ELECTRONIC SUPPLEMENTARY INFORMATION

Stabilization of Reactive Rare Earth Alkyl Complexes through Mechanistic Studies

Elias Tanuhadi[†,‡], Anna S. Bair[†,‡], Mary Johnson[†,‡], Philip Fontaine[‖], Jerzy Klosin[‖*], Sudipta Pal[‖], and Polly L. Arnold[†,‡,*]

[†] Dept of Chemistry, University of California, Berkeley, Berkeley, CA, 94720, USA. E-mail: pla@berkeley.edu

[‡] Chemical Sciences Division, Lawrence Berkeley National Laboratory, Berkeley, CA 94720, USA

[‖] Corporate R&D, The Dow Chemical Company, Midland, Michigan 48674, USA; E-mail: jklosin@dow.com

Content

Compound numbering

known:

$M(r)_3(THF)_2$; M = Sm(III), Y(III), Lu(III), Sc(III)

$Y(r)_3$(donor); donor = (DMPE)(THF), TMEDA

new:

$M(r)_3(C_6H_{14}O_3)$ (**M-G_2**); M = Sm(III), Y(III), Lu(III), Sc(III);

$M(CH_2SiMe_3)_3(C_8H_{18}O_4)$ (**M-G_3**); M = Sm(III), Y(III), Lu(III);

$M(CH_2SiMe_3)_3(Me_2NCH_2CH_2NMe_2)$ (**M-TMEDA**); M = Sm(III), Lu(III); Sc(III)

$M(CH_2SiMe_3)_3(C_6H_{16}P_2)(C_4H_8O)_n$ (**M-DMPE**); M = Lu(III), n = 1; Sc(III), n = 0

G_2 = diglyme, $(CH_3(OCH_2CH_2)_2O)$

G_3 = triglyme $(CH_3(OCH_2CH_2)_3O)$

1. General Information

NMR spectra were recorded on Bruker AVQ 400 and 600 MHz spectrometers and are referenced to residual protio solvent for ^{1}H NMR spectroscopy. C_6D_6 was used as solvent for NMR spectroscopic experiments, and was referenced to added hexamethylbenzene (HMB) (2.12 ppm for both ^{1}H and ^{13}C[3] NMR spectroscopic experiments). Chemical shifts are quoted in ppm and coupling constants in Hz. NMR spectra were taken at 25°C. Quantitative ^{1}H NMR data were acquired with the delay time set to 5x the longest T_1 value present.

Elemental analysis: Elemental analyses were carried out by Dr Elena Kreimer at the microanalytic services in the College of Chemistry at the University of California, Berkeley.

Single crystal X-ray diffraction (SXRD): Single crystal X-ray diffraction data of **LuG_3** were collected using a Rigaku XtaLab P200 diffractometer fitted with a Pilatus3 R 200K-A Shutterless Detector and using a MicroMax 007HF Dual Rotating Anode (MoKα radiation) at 150 K. X-ray diffraction data of all other compounds were collected using a Rigaku Xtalab Synergy-S diffractometer fitted with a HyPix-6000HE photon counting detector using MoKα (λ = 0.71073 Å) or CuKα (λ = 0.1.5418Å) radiation. All structures were solved using SHELXT in Olex2 and refined using SHELXL in Olex2.[6,7] Absorption corrections were completed using CrysAlis PRO (Rigaku Oxford Diffraction) software. Analytical numeric absorption corrections used a multifaceted crystal model based on expressions derived by Clark and Reid.[8] Numerical absorption correction was based on a Gaussian integration over a multifaceted crystal model.

2. Additional Synthesis Procedures and Characterization

2.1. Synthesis of d_2-(chloromethyl)trimethylsilane ($ClCD_2Si(CH_3)_3$)

To a stirred solution of d_2 – chloroiodomethane (1 g, 5.6 mmol, 1 eq.) and chlorotrimethylsilane (TMSCl, 0.913 g; 8.4 mmol, 1.5 eq.) in THF (5 mL), methyllithium, CH_3Li (MeLi) [1.6 M in Et_2O] (7.9 mL, 12.6 mmol; 2.25 eq.) was added dropwise at -78°C. The resulting reaction mixture was stirred for 90 min. at -78°C followed by separation of the volatile product from any solids by vacuum transfer. Et_2O was removed under reduced pressure. Residual THF was removed by extraction of the product into hexanes (hexanes/H_2O). The combined hexanes extracts were distilled off P_2O_5 to yield the title compound $ClCD_2Si(CH_3)_3$ as a colorless liquid in a hexanes solution 20% yield, based on d_2 – chloroiodomethane; determined by integration against internal HMB standard.

^1H NMR (700 MHz, C_6D_6) δ -0.04 (s, 9H). ^2H NMR (92 MHz, C_6D_6) δ 2.37 (s, 2H).

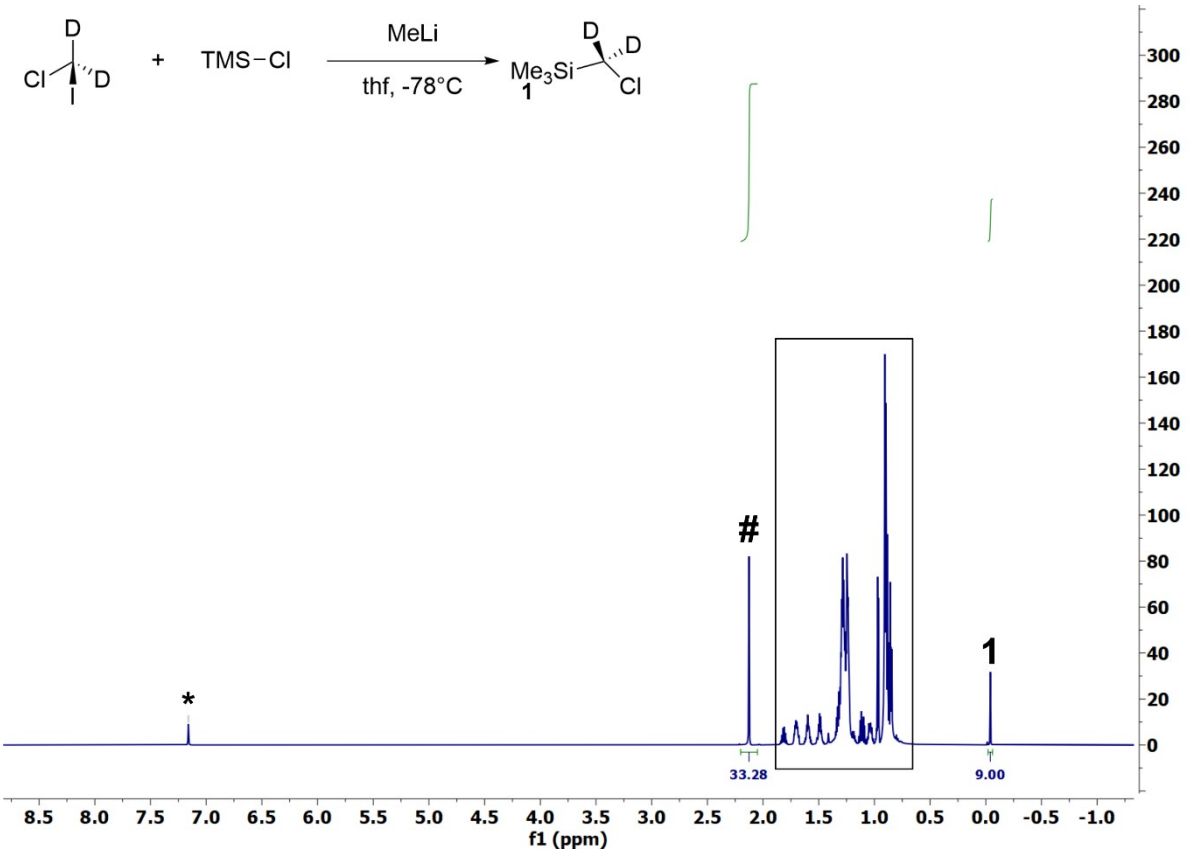

Figure S 1 ^1H NMR spectrum (700 MHz) of $ClCD_2Si(CH_3)_3$ in d_6-benzene. The solvent residual resonance is marked with an asterisk, # shows the hexamethyl benzene (HMB) internal standard, hexanes from the extraction step, boxed for clarity.

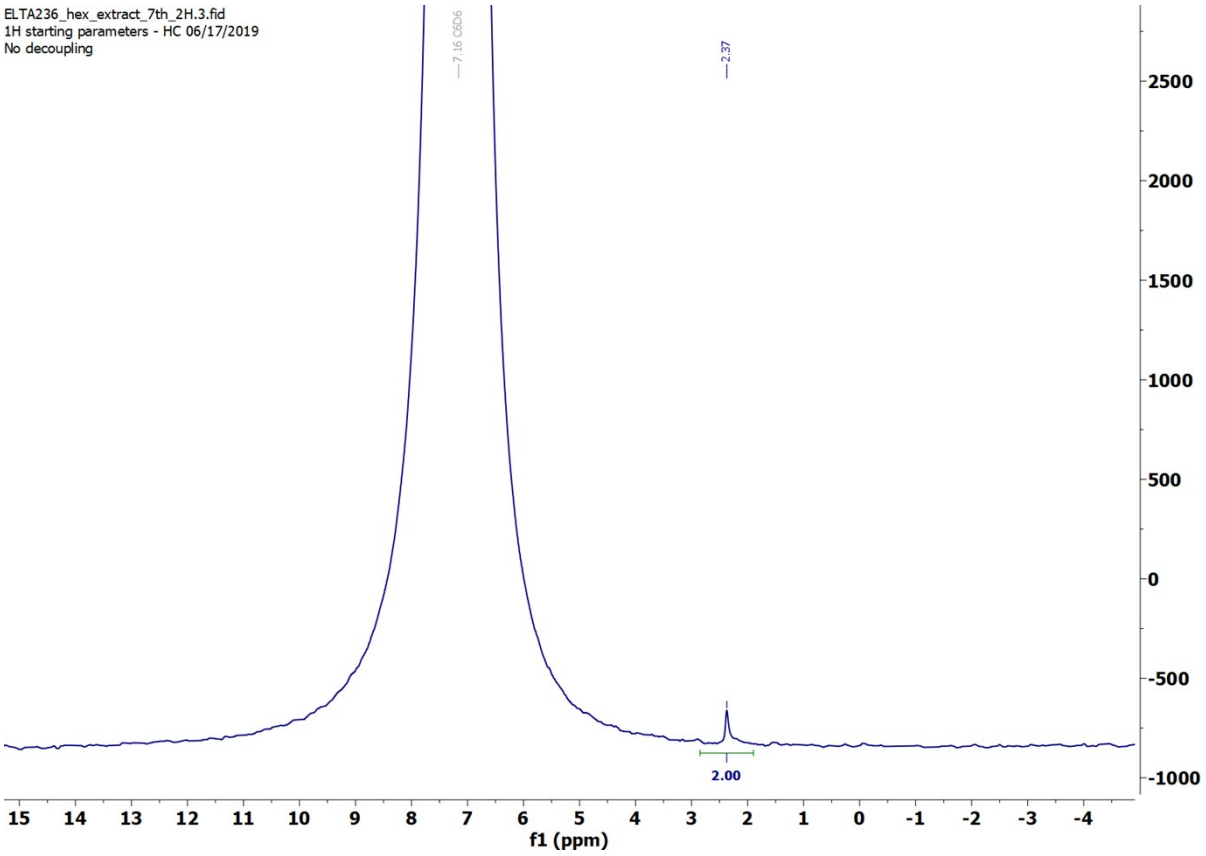

Figure S 2 ^{2}H NMR (92 MHz, C_6D_6) of $ClCD_2Si(CH_3)_3$ in d_6-benzene.

2.2. Synthesis of d_2-((trimethylsilyl)methyl)lithium ($LiCD_2Si(CH_3)_3$)

In an Ar-filled glovebox, a 20 mL scintillation vial was charged with 17 mL of $ClCD_2Si(CH_3)_3$ (70.9 mM in hexanes, dried over P_2O_5) and lithium sand (138 mg, 19.88 mmol). The resulting reaction mixture was stirred at 60°C overnight and the purple suspension filtered followed by solvent removal under reduced pressure offering the title compound $LiCD_2Si(CH_3)_3$ as a white crystalline solid. Yield: 85%, 100 mg based on $ClCD_2Si(CH_3)_3$.

^{1}H NMR (400 MHz, C_6D_6) δ 0.13 (s, 9H). ^{7}Li NMR (156 MHz, C_6D_6) δ 2.63.

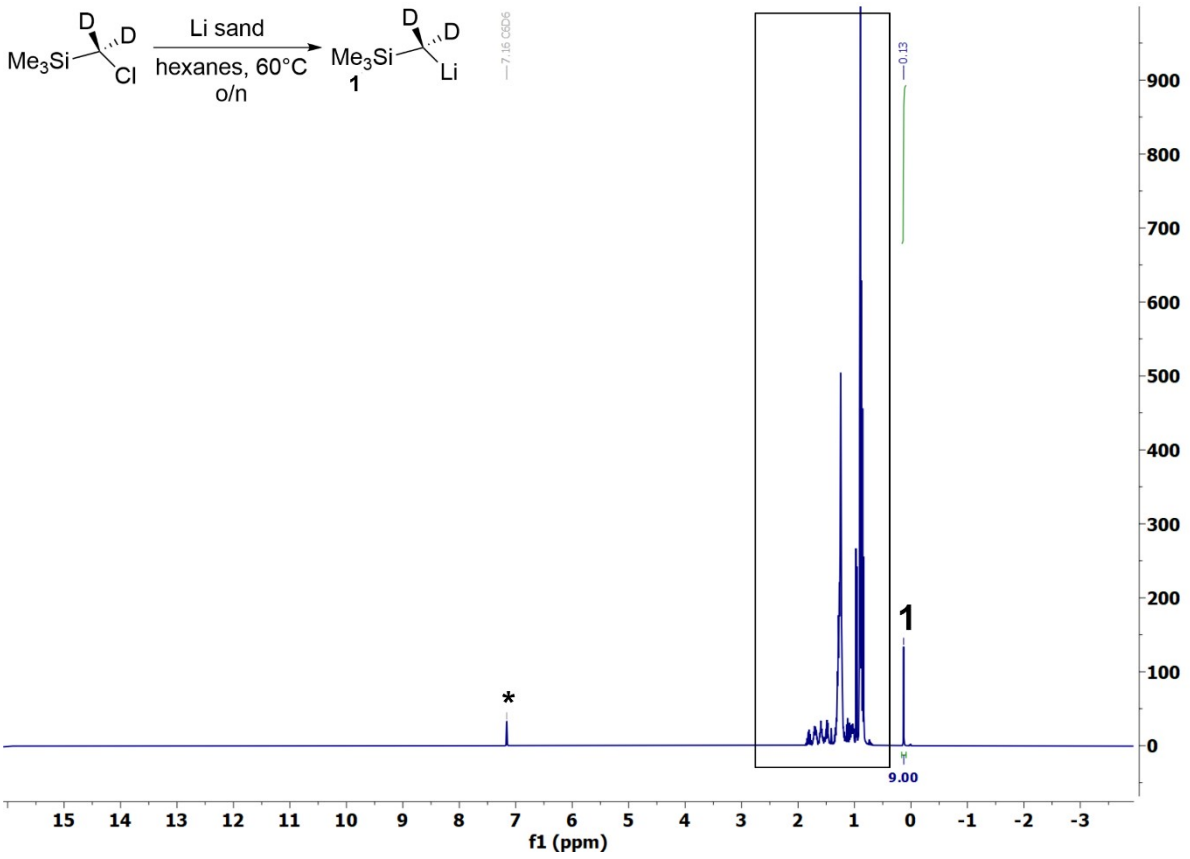

Figure S 3 ^{1}H NMR spectrum (400 MHz) of $LiCD_2Si(CH_3)_3$ in d_6-benzene. The solvent residual resonance is marked with an asterisk, hexanes from the extraction step, boxed for clarity. o/n = overnight.

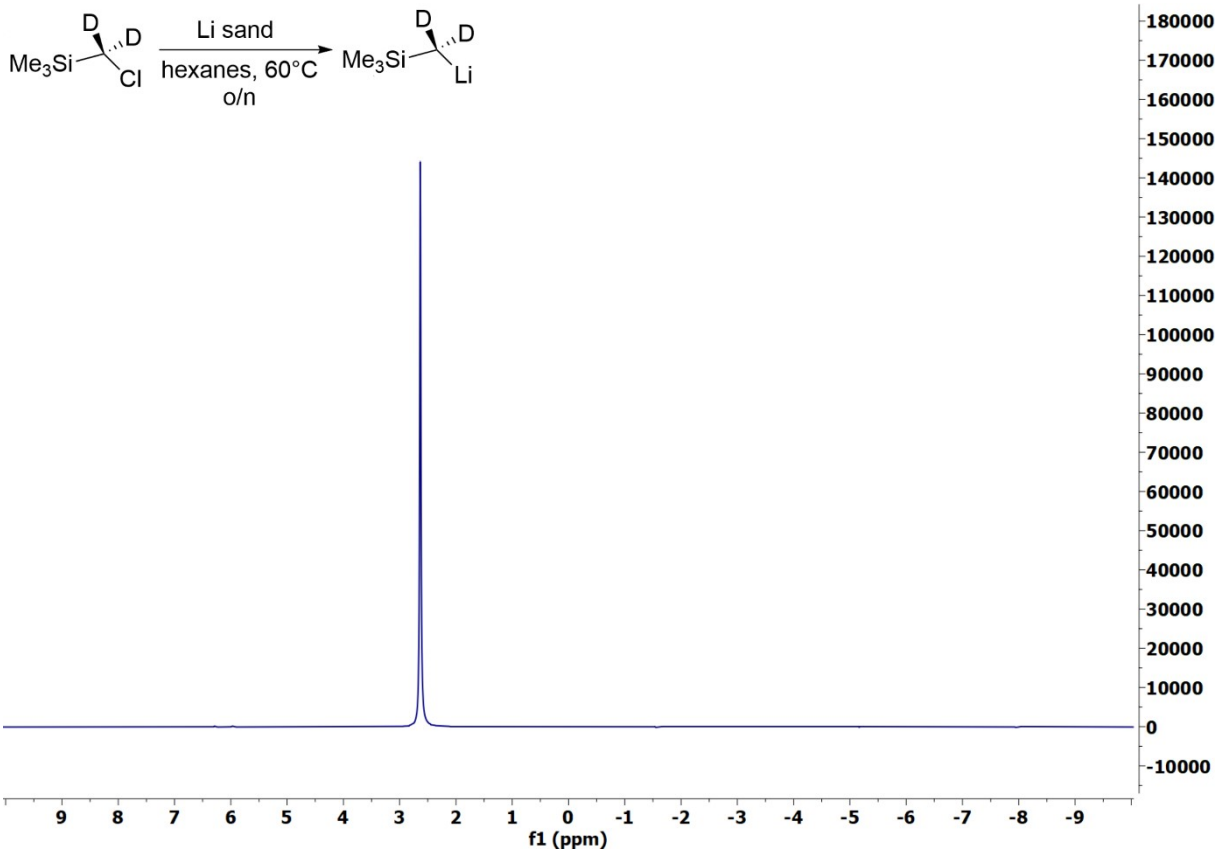

Figure S 4 ^{7}Li NMR spectrum (156 MHz) of $LiCD_2Si(CH_3)_3$ in d_6-benzene. o/n = overnight.

2.3. $Sm(CH_2SiMe_3)_3(C_6H_{14}O_3)$ (**Sm-G$_2$**)

^{1}H NMR (600 MHz, C_6D_6) δ 5.46 (s, 6H), 5.29 (s, 6H), 0.44 (s, 27H), -0.14 (s, 4H), -1.53 (s, 4H). ^{13}C NMR (151 MHz, C_6D_6) δ 131.79, 31.97, 23.05, 14.34, 2.84.

Anal. Calcd for $SmC_{18}H_{47}Si_3O_3$: C, 39.58, H, 8.67. Found: C, 39.29; H, 8.30.

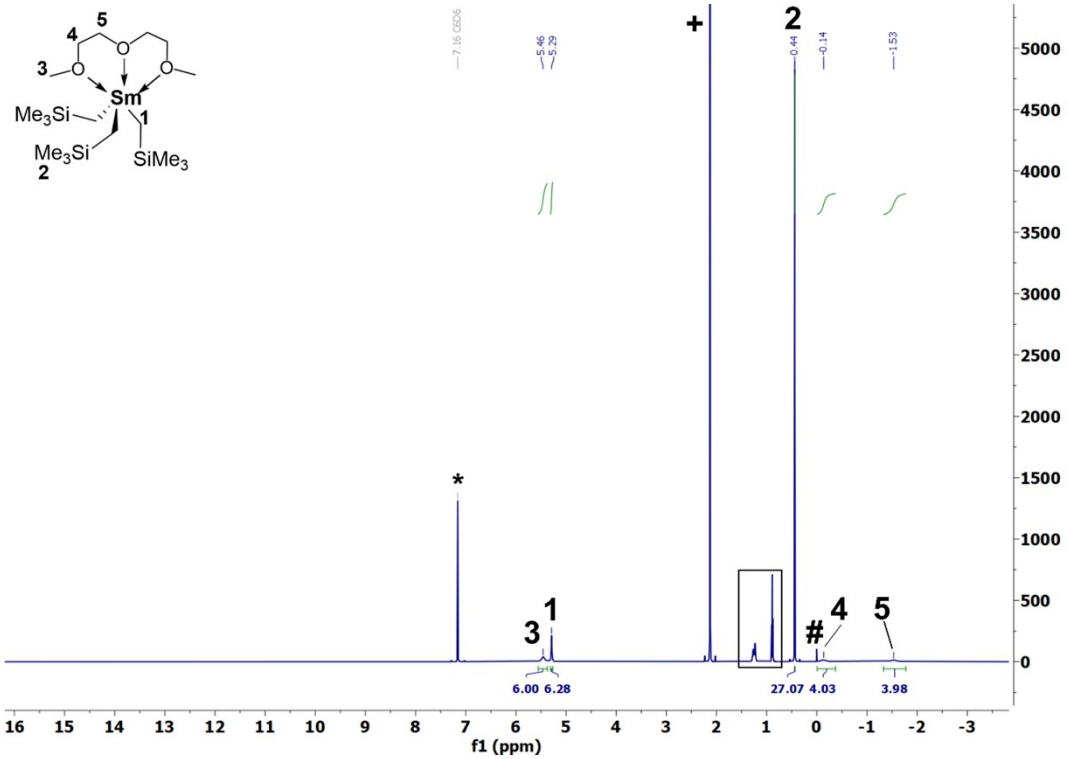

Figure S 5 ^{1}H NMR spectrum (600 MHz) of **Sm-G$_2$** in d_6-benzene. The solvent residual resonance is marked with an asterisk, # shows TMS arising from the onset of decomposition, + shows the hexamethyl benzene (HMB) internal standard, hexanes from the recrystallization, boxed for clarity.

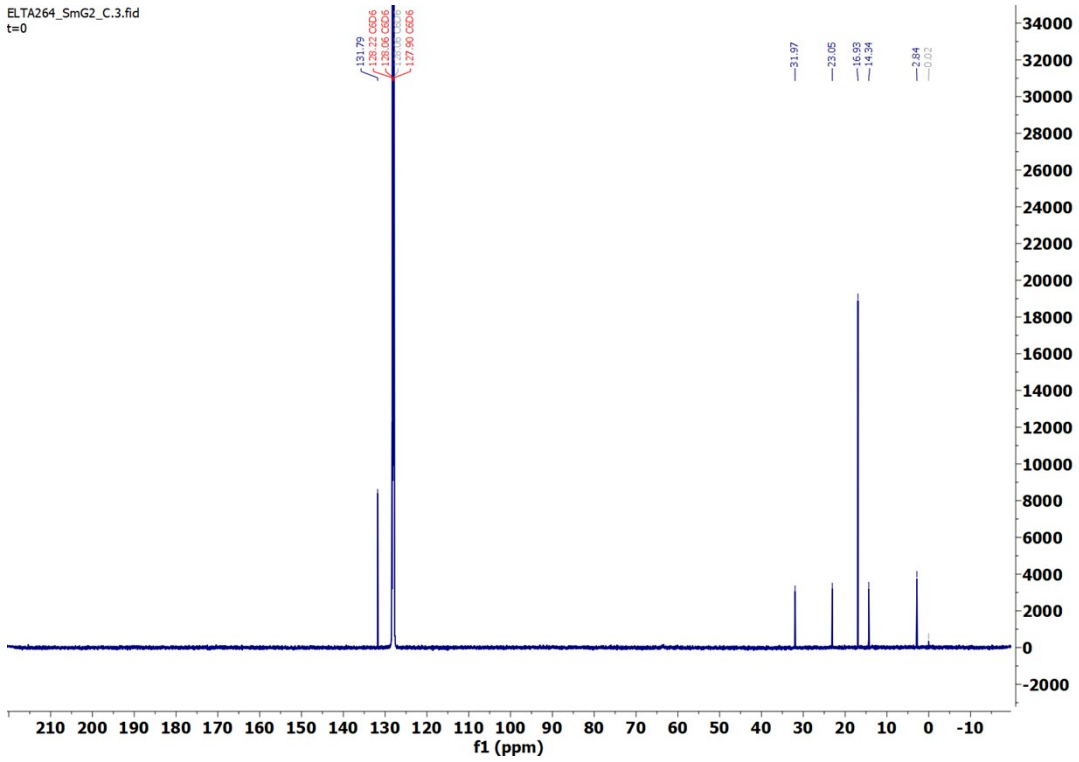

Figure S 6 $^{13}C\{^{1}H\}$ NMR spectrum (151 MHz) of **Sm-G$_2$** in d_6-benzene.

2.4. $Y(CH_2SiMe_3)_3(C_6H_{14}O_3)$ (**Y-G$_2$**)

^{1}H NMR (600 MHz, C_6D_6) δ 3.07 (s, 6H), 2.97 (s, 4H), 2.68 (s, 4H), 0.44 (s, 27H), -0.42 (d, *J* = 2.9 Hz, 6H). ^{13}C NMR (151 MHz, C_6D_6) δ 69.18, 67.97, 60.68, 35.42 (d, *J* = 36.5 Hz), 4.78.

Anal. Calcd for $YC_{18}H_{47}Si_3O_3$: C, 44.60, H, 9.77. Found: C, 42.37; H, 9.16.

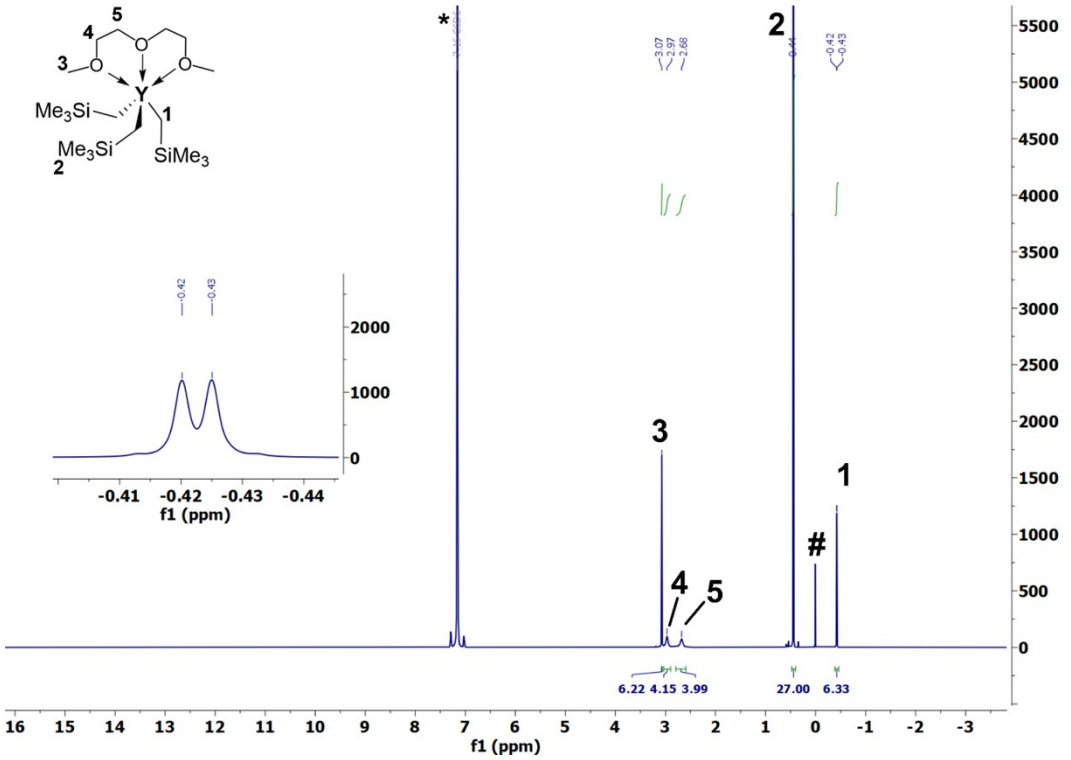

Figure S 7 ^{1}H NMR spectrum (600 MHz) of **Y-G$_2$** in d_6-benzene. The solvent residual resonance is marked with an asterisk, # shows TMS arising from the onset of decomposition. CH_2-doublet arising from $^2J_{YH}$ coupling highlighted in inset.

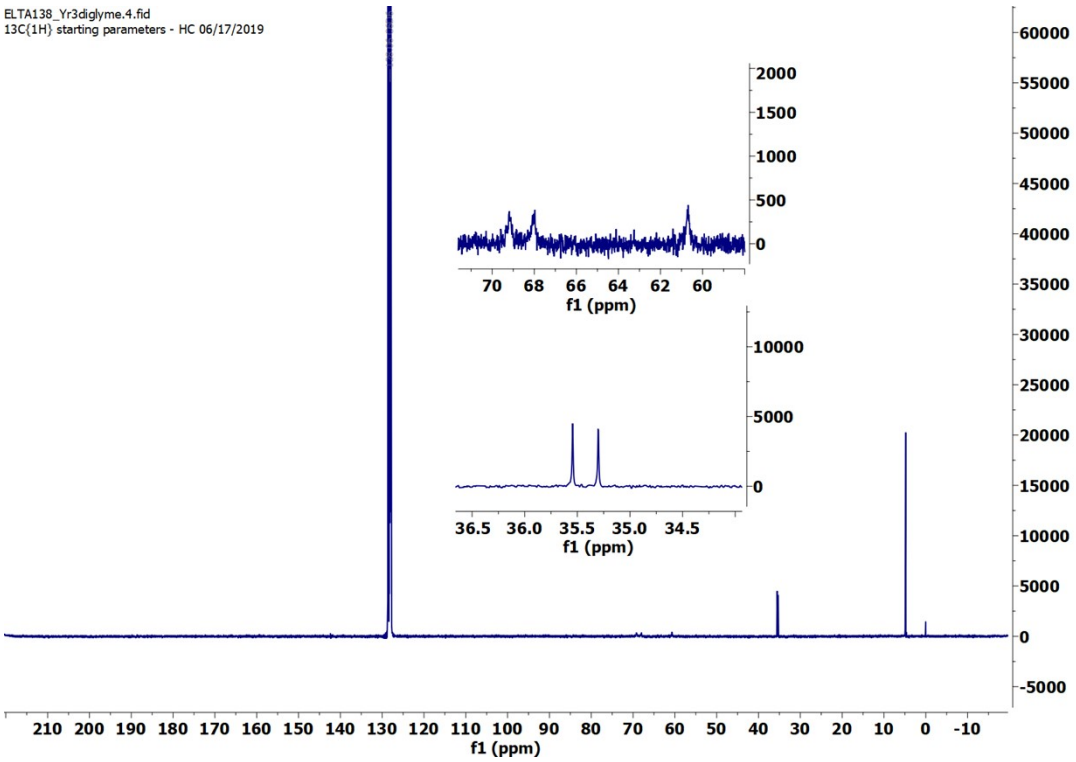

Figure S 8 ^{13}C{^{1}H} NMR spectrum (151 MHz) of **Y-G$_2$** in d_6-benzene.

2.5. $Lu(CH_2SiMe_3)_3(C_6H_{14}O_3)$ (**Lu-G$_2$**)

^{1}H NMR (600 MHz, C_6D_6) δ 3.04 (s, 6H), 2.96 (t, *J* = 5.3 Hz, 4H), 2.61 (t, *J* = 5.3 Hz, 4H), 0.44 (s, 27H), -0.66 (s, 6H). ^{13}C NMR (151 MHz, C_6D_6) δ 69.41, 68.43, 60.70, 41.60, 4.91.

Anal. Calcd for $LuC_{18}H_{47}Si_3O_3$: C, 37.88, H, 8.30. Found: C, 37.54; H, 8.13.

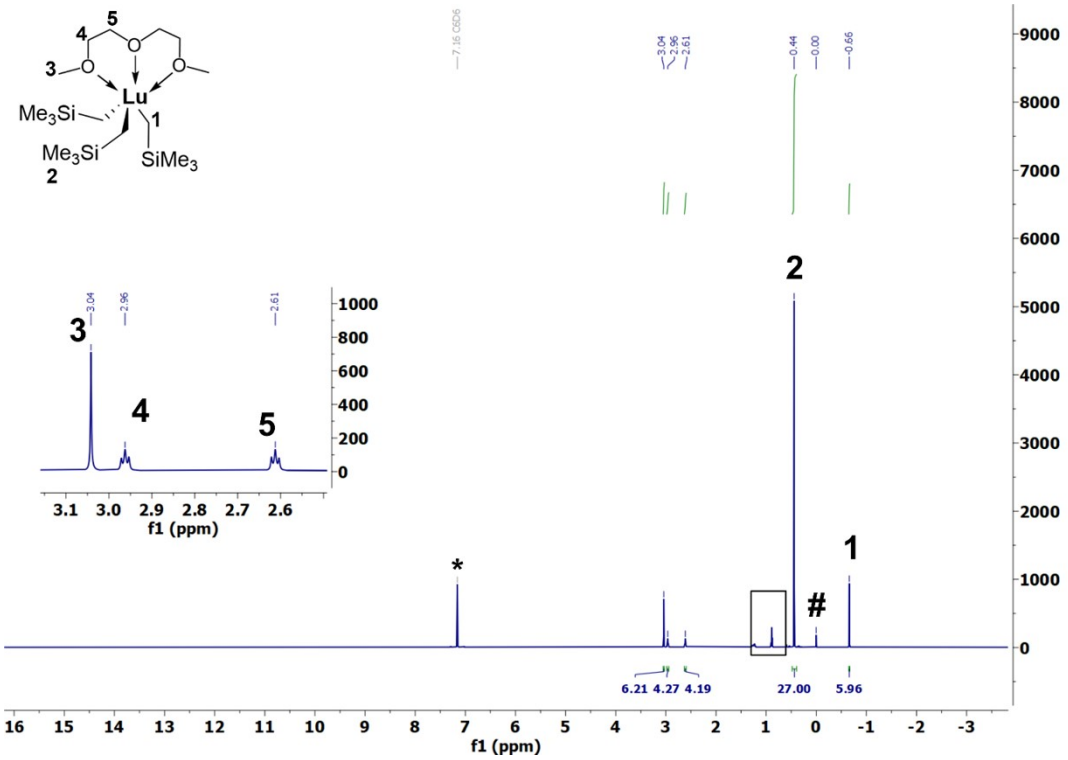

Figure S 9 ^{1}H NMR spectrum (600 MHz) of **Lu-G$_2$** in d_6-benzene. The solvent residual resonance is marked with an asterisk, # shows TMS arising from the onset of decomposition, hexanes from the recrystallization, boxed for clarity.

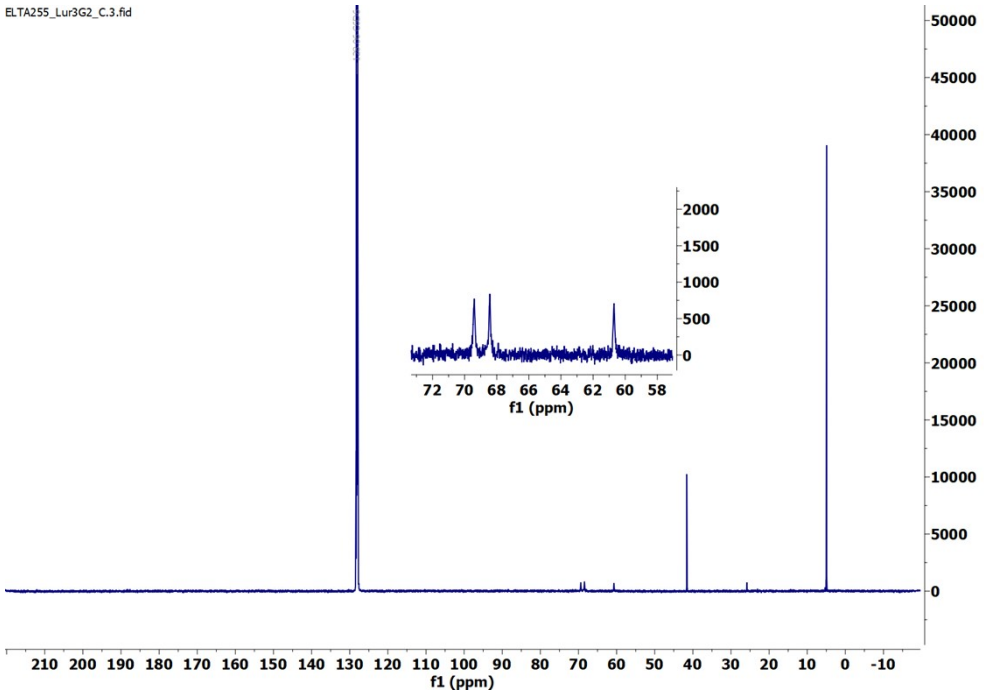

Figure S 10 ^{13}C{^{1}H} NMR spectrum (151 MHz) of **Lu-G$_2$** in d_6-benzene.

2.6. $Sc(CH_2SiMe_3)_3(C_6H_{14}O_3)$ (**Sc-G$_2$**)

^{1}H NMR (600 MHz, C_6D_6) δ 3.23 (t, *J* = 5.2 Hz, 3H), 3.02 (s, 6H), 2.76 (t, *J* = 5.3 Hz, 5H), 0.41 (s, 36H), 0.09 (s, 6H). ^{13}C NMR (151 MHz, C_6D_6) δ 70.05, 69.71, 60.73, 4.33.

Anal. Calcd for $ScC_{18}H_{47}Si_3O_3$: C, 49.05, H, 10.75. Found: C, 48.97; H, 10.66.

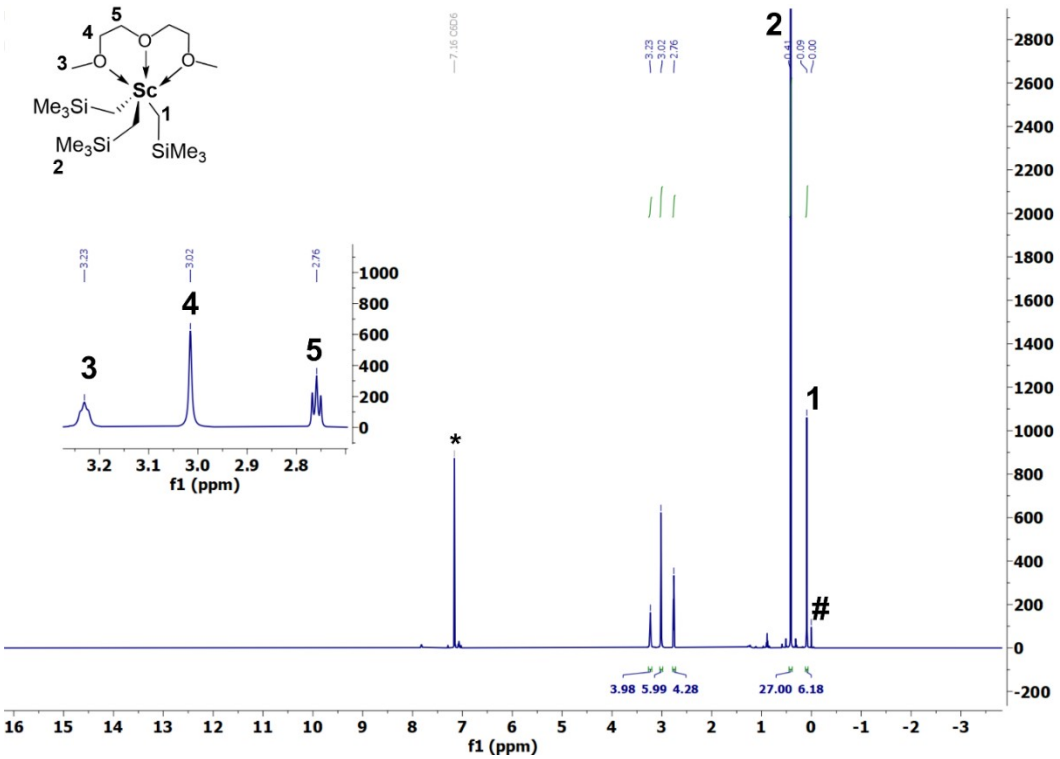

Figure S 11 ^{1}H NMR spectrum (600 MHz) of **Sc-G$_2$** in d_6-benzene. The solvent residual resonance is marked with an asterisk, # shows TMS arising from the onset of decomposition.

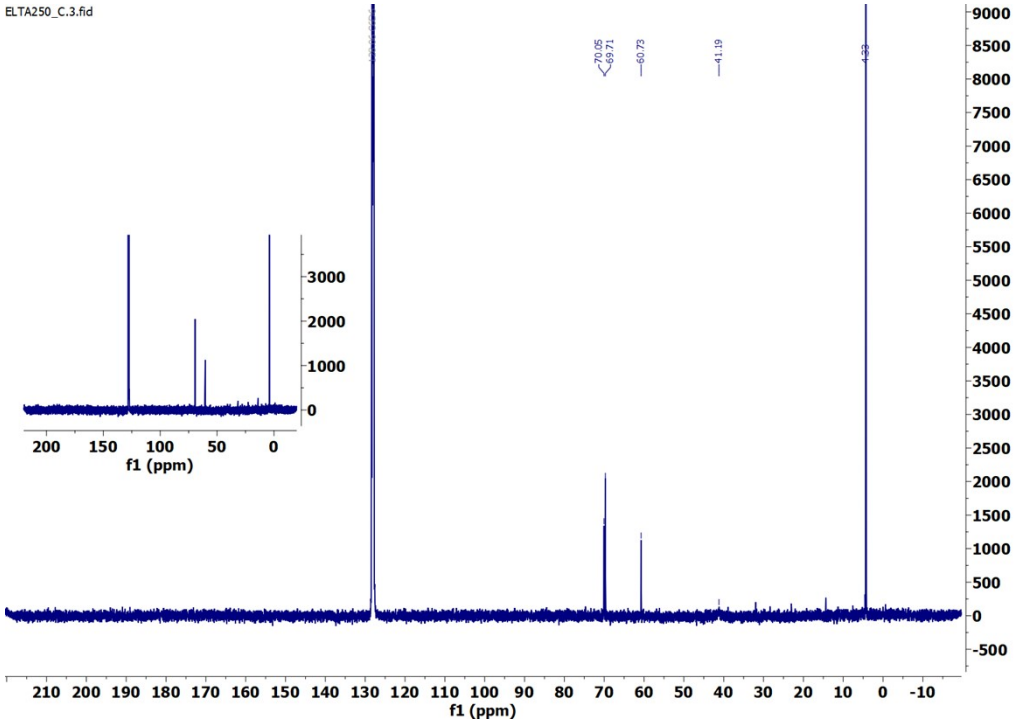

Figure S 12 ^{13}C{^{1}H} NMR spectrum (151 MHz) of **Sc-G$_2$** in d_6-benzene.

2.7. $Sm(CH_2SiMe_3)_3(CH_3(OCH_2CH_2)_3O)$ (**Sm-G$_3$**)

^{1}H NMR (600 MHz, C_6D_6) δ 10.25 (s, 1H), 6.00 (s, 1H), 1.39 (s, 6H), -1.80 (s, 1H), -3.79 (s, 1H). ^{13}C NMR (151 MHz, C_6D_6) δ 152.17, 86.66, 72.19, 70.77, 69.74, 67.62, 58.73, 3.61.

Anal. Calcd for $SmC_{20}H_{51}Si_3O_4$: C, 40.7, H, 8.71. Found: C, 40.32; H, 8.43.

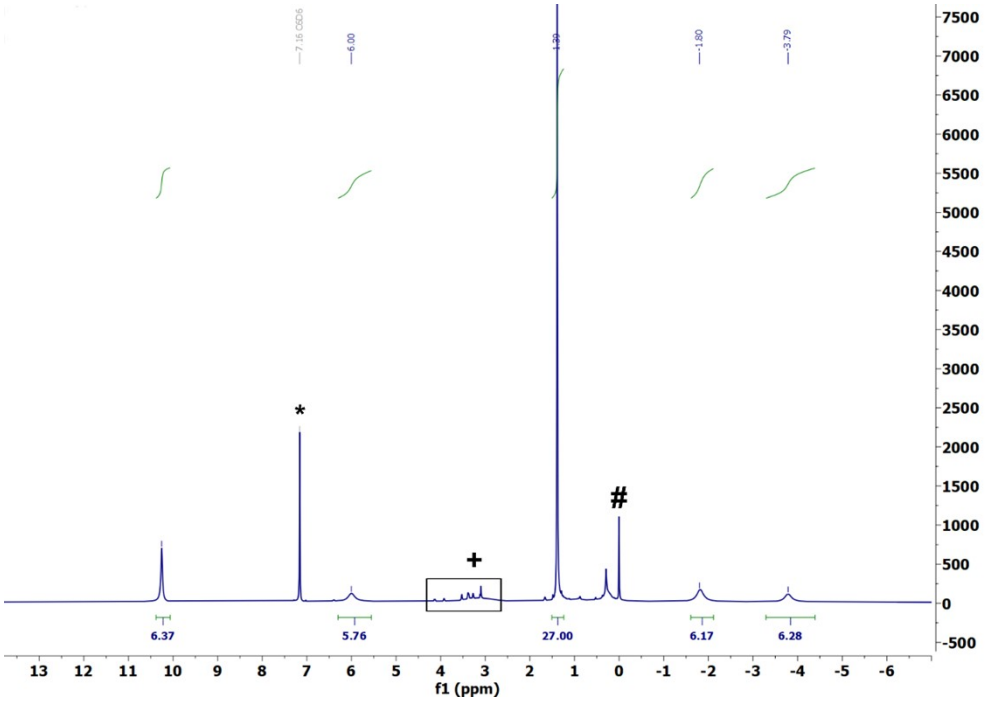

Figure S 13 ^{1}H NMR spectrum (600 MHz) of **Sm-G$_3$** in d_6-benzene. The solvent residual resonance is marked with an asterisk, # shows TMS arising from the onset of decomposition, + for decomposition products resulting from G_3 decomposition.

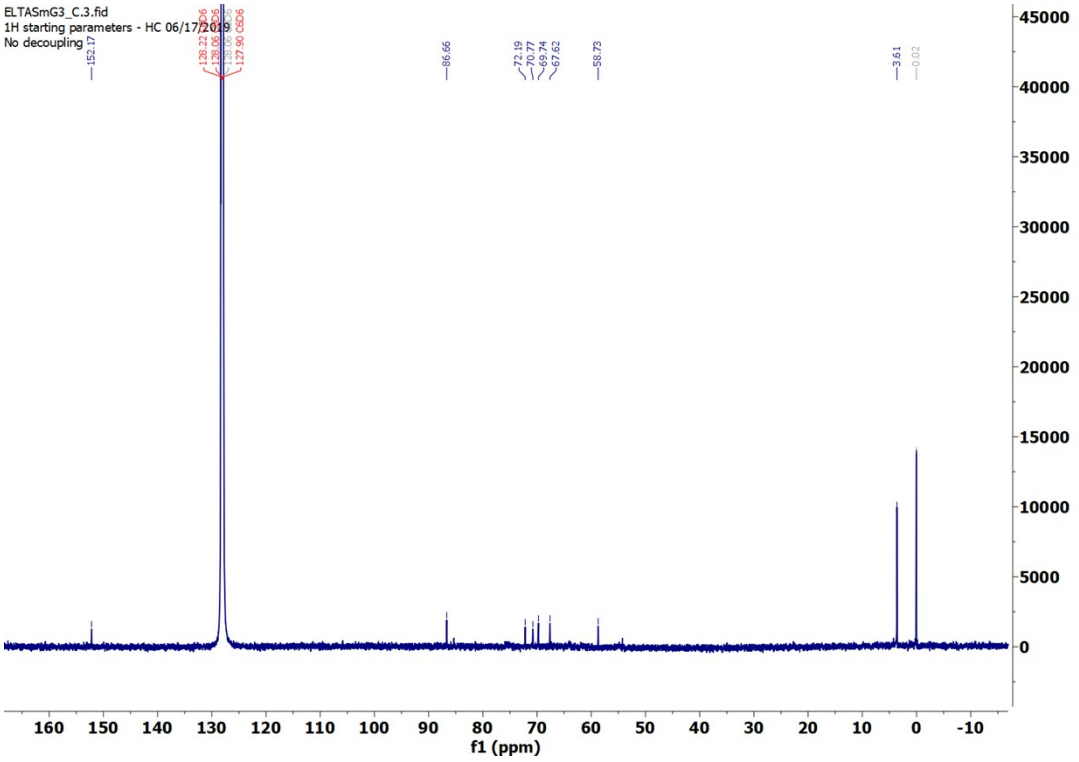

Figure S 14 $^{13}C\{^{1}H\}$ NMR spectrum (151 MHz) of **Sm-G$_3$** in d_6-benzene.

2.8. Y(CH$_2$SiMe$_3$)$_3$((OCH$_2$CH$_2$)$_3$O) (**Y-G$_3$**)

^{1}H NMR (400 MHz, C_6D_6) δ 3.47 (s, 6H), 3.09 (t, J = 4.8 Hz, 4H), 3.03 – 2.93 (m, 8H), 0.39 (s, 27H), -1.00 – -1.15 (m, 6H). ^{13}C NMR (151 MHz, C_6D_6) δ 72.32, 71.98, 69.51, 68.37, 5.27, 4.92.

Anal. Calcd for $YC_{20}H_{51}Si_3O_4$: C, 45.43, H, 9.72. Found: C, 45.38; H, 9.76.

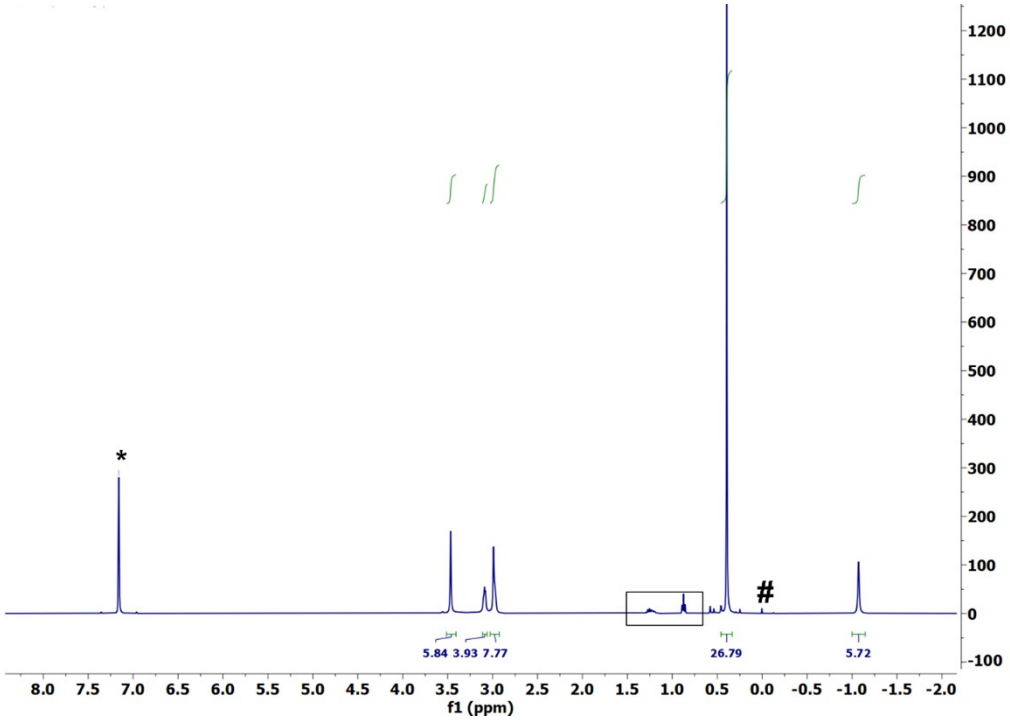

Figure S 15 ^{1}H NMR spectrum (400 MHz) of **Y-G$_3$** in d_6-benzene. The solvent residual resonance is marked with an asterisk, # shows TMS arising from the onset of decomposition, hexanes from recrystallization boxed.

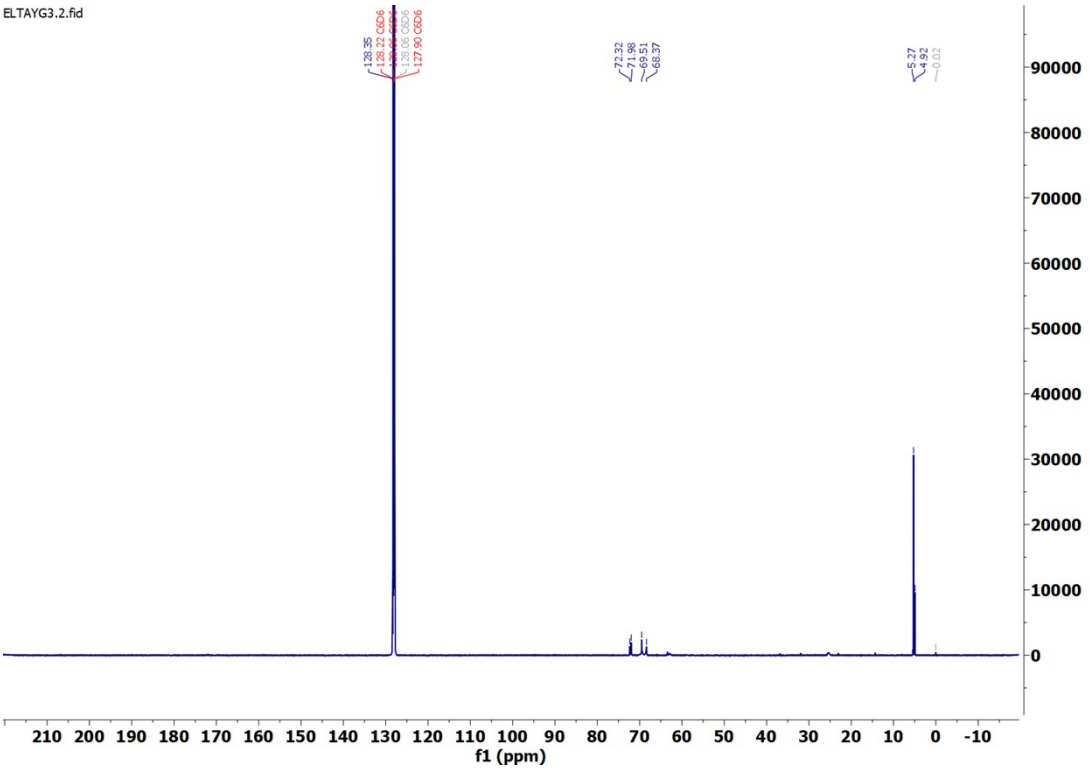

Figure S 16 $^{13}C\{^{1}H\}$ NMR spectrum (151 MHz) of **Y-G$_3$** in d_6-benzene.

2.9. Lu(CH$_2$SiMe$_3$)$_3$((OCH$_2$CH$_2$)$_3$O) (**Lu-G$_3$**)

^{1}H NMR (600 MHz, C_6D_6) δ 3.23 (t, J = 4.9 Hz, 4H), 3.13 (d, J = 8.5 Hz, 10H), 2.97 (t, J = 5.2 Hz, 4H), 0.42 (s, 27H), -0.82 (s, 6H). ^{13}C NMR (151 MHz, C_6D_6) δ 71.53, 69.69, 69.26, 60.51, 38.44, 34.45, 22.73, 14.27, 5.06.

Anal. Calcd for $LuC_{20}H_{51}Si_3O_4$: C, 39.07, H, 8.36. Found: C, 38.69; H, 8.11.

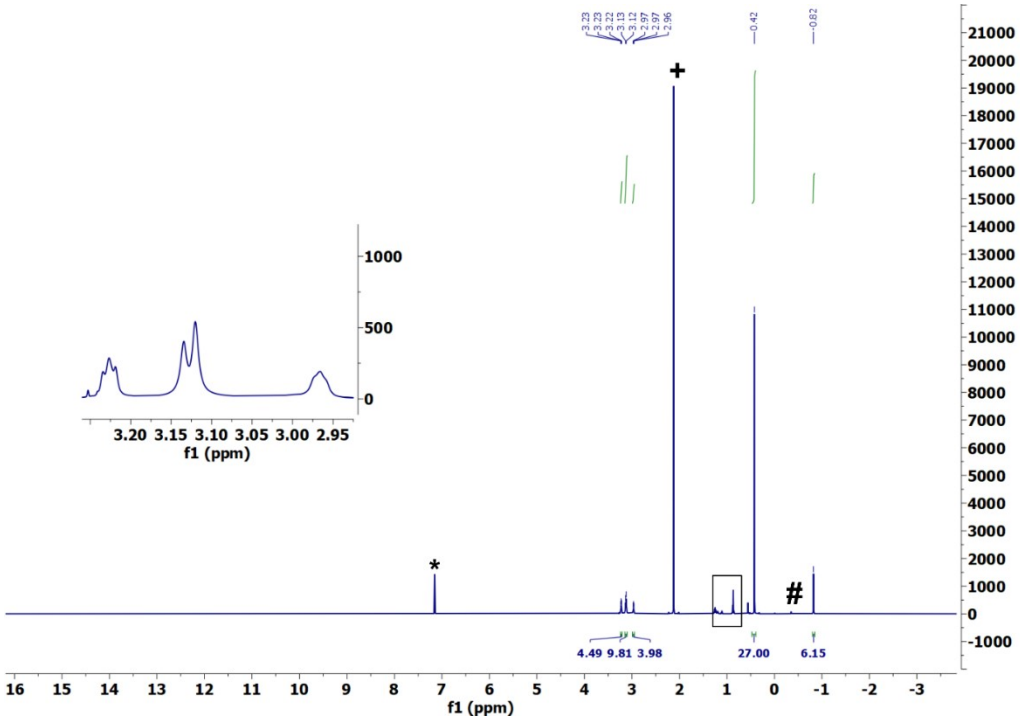

Figure S 17 ^{1}H NMR spectrum (600 MHz) of **Lu-G$_3$** in d_6-benzene. The solvent residual resonance is marked with an asterisk, # shows TMS arising from the onset of decomposition, + shows the hexamethyl benzene (HMB) internal standard, hexanes from the recrystallization, boxed for clarity.

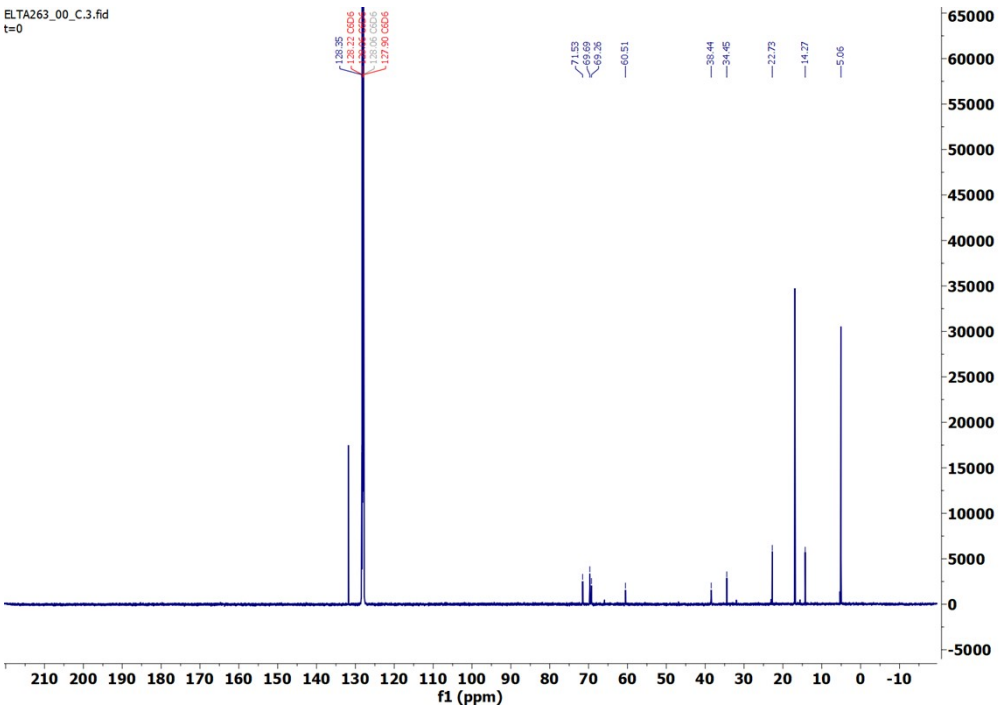

Figure S 18 $^{13}C\{^{1}H\}$ NMR spectrum (151 MHz) of **Lu-G_3** in d_6-benzene.

2.10. Sm(CH$_2$SiMe$_3$)$_3$(Me$_2$NCH$_2$CH$_2$NMe$_2$) (**Sm-TMEDA**)

^{1}H NMR (600 MHz, C_6D_6) δ 4.50 (s, 6H), 2.10 (s, 12H), 0.21 (s, 27H), -2.68 (s, 4H). ^{13}C NMR (151 MHz, C_6D_6) δ 58.45, 46.03.

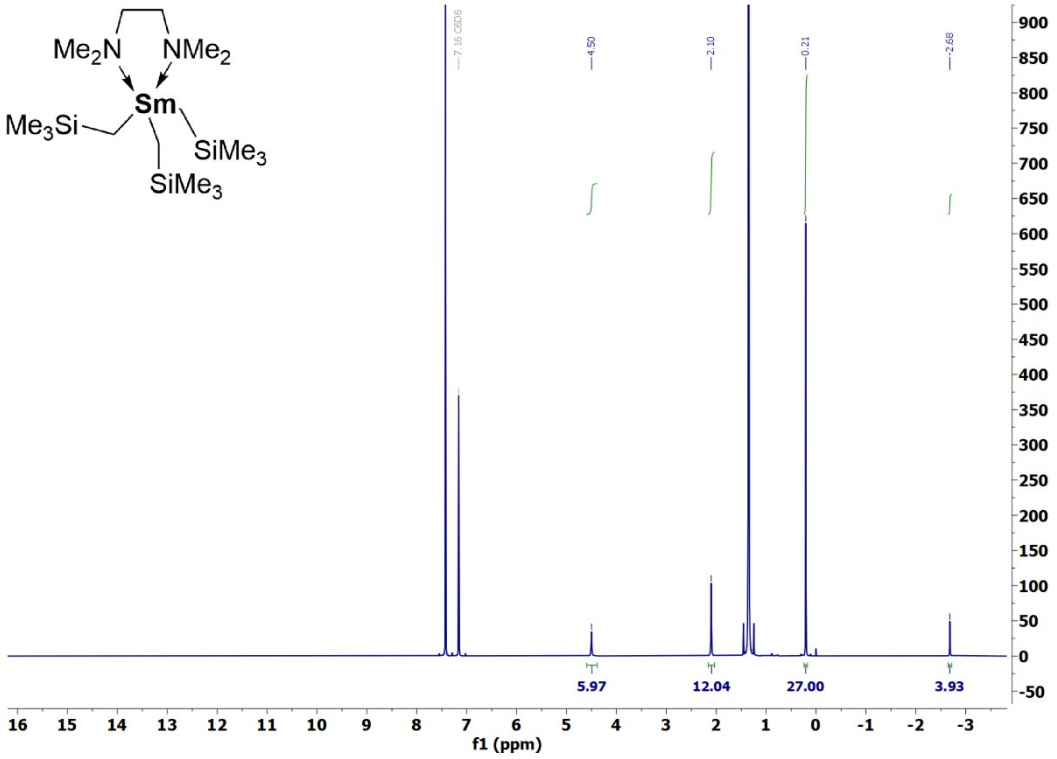

Figure S 19 ^{1}H NMR spectrum (600 MHz) of **Sm-TMEDA** in d_6-benzene.

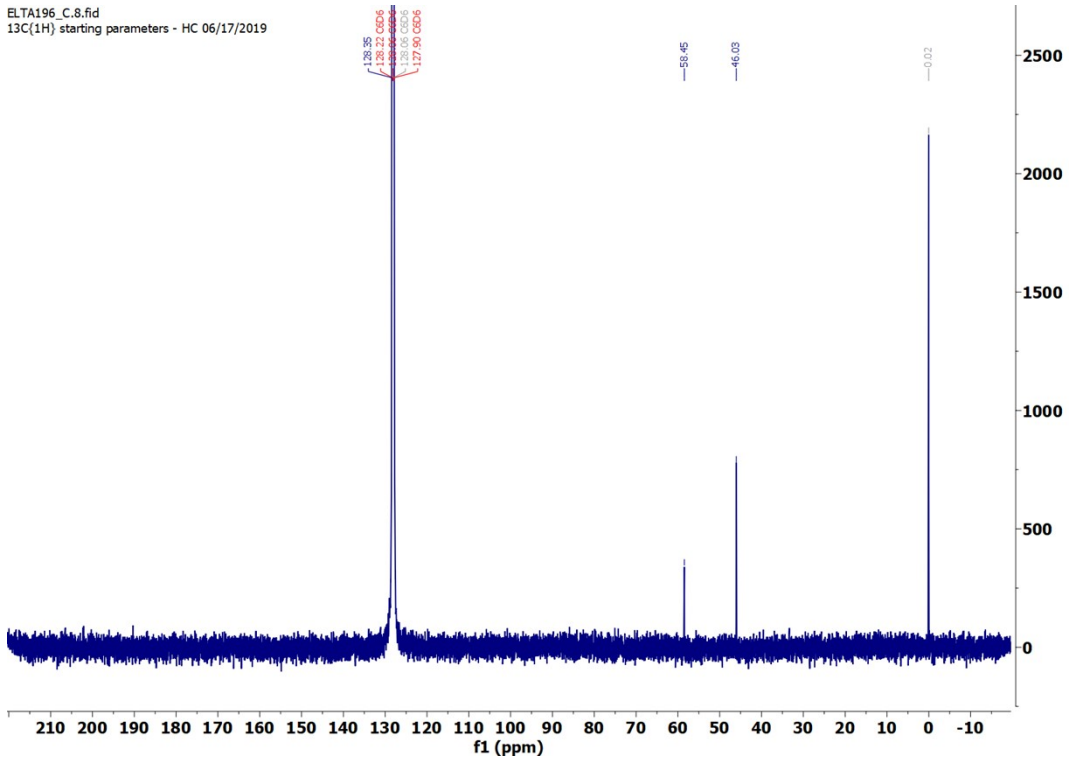

Figure S 20 ^{13}C{^{1}H} NMR spectrum (151 MHz) of **Sm-TMEDA** in d_6-benzene

2.11. Lu(CH_2SiMe_3)$_3$($Me_2NCH_2CH_2NMe_2$) (**Lu-TMEDA**)

^{1}H NMR (600 MHz, C_6D_6) δ 1.82 (s, 12H), 1.48 (s, 4H), 0.41 (s, 27H), -0.61 (s, 6H). ^{13}C NMR (151 MHz, C_6D_6) δ 56.60, 46.23, 45.51, 4.87.

Anal. Calcd for $LuC_{18}H_{49}Si_3N_2$: C, 39.11, H, 8.93; N, 5.07. Found: C, 39.11; H, 8.97; N, 4.99.

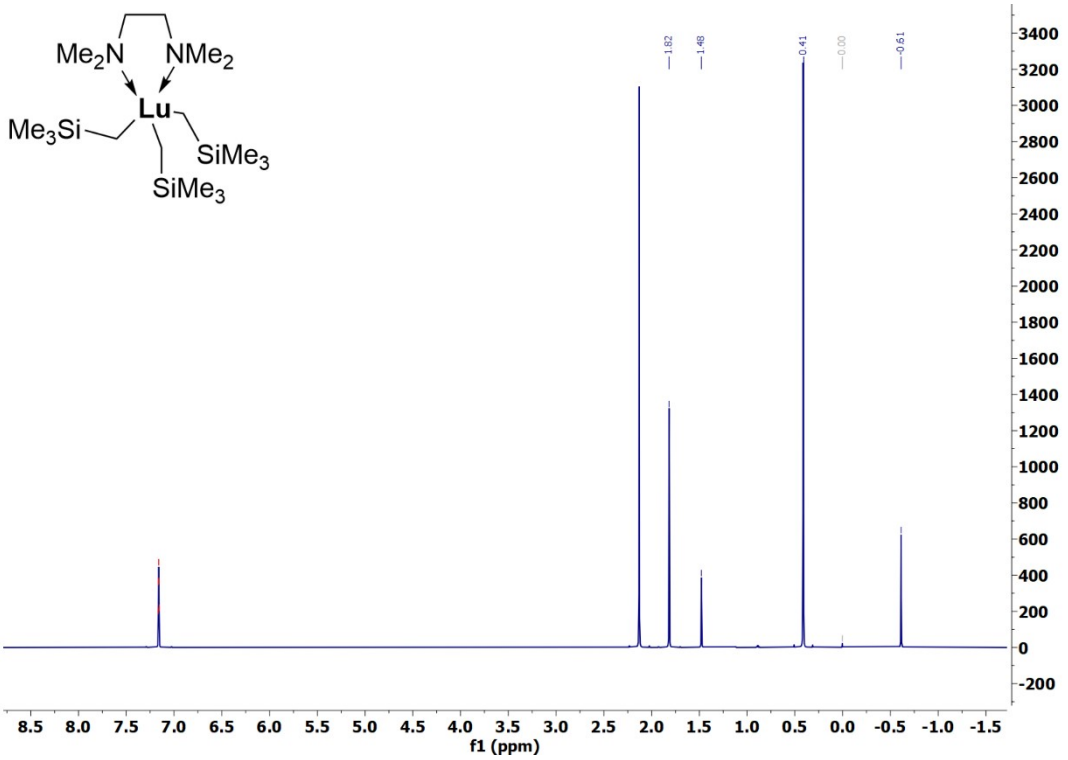

Figure S 21 ^{1}H NMR spectrum (600 MHz) of **Lu-TMEDA** in d_6-benzene.

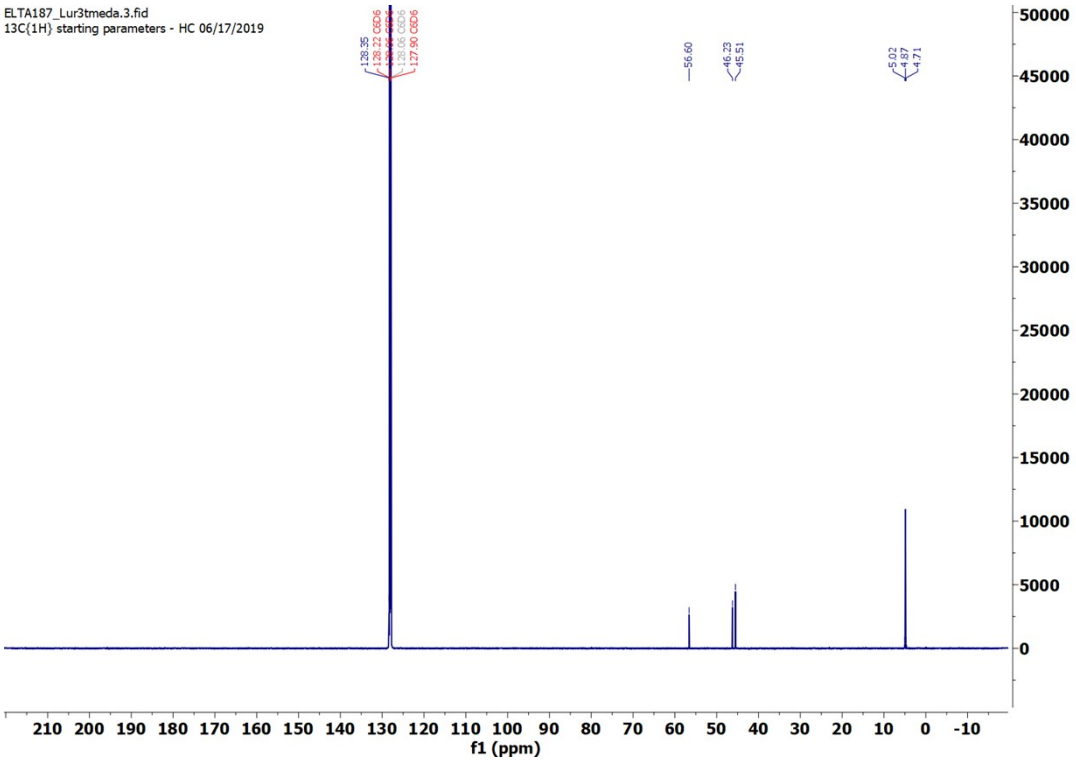

Figure S 22 ^{13}C{^{1}H} NMR spectrum (151 MHz) of **Lu-TMEDA** in d_6-benzene

2.12. $Sc(CH_2SiMe_3)_3(Me_2NCH_2CH_2NMe_2)$ (**Sc-TMEDA**)

^1H NMR (600 MHz, C_6D_6) δ 1.91 (s, 12H), 1.57 (s, 4H), 0.40 (s, 27H), 0.10 (s, 6H). ^{13}C NMR (151 MHz, C_6D_6) δ 56.85, 46.69, 16.93, 4.41.

Anal. Calcd for $ScC_{18}H_{49}Si_3N_2$: C,51.13, H, 11.68; N, 6.63. Found: C, 50.97; H, 11.59; N, 6.57.

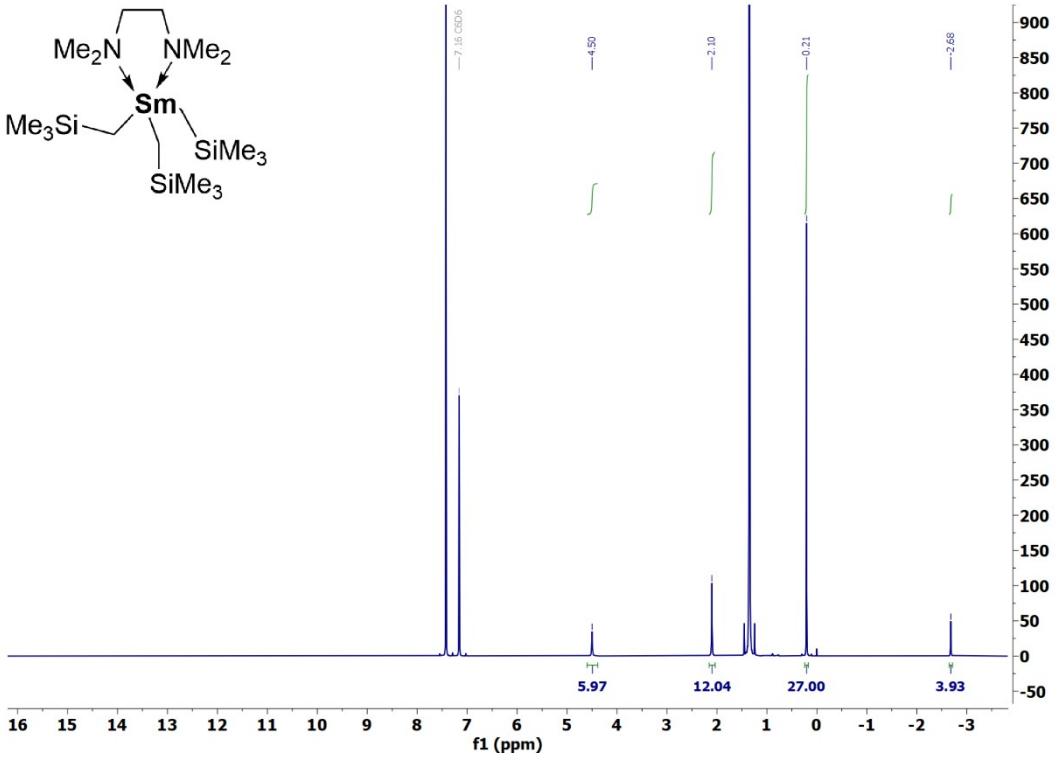

Figure S 23 ^1H NMR spectrum (600 MHz) of **Sc-TMEDA** in d_6-benzene.

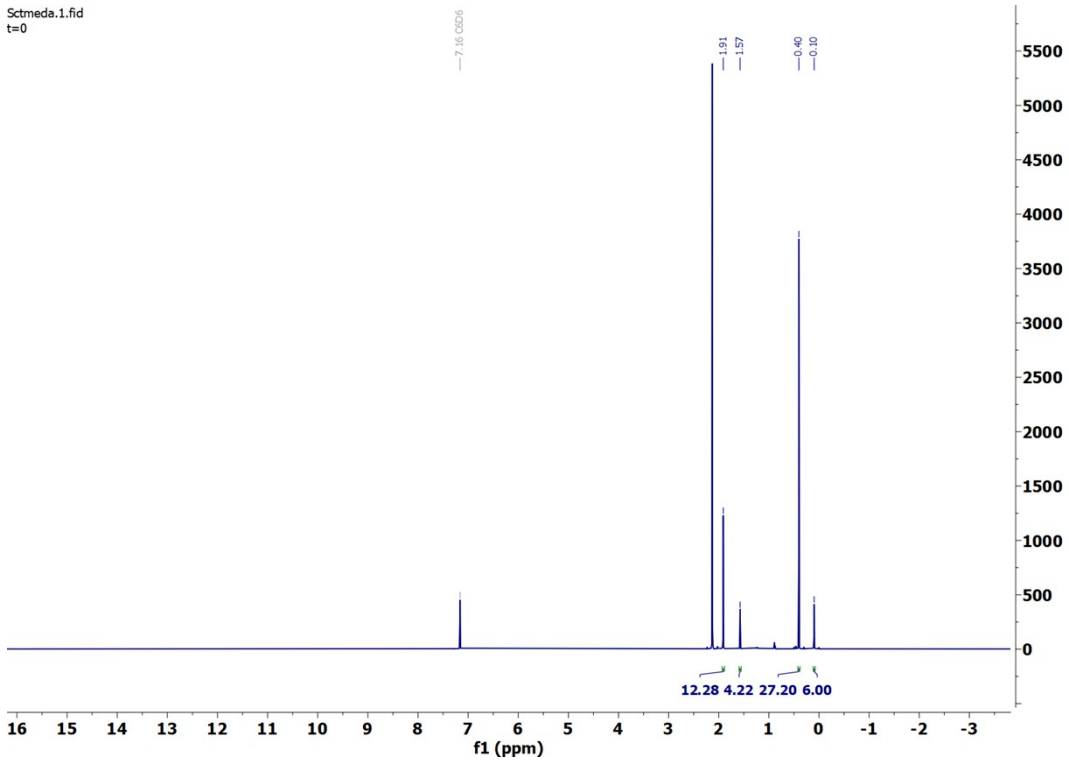

Figure S 24 $^{13}C\{^1H\}$ NMR spectrum (151 MHz) of **Sc-TMEDA** in d_6-benzene

2.13. Lu(CH$_2$SiMe$_3$)$_3$(C$_6$H$_{16}$P$_2$)(C$_4$H$_8$O) (**Lu-DMPE**)

^{1}H NMR (600 MHz, C_6D_6) δ 3.91 (s, 4H), 1.36 – 1.28 (m, 4H), 1.12 (t, *J* = 7.0 Hz, 4H), 0.78 (s, 12H), 0.36 (s, 27H), -0.63 (s, 6H). ^{13}C NMR (151 MHz, C_6D_6) δ 25.13, 12.30, 4.77. ^{31}P NMR (243 MHz, C_6D_6) δ -38.88.

Anal. Calcd for $LuC_{22}H_{57}Si_3P_2O$: C,40.1; H, 8.72. Found: C, 39.89; H, 8.62.

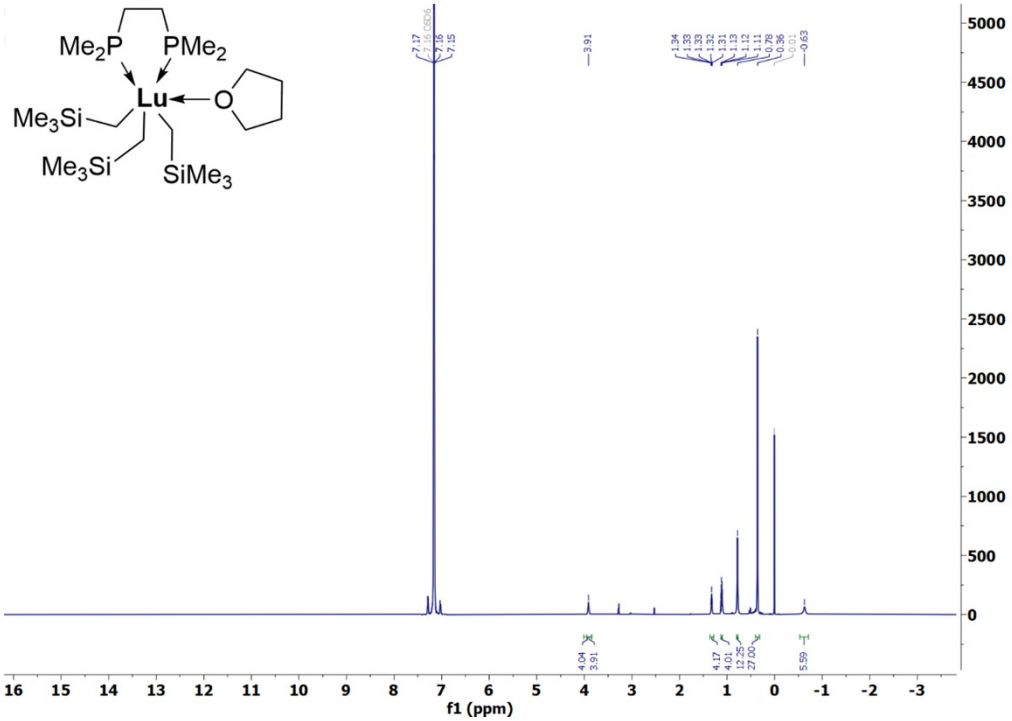

Figure S 25 ^{1}H NMR spectrum (600 MHz) of **Lu-DMPE** in d_6-benzene.

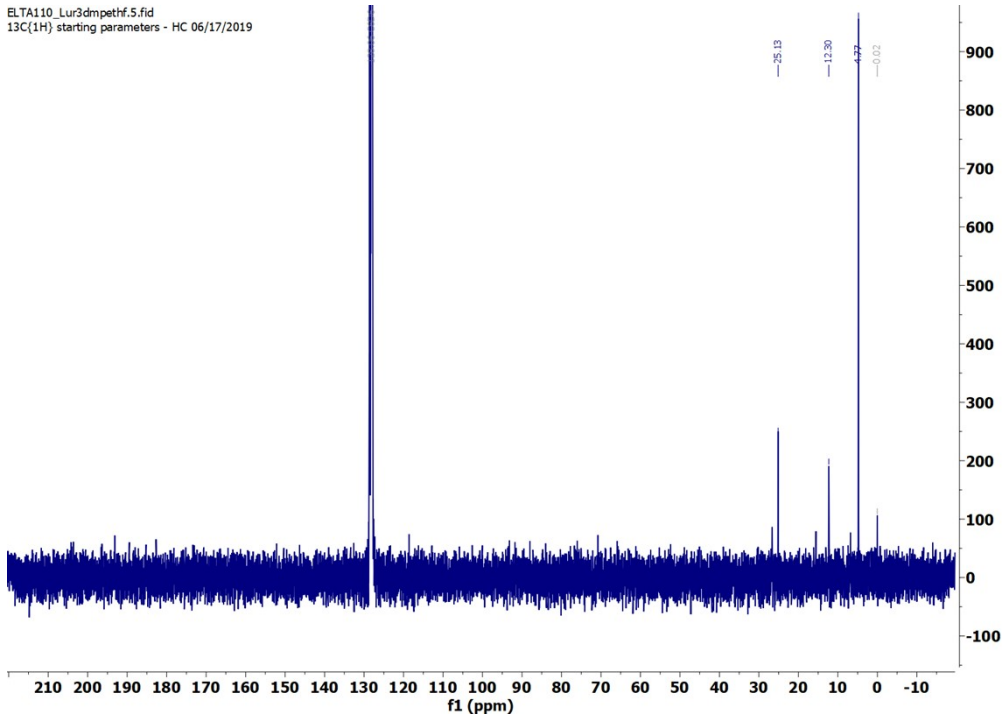

Figure S 26 ^{13}C{^{1}H} NMR spectrum (151 MHz) of **Lu-DMPE** in d_6-benzene

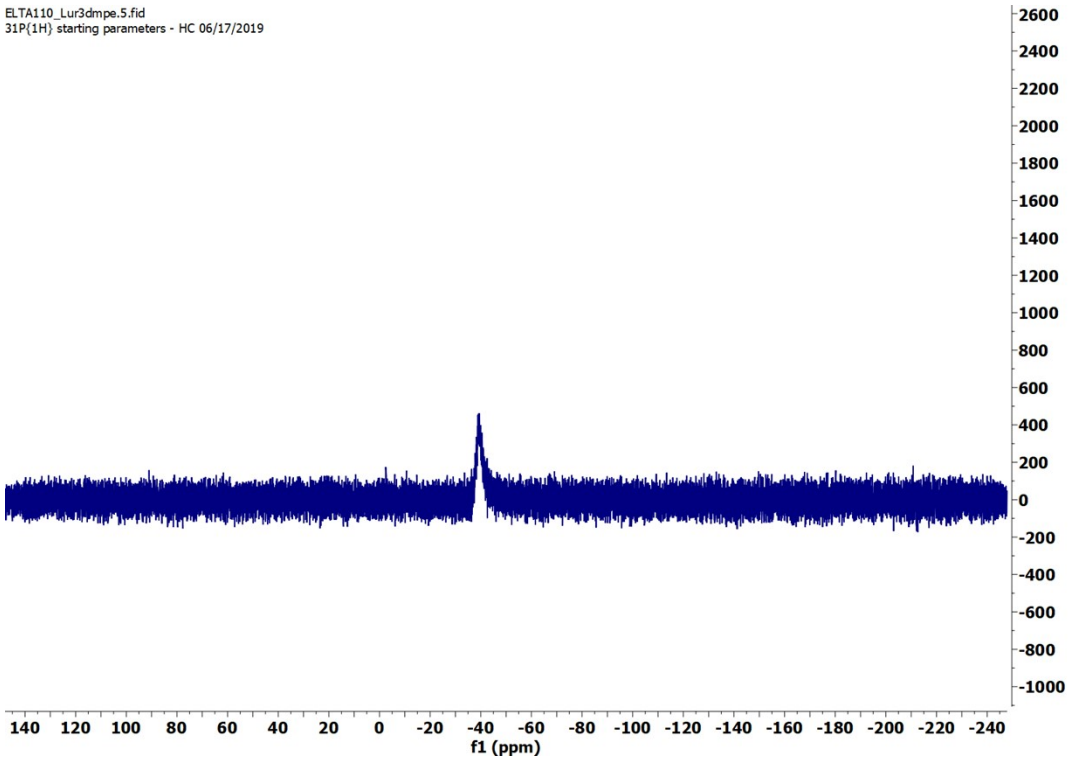

Figure S 27 ^{31}P NMR spectrum (243 MHz, C_6D_6) of **Lu-DMPE** in d_6-benzene.

2.14. $Sc(CH_2SiMe_3)_3(C_6H_{16}P_2)$ (**Sc-DMPE**)

^{1}H NMR (600 MHz, C_6D_6) δ 0.92 (s, 4H), 0.76 (t, J = 1.6 Hz, 12H), 0.40 (s, 27H), 0.26 (s, 6H). ^{13}C NMR (151 MHz, C_6D_6) δ 28.15, 14.04, 14.01, 13.97, 13.94. ^{31}P NMR (243 MHz, C_6D_6) δ -36.30.

Anal. Calcd for $ScC_{18}H_{49}Si_3P_2$: C,47.33; H, 10.81. Found: C, 46.95; H, 10.56.

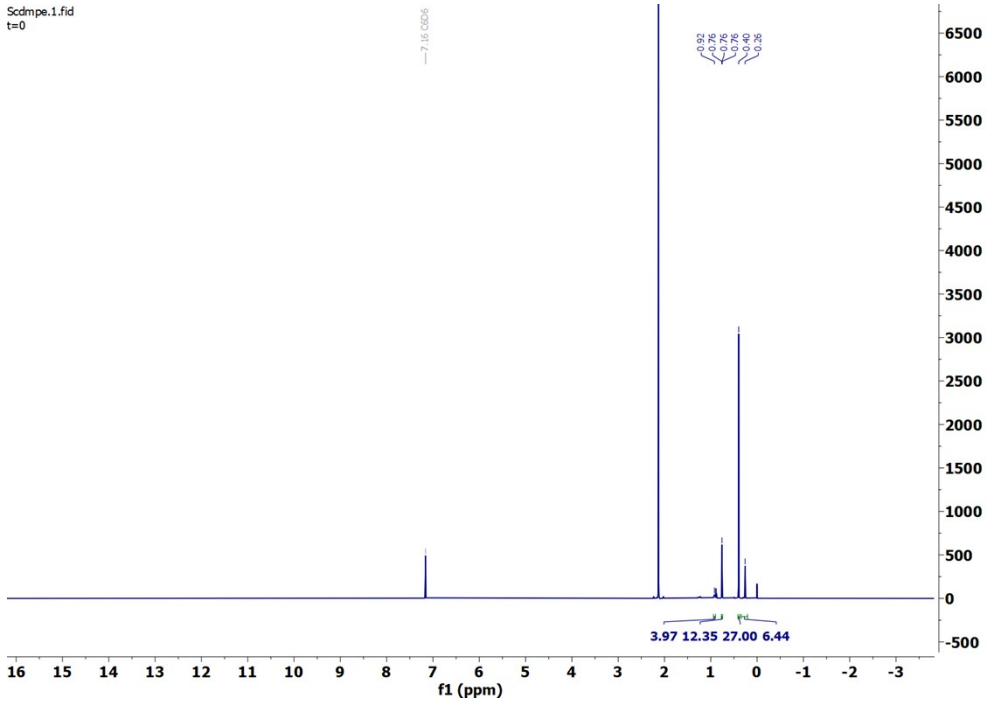

Figure S 28 ^{1}H NMR spectrum (600 MHz) of **Sc-DMPE** in d_6-benzene.

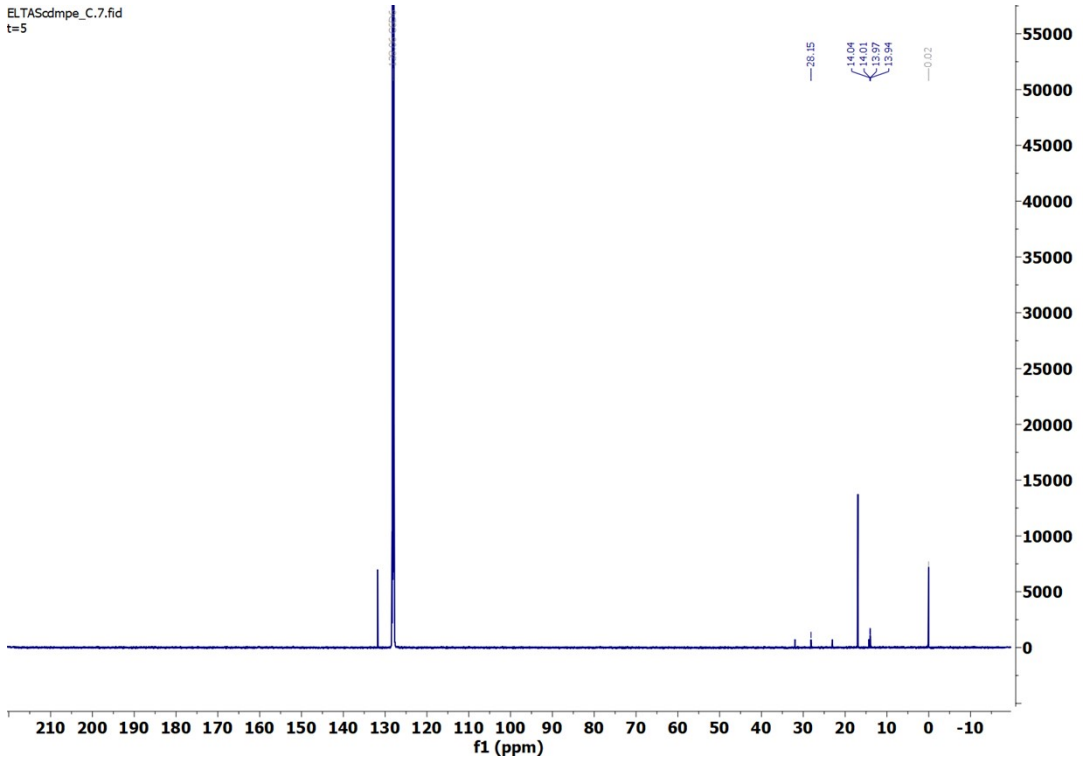

Figure S 29 $^{13}C\{^{1}H\}$ NMR spectrum (151 MHz) of **Sc-DMPE** in d_6-benzene.

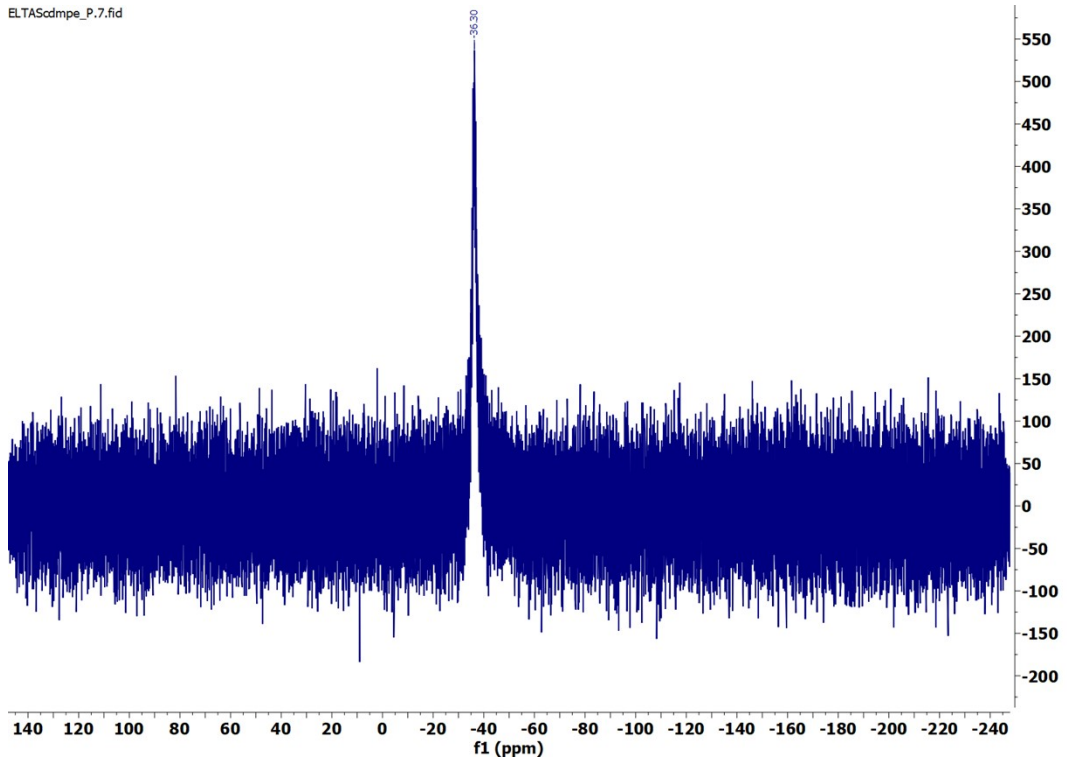

Figure S 30 ^{31}P NMR spectrum (243 MHz, C_6D_6) of **Sc-DMPE** in d_6-benzene.

2.15. Synthesis of LiCl-free $Y(CH_2SiMe_3)_3(C_4H_8O)_2$ (**Y-THF**)

In an Ar-filled glovebox, anhydrous YCl_3 (26 mg, 0.133 mmol) was suspended in 260 μL THF and 2.6 mL Et_2O/pentane (1/1). The resulting white suspension was cooled to -78°C and $NaCH_2SiMe_3$ (44 mg, 0.4 mmol, 3 eq.) was added portionwise as a solid. After stirring the resulting white suspension for 1 h at -78°C, it was warmed to room temperature for 15 min. Filtration and removal of the solvent at -40°C yielded the title compound as a white crystalline solid. Yield: 28 mg, 44% based on YCl_3.

^{1}H NMR (600 MHz, C_6D_6) δ 3.88 (s, 8H), 1.34 – 1.32 (m, 8H), 0.30 (s, 27H), -0.68 (d, *J* = 2.7 Hz, 6H).
^{13}C NMR (151 MHz, C_6D_6) δ 65.90, 25.15, 15.55, 4.63.

Anal. Calcd for $YC_{20}H_{49}Si_3O_2$: C, 48.55; H, 9.98. Found: C, 48.43; H, 9.81.

3. Single-Crystal X-ray Diffraction Data (SXRD)

CCDC submission summary for codes 2351142-2351150, 2369795

Summary of Data - Deposition Number 2351142

Compound Name:
Data Block Name: data_pla23171_auto
Unit Cell Parameters: a 9.9283(3) b 32.1189(7) c 10.3633(3) P21/n
---

Summary of Data - Deposition Number 2351143

Compound Name:
Data Block Name: data_lug3_abair_arnold
Unit Cell Parameters: a 10.6318(3) b 9.5844(3) c 29.2885(7) P21/c
---

Summary of Data - Deposition Number 2351144

Compound Name:
Data Block Name: data_pla25059_refinalized
Unit Cell Parameters: a 10.26960(10) b 15.03040(10) c 17.60830(10) P212121

Summary of Data - Deposition Number 2351145

Compound Name:
Data Block Name: data_pla24006_refinalized
Unit Cell Parameters: a 9.48680(10) b 15.77720(10) c 18.69720(10) P21/n
---

Summary of Data - Deposition Number 2351146

Compound Name:
Data Block Name: data_pla24028_refinalized
Unit Cell Parameters: a 19.06420(10) b 15.98610(10) c 19.10330(10) P21/n
---

Summary of Data - Deposition Number 2351147

Compound Name:
Data Block Name: data_pla23043_refinalized
Unit Cell Parameters: a 11.1358(2) b 18.3119(3) c 13.4974(2) P21/n
---

Summary of Data - Deposition Number 2351148

Compound Name:
Data Block Name: data_pla23105_refinalized
Unit Cell Parameters: a 10.49690(10) b 18.04320(10) c 18.05330(10) P212121

Summary of Data - Deposition Number 2351149

Compound Name:
Data Block Name: data_pla24060_refinalized
Unit Cell Parameters: a 16.9327(2) b 9.51690(10) c 18.2023(2) Pna21

Summary of Data - Deposition Number 2351150

Compound Name:
Data Block Name: data_pla23157_auto
Unit Cell Parameters: a 9.76140(10) b 16.1956(2) c 17.1923(2) P212121

Summary of Data - Deposition Number 2369795

Compound Name:
Data Block Name: data_pla24134_refinalized
Unit Cell Parameters: a 9.87370(10) b 16.22530(10) c 17.35450(10) P212121

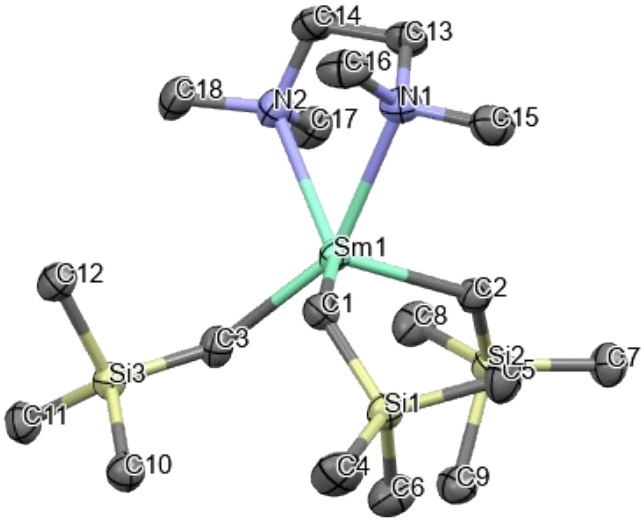

Fig. S31 Molecular structure of Sm-**TMEDA** with thermal ellipsoids at 50% probability with hydrogen atoms are omitted for the clarity. Sm: turquoise, C: grey, N: blue, Si: yellow.

Table S1. Sample and crystal data of Sm-**TMEDA**

Chemical formula	**$SmC_{18}H_{49}Si_3N_2$**	**Crystal system**	**orthorhombic**	
Formula weight [g/mol]	528.21	**Space group**	$P2_12_12_1$	
Temperature [K]	99.9(4)	**Z**	1	
Measurement method	ϕ and ω scans	**Volume [Å^3]**	2780.26(4)	
Radiation (Wavelength [Å])	Cu Kα (λ = 1.54184)	**Unit cell dimensions [Å] and [°]**	9.87370(10)	90
Crystal size / [mm^3]	0.216 × 0.159 × 0.074		16.22530(10)	90
Crystal habit	clear yellow block		17.35450(10)	90
Density (calculated) / [g/cm^3]	1.262	**Absorption coefficient / [mm^{-1}]**	17.107	
Abs. correction Tmin	0.119	**Abs. correction Tmax**	0.364	
Abs. correction type	multi-scan	**F(000) [e$^-$]**	1100.0	
Index ranges	-12 ≤ h ≤ 12, -20 ≤ k ≤ 20, -22 ≤ l ≤ 20	**Theta range for data collection [°]**	7.458 to 159.862	
Reflections number	58576	**Data / restraints / parameters**	6043/0/230	
Refinement method	Least squares	**Final R indices**	all data	R_1 = 0.0313, wR_2 = 0.0856
Function minimized	$\Sigma\, w(F_o^2 - F_c^2)^2$		I>2σ(I)	R_1 = 0.0311, wR_2 = 0.0855
Goodness-of-fit on F^2	1.111	**Weighting scheme**	$w=1/[\sigma^2(F_o^2)+(0.0552P)^2+2.6302P]$	
Largest diff. peak and hole [e Å^{-3}]	1.32/-1.14		where $P=(F_o^2+2F_c^2)/3$	

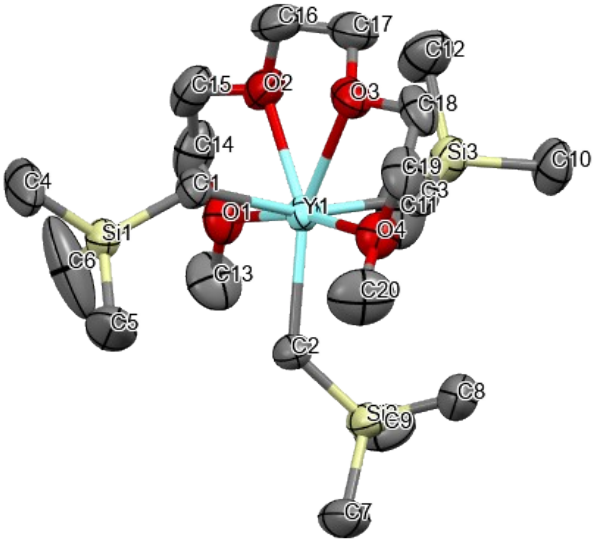

Fig. S32 Molecular structure of Y-**G_3** with thermal ellipsoids at 50% probability with hydrogen atoms are omitted for the clarity. Y: turquoise, C: grey, O: red, Si: yellow.

Table S2. Sample and crystal data of **Y-G_3**

Chemical formula	$Y(CH_2SiMe_3)_3(C_8H_{18}O_4)$	**Crystal system**	**monoclinic**	
Formula weight [g/mol]	528.78	**Space group**	$P2_1/n$	
Temperature [K]	199.99(10)	**Z**	1	
Measurement method	ϕ and ω scans	**Volume [Å^3]**	3052.23(17)	
Radiation (Wavelength [Å])	Cu Kα (λ = 1.54184)	**Unit cell dimensions [Å] and [°]**	9.9283(3)	90
Crystal size / [mm^3]	0.16 × 0.11 × 0.1		32.1189(7)	112.542(4)
Crystal habit	clear colorless block		10.3633(3)	90
Density (calculated) / [g/cm^3]	1.151	**Absorption coefficient / [mm^{-1}]**	3.965	
Abs. correction Tmin	0.569	**Abs. correction Tmax**	0.693	
Abs. correction type	multi-scan	**F(000) [e$^-$]**	1136.0	
Index ranges	$-12 \le h \le 12$, $-21 \le k \le 40$, $-13 \le l \le 13$	**Theta range for data collection [°]**	5.502 to 160.098	
Reflections number	18955	**Data / restraints / parameters**	6475/0/272	
Refinement method	Least squares	**Final R indices**	all data	R_1 = 0.0563, wR_2 = 0.1499
Function minimized	$\Sigma\, w(F_o^2 - F_c^2)^2$		I>2σ(I)	R_1 = 0.0490, wR_2 = 0.1440
Goodness-of-fit on F²	1.070	**Weighting scheme**	$w=1/[\sigma^2(F_o^2)+(0.0873P)^2+0.9693P]$	
Largest diff. peak and hole [e Å^{-3}]	0.63/-0.72		where $P=(F_o^2+2F_c^2)/3$	

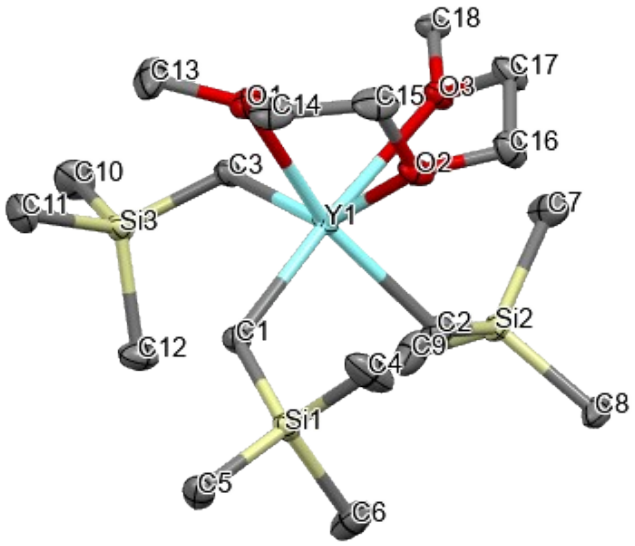

Fig. S33 Molecular structure of Y-$\mathbf{G_2}$ with thermal ellipsoids at 50% probability with hydrogen atoms are omitted for the clarity. Y: turquoise, C: grey, O: red, Si: yellow.

Table S3. Sample and crystal data of **Y-G_2**

Chemical formula	$Y(CH_2SiMe_3)_3(C_6H_{14}O_3)$	**Crystal system**	**monoclinic**	
Formula weight [g/mol]	484.73	**Space group**	$P2_1/n$	
Temperature [K]	99.99(11)	**Z**	1	
Measurement method	ϕ and ω scans	**Volume [Å^3]**	2750.13(8)	
Radiation (Wavelength [Å])	Mo Kα (λ = 0.71073)	**Unit cell dimensions [Å] and [°]**	11.1358(2)	90
Crystal size / [mm^3]	0.428 × 0.112 × 0.109		18.3119(3)	92.304(2)
Crystal habit	clear colorless block		13.4974(2)	90
Density (calculated) / [g/cm^3]	1.171	**Absorption coefficient / [mm^{-1}]**	2.264	
Abs. correction Tmin	0.444	**Abs. correction Tmax**	0.790	
Abs. correction type	multi-scan	**F(000) [e$^-$]**	1040.0	
Index ranges	$-15 \le h \le 16$, $-26 \le k \le 26$, $-20 \le l \le 19$	**Theta range for data collection [°]**	3.75 to 64.742	
Reflections number	74421	**Data / restraints / parameters**	8757/0/237	
Refinement method	Least squares	**Final R indices**	all data	R_1 = 0.0389, wR_2 = 0.0547
Function minimized	$\Sigma\, w(F_o^2 - F_c^2)^2$		I>2σ(I)	R_1 = 0.0302, wR_2 = 0.0531
Goodness-of-fit on F^2	1.099	**Weighting scheme**	$w=1/[\sigma^2(F_o^2)+(0.0199P)^2+0.9981P]$	
Largest diff. peak and hole [e Å^{-3}]	0.46/-0.29		where $P=(F_o^2+2F_c^2)/3$	

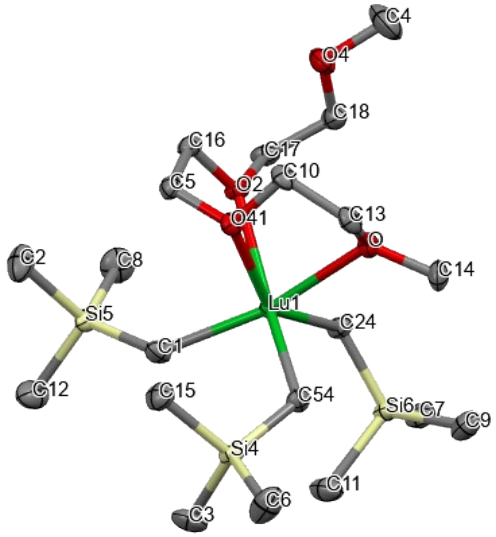

Fig. S34 Molecular structure of Lu-$\mathbf{G_3}$ with thermal ellipsoids at 50% probability with hydrogen atoms are omitted for the clarity. Lu: green, C: grey, O: red, Si: yellow.

Table S4. Sample and crystal data of **Lu-$\mathbf{G_3}$**

Chemical formula	$Lu(CH_2SiMe_3)_3(C_8H_{18}O_4)$	**Crystal system**	**monoclinic**	
Formula weight [g/mol]	614.84	**Space group**	$P2_1/c$	
Temperature [K]	293(2)	**Z**	1	
Measurement method	ϕ and ω scans	**Volume [Å^3]**	2984.40(14)	
Radiation (Wavelength [Å])	MoKα (λ = 0.71073)	**Unit cell dimensions [Å] and [°]**	10.6318(3)	90
Crystal size / [mm^3]	0.32 × 0.25 × 0.21		9.5844(3)	90.415(2)
Crystal habit	clear colorless block		29.2885(7)	90
Density (calculated) / [g/cm^3]	1.368	**Absorption coefficient / [mm^{-1}]**	3.448	
Abs. correction Tmin	0.405	**Abs. correction Tmax**	0.531	
Abs. correction type	multi-scan	**F(000) [e$^-$]**	1264.0	
Index ranges	$-13 \le h \le 13$, $-11 \le k \le 11$, $-36 \le l \le 36$	**Theta range for data collection [°]**	5.882 to 52.74	
Reflections number	44266	**Data / restraints / parameters**	6086/0/265	
Refinement method	Least squares	**Final R indices**	all data	R_1 = 0.0253, wR_2 = 0.0566
Function minimized	$\Sigma\, w(F_o^2 - F_c^2)^2$		I>2σ(I)	R_1 = 0.0240, wR_2 = 0.0558
Goodness-of-fit on F^2	1.090	**Weighting scheme**	$w=1/[\sigma^2(F_o^2)+(0.0161P)^2+9.2682P]$	
Largest diff. peak and hole [e Å^{-3}]	1.87/-1.17		where $P=(F_o^2+2F_c^2)/3$	

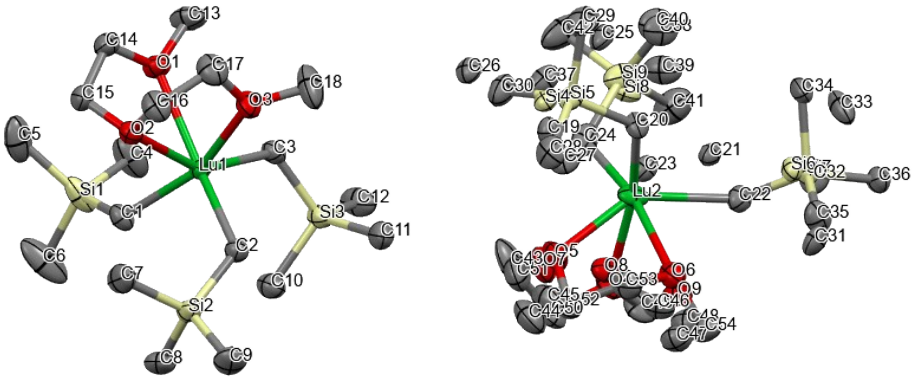

Fig. S35 Molecular structure of Lu-$\mathbf{G_2}$ with thermal ellipsoids at 50% probability with hydrogen atoms are omitted for the clarity. Lu: green, C: grey, O: red, Si: yellow. Bonds at the suppressed positions (45.4% occupancy) in the disordered molecule are omitted for clarity.

Table S5. Sample and crystal data of **Lu-$\mathbf{G_2}$**

Chemical formula	$Lu(CH_2SiMe_3)_3(C_6H_{14}O_3)$	**Crystal system**	**monoclinic**	
Formula weight [g/mol]	4562.31	**Space group**	$P2_1/n$	
Temperature [K]	100.00(10)	**Z**	2	
Measurement method	ϕ and ω scans	**Volume [Å^3]**	5562.61(6)	
Radiation (Wavelength [Å])	Cu Kα (λ = 1.54184)	**Unit cell dimensions [Å] and [°]**	19.06420(10)	90
Crystal size / [mm^3]	0.246 × 0.179 × 0.127		15.98610(10)	107.1660(10)
Crystal habit	clear colorless block		19.10330(10)	90
Density (calculated) / [g/cm^3]	1.362	**Absorption coefficient / [mm^{-1}]**	8.121	
Abs. correction Tmin	0.240	**Abs. correction Tmax**	0.425	
Abs. correction type	multi-scan	**F(000) [e$^-$]**	2332.0	
Index ranges	$-24 \le h \le 24$, $-20 \le k \le 14$, $-24 \le l \le 24$	**Theta range for data collection [°]**	5.754 to 160.398	
Reflections number	123523	**Data / restraints / parameters**	12072/0/665	
Refinement method	Least squares	**Final R indices**	all data	R_1 = 0.0386, wR_2 = 0.0971
Function minimized	$\Sigma\, w(F_o^2 - F_c^2)^2$		I>2σ(I)	R_1 = 0.0363, wR_2 = 0.0950
Goodness-of-fit on F^2	1.079	**Weighting scheme**	$w=1/[\sigma^2(F_o^2)+(0.0458P)^2+12.7298P]$	
Largest diff. peak and hole [e Å^{-3}]	1.77/-2.15		where $P=(F_o^2+2F_c^2)/3$	

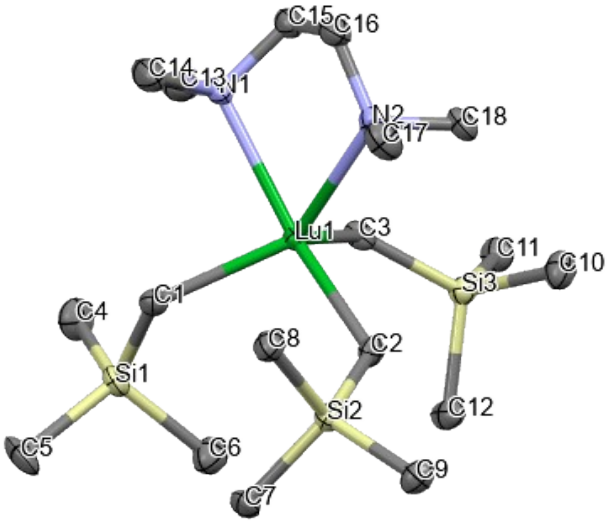

Fig. S36 Molecular structure of Lu-**TMEDA** with thermal ellipsoids at 50% probability with hydrogen atoms are omitted for the clarity. Lu: green, C: grey, N: blue, Si: yellow.

Table S6. Sample and crystal data of **Lu-TMEDA**

Chemical formula	$LuC_{18}H_{49}Si_3N_2$	**Crystal system**	**orthorhombic**	
Formula weight [g/mol]	552.83	**Space group**	$P2_12_12_1$	
Temperature [K]	99.97(11)	**Z**	1	
Measurement method	ϕ and ω scans	**Volume [Å^3]**	2717.96(5)	
Radiation (Wavelength [Å])	Cu Kα (λ = 1.54184)	**Unit cell dimensions [Å] and [°]**	9.76140(10)	90
Crystal size / [mm^3]	0.12 × 0.06 × 0.05		16.1956(2)	90
Crystal habit	clear colorless block		17.1923(2)	90
Density (calculated) / [g/cm^3]	1.351	**Absorption coefficient / [mm^{-1}]**	8.228	
Abs. correction Tmin	0.438	**Abs. correction Tmax**	0.684	
Abs. correction type	multi-scan	**F(000) [e$^-$]**	1136.0	
Index ranges	$-12 \le h \le 12$, $-20 \le k \le 18$, $-21 \le l \le 21$	**Theta range for data collection [°]**	7.5 to 159.812	
Reflections number	59230	**Data / restraints / parameters**	5898/0/246	
Refinement method	Least squares	**Final R indices**	all data	R_1 = 0.0397, wR_2 = 0.0909
Function minimized	$\Sigma\, w(F_o^2 - F_c^2)^2$		I>2σ(I)	R_1 = 0.0389, wR_2 = 0.0907
Goodness-of-fit on F^2	1.049	**Weighting scheme**	$w=1/[\sigma^2(F_o^2)+(0.0264)^2+18.3519P]$	
Largest diff. peak and hole [e Å^{-3}]	1.22/-1.30		where $P=(F_o^2+2F_c^2)/3$	

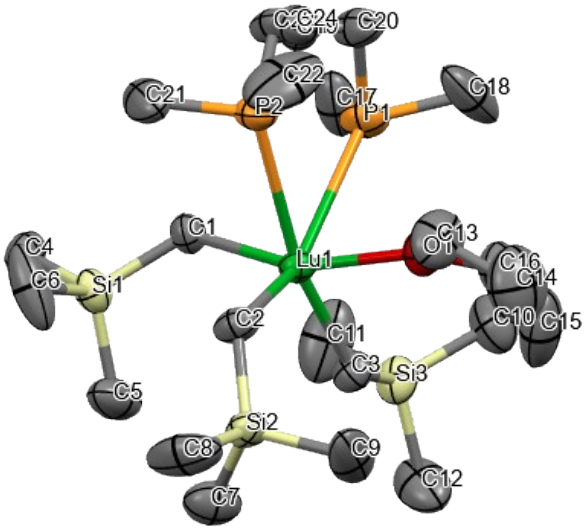

Fig. S37 Molecular structure of Lu-**DMPE** with thermal ellipsoids at 50% probability with hydrogen atoms are omitted for the clarity. Lu: green, C: grey, P: orange, Si: yellow, O: red.

Table S7. Sample and crystal data of **Lu-DMPE**

Chemical formula	$LuC_{22}H_{57}Si_3P_2O$	**Crystal system**	**orthorhombic**	
Formula weight [g/mol]	658.85	**Space group**	$P2_12_12_1$	
Temperature [K]	99.98(13)	**Z**	1	
Measurement method	ϕ and ω scans	**Volume [Å³]**	3419.25(4)	
Radiation (Wavelength [Å])	Cu Kα (λ = 1.54184)	**Unit cell dimensions [Å] and [°]**	10.49690(10)	90
Crystal size / [mm³]	0.23 × 0.1 × 0.08		18.04320(10)	90
Crystal habit	clear colorless block		18.05330(10)	90
Density (calculated) / [g/cm³]	1.268	**Absorption coefficient / [mm⁻¹]**	7.485	
Abs. correction Tmin	0.278	**Abs. correction Tmax**	0.586	
Abs. correction type	multi-scan	**F(000) [e⁻]**	1336.0	
Index ranges	$-13 \le h \le 13$, $-22 \le k \le 23$, $-23 \le l \le 22$	**Theta range for data collection [°]**	6.926 to 161.3	
Reflections number	229465	**Data / restraints / parameters**	7472/6/293	
Refinement method	Least squares	**Final R indices**	all data	R_1 = 0.0314, wR_2 = 0.0861
Function minimized	$\Sigma\, w(F_o^2 - F_c^2)^2$		I>2σ(I)	R_1 = 0.0308, wR_2 = 0.0855
Goodness-of-fit on F²	1.054	**Weighting scheme**	$w=1/[\sigma^2(F_o^2)+(0.0516P)^2+2.9340P]$	
Largest diff. peak and hole [e Å⁻³]	1.17/-0.64		where $P=(F_o^2+2F_c^2)/3$	

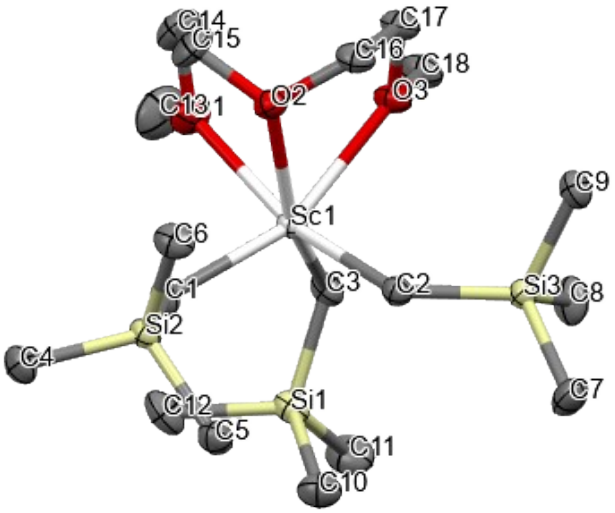

Fig. S38 Molecular structure of Sc-$\mathbf{G_2}$ with thermal ellipsoids at 50% probability with hydrogen atoms are omitted for the clarity. Sc: grey, C: grey, Si: yellow, O: red.

Table S8. Sample and crystal data of **Sc-G_2**

Chemical formula	$ScC_{18}H_{47}Si_3O_3$	**Crystal system**	**monoclinic**	
Formula weight [g/mol]	440.78	**Space group**	$P2_1/n$	
Temperature [K]	99.98(10)	**Z**	1	
Measurement method	ϕ and ω scans	**Volume [Å^3]**	2737.80(4)	
Radiation (Wavelength [Å])	Cu Kα (λ = 1.54184)	**Unit cell dimensions [Å] and [°]**	9.48680(10)	90
Crystal size / [mm^3]	0.2 × 0.15 × 0.09		15.77720(10)	101.9560(10)
Crystal habit	clear colorless block		18.69720(10)	90
Density (calculated) / [g/cm^3]	1.069	**Absorption coefficient / [mm^{-1}]**	3.648	
Abs. correction Tmin	0.529	**Abs. correction Tmax**	0. 735	
Abs. correction type	multi-scan	**F(000) [e$^-$]**	968.0	
Index ranges	$-10 \le h \le 12$, $-20 \le k \le 20$, $-23 \le l \le 23$	**Theta range for data collection [°]**	7.4 to 160.086	
Reflections number	61454	**Data / restraints / parameters**	5972/0/253	
Refinement method	Least squares	**Final R indices**	all data	R1 = 0.0315, wR2 = 0.0851
Function minimized	$\Sigma\, w(F_o^2 - F_c^2)^2$		I>2σ(I)	R1 = 0.0303, wR2 = 0.0841
Goodness-of-fit on F^2	1.110	**Weighting scheme**	$w=1/[\sigma^2(F_o^2)+(0.0495P)^2+0.6268P]$	
Largest diff. peak and hole [e Å^{-3}]	0.66/-0.31		where $P=(F_o^2+2F_c^2)/3$	

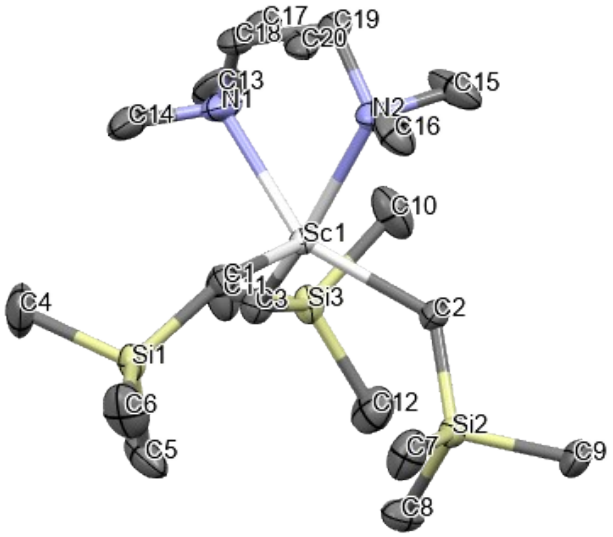

Fig. S39 Molecular structure of Sc-**TMEDA** with thermal ellipsoids at 50% probability with hydrogen atoms are omitted for the clarity. Sc: grey, C: grey, Si: yellow, N: blue.

Table S9. Sample and crystal data of **Sc-TMEDA**

Chemical formula	$ScC_{18}H_{49}Si_3N_2$	**Crystal system**	**orthorhombic**	
Formula weight [g/mol]	422.82	**Space group**	$P2_12_12_1$	
Temperature [K]	100.00(11)	**Z**	1	
Measurement method	ϕ and ω scans	**Volume [Å³]**	2717.95(4)	
Radiation (Wavelength [Å])	Cu Kα (λ = 1.54184)	**Unit cell dimensions [Å] and [°]**	10.26960(10)	90
Crystal size / [mm³]	0.252 × 0.143 × 0.098		15.03040(10)	90
Crystal habit	clear colorless block		17.60830(10)	90
Density (calculated) / [g/cm³]	1.033	**Absorption coefficient / [mm⁻¹]**	3.592	
Abs. correction Tmin	0.465	**Abs. correction Tmax**	0.720	
Abs. correction type	multi-scan	**F(000) [e⁻]**	936.0	
Index ranges	$-13 \le h \le 13$, $-11 \le k \le 18$, $-22 \le l \le 22$	**Theta range for data collection [°]**	7.734 to 160.12	
Reflections number	63925	**Data / restraints / parameters**	5902/0/272	
Refinement method	Least squares	**Final R indices**	all data	R_1 = 0.0260, wR_2 = 0.0682
Function minimized	$\Sigma\, w(F_o^2 - F_c^2)^2$		I>2σ(I)	R_1 = 0.0258, wR_2 = 0.0680
Goodness-of-fit on F²	1.070	**Weighting scheme**	$w=1/[\sigma^2(F_o^2)+(0.0380P)^2+0.6975P]$	
Largest diff. peak and hole [e Å⁻³]	0.24/-0.31		where $P=(F_o^2+2F_c^2)/3$	

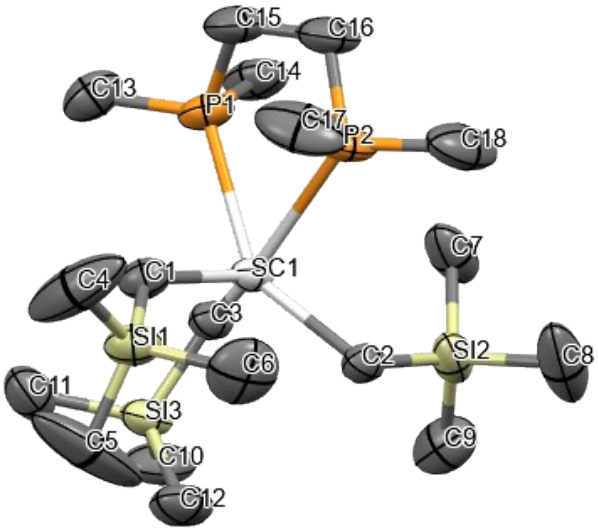

Fig. S40 Molecular structure of Sc-**DMPE** with thermal ellipsoids at 50% probability with hydrogen atoms are omitted for the clarity. Sc: grey, C: grey, Si: yellow, P: orange.

Table S10. Sample and crystal data of **Sc-DMPE**

Chemical formula	$ScC_{18}H_{49}Si_3P_2$	**Crystal system**	**orthorhombic**	
Formula weight [g/mol]	456.74	**Space group**	$Pna2_1$	
Temperature [K]	100.00(10)	**Z**	1	
Measurement method	ϕ and ω scans	**Volume [Å³]**	2933.24(6)	
Radiation (Wavelength [Å])	Cu Kα (λ = 1.54184)	**Unit cell dimensions [Å] and [°]**	16.9327(2)	90
Crystal size / [mm³]	0.257 × 0.218 × 0.129		9.51690(10)	90
Crystal habit	clear colorless block		18.2023(2)	90
Density (calculated) / [g/cm³]	1.034	**Absorption coefficient / [mm⁻¹]**	4.339	
Abs. correction Tmin	0.402	**Abs. correction Tmax**	0.604	
Abs. correction type	multi-scan	**F(000) [e⁻]**	1000.0	
Index ranges	$-21 \le h \le 21$, $-12 \le k \le 12$, $-23 \le l \le 21$	**Theta range for data collection [°]**	9.718 to 160.89	
Reflections number	62263	**Data / restraints / parameters**	5912/7/238	
Refinement method	Least squares	**Final R indices**	all data	R_1 = 0.0604, wR_2 = 0.1435
Function minimized	$\Sigma\, w(F_o^2 - F_c^2)^2$		I>2σ(I)	R_1 = 0.0598, wR_2 = 0.1431
Goodness-of-fit on F²	1.080	**Weighting scheme**	$w=1/[\sigma^2(F_o^2)+(0.0459P)^2+4.6572P]$	
Largest diff. peak and hole [e Å⁻³]	0.64/-0.36		where $P=(F_o^2+2F_c^2)/3$	

4. Thermal stability studies

4.1. General procedure for thermolysis studies

In an Ar-filled glovebox, a 9.1 mM solution of the corresponding M complex was prepared in C_6D_6 with hexamethylbenzene as an internal standard, in a YT NMR tube. The NMR sample was incubated at 30°C in an oil bath with a thermocouple. The thermolysis process was monitored by ^{1}H NMR spectroscopy for at least two half-lives.

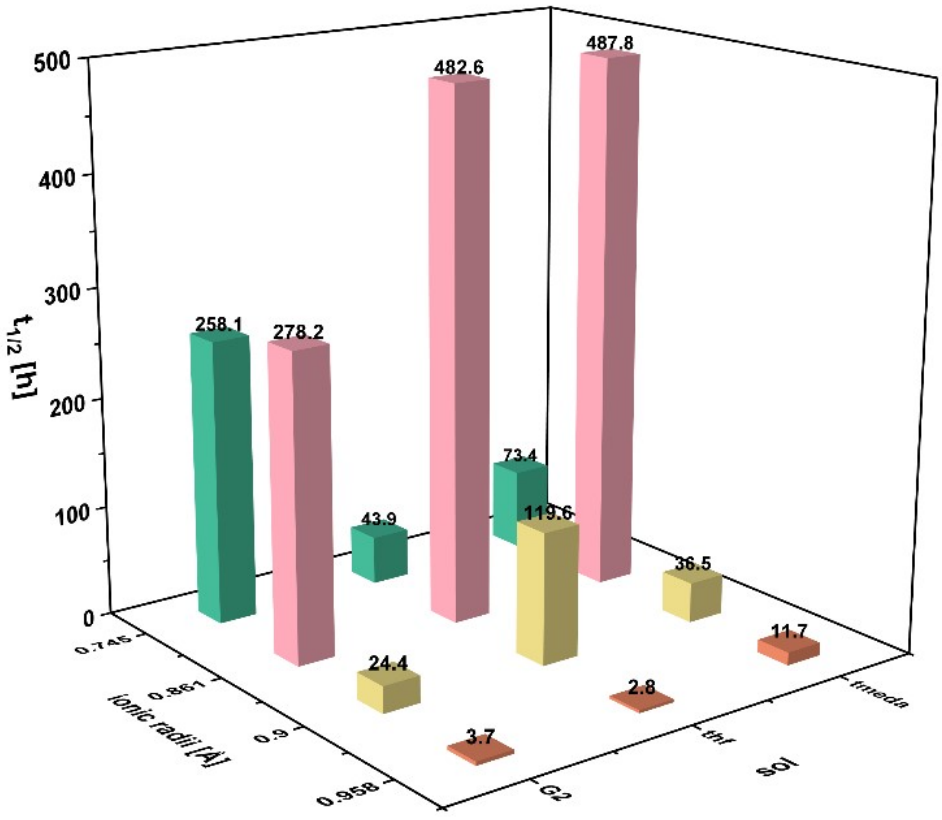

Figure S 41 Thermal stability, defined as half-life of a solution of M(r)$_3$(donor) (**M-donor**) in benzene solution, for a range of rare earth neosilyl organized in increasing metal ionic radius, Sc (green), Lu (pink), Y (yellow), Sm (rust), and coordinated donor ligand(s), donor for donor = $(THF)_2$, TMEDA, G_2 = diglyme, $(CH_3(OCH_2CH_2)_2O)$. Plots with additional data for selected metals are included in the SI.

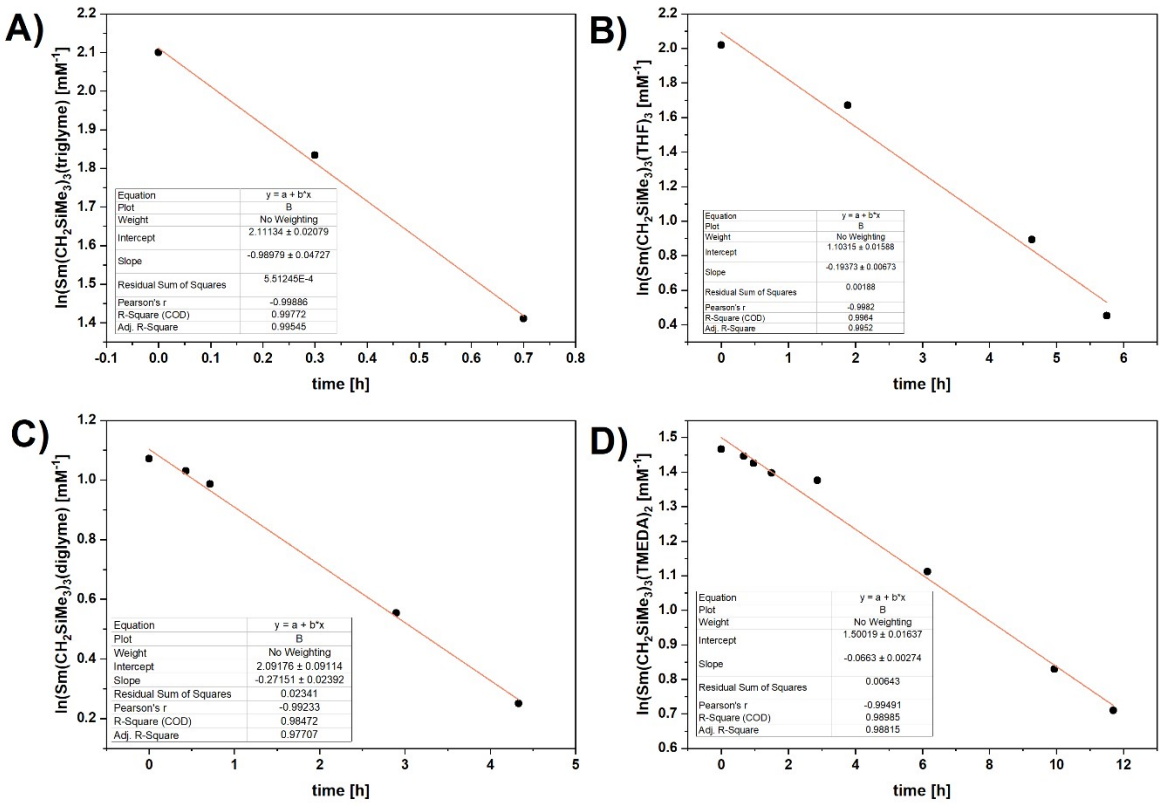

Figure S 42 Thermal stability of **A) Sm-G_3**, **B) Sm-THF**, **C) Sm-G_2**, and **D) Sm-TMEDA** expressed by the decrease of **Sm-donor** concentration as a function of time using the logarithmic **Sm-donor** concentration values obtained from the NMR integration values after incubation in C_6D_6, room temperature (30°C).

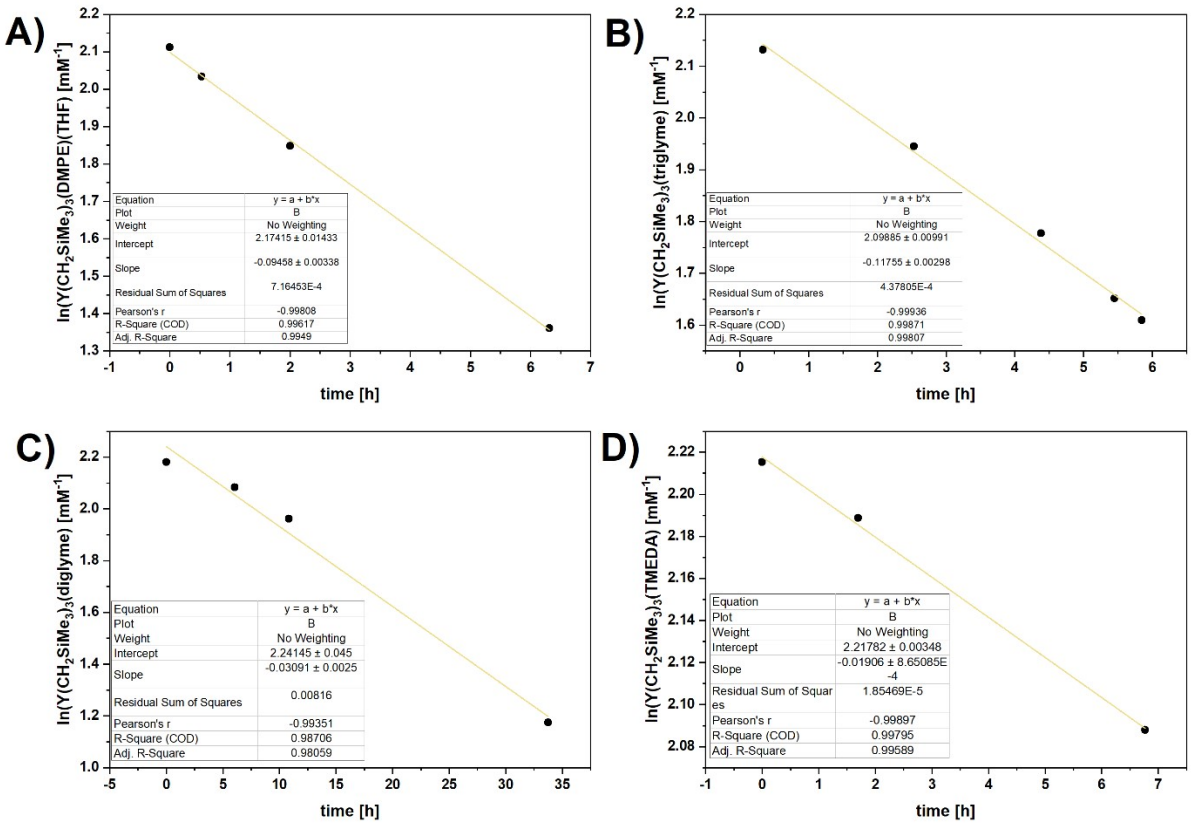

Figure S 43 Thermalstability of **A) Y-DMPE**, **B) Y-G_3**, **C) Y-G_2**, and **D) Y-TMEDA** expressed by the decrease of **Y-donor** concentration as a function of time using the logarithmic **Y-donor** concentration values obtained from the NMR integration values after incubation in C_6D_6, room temperature (30°C).

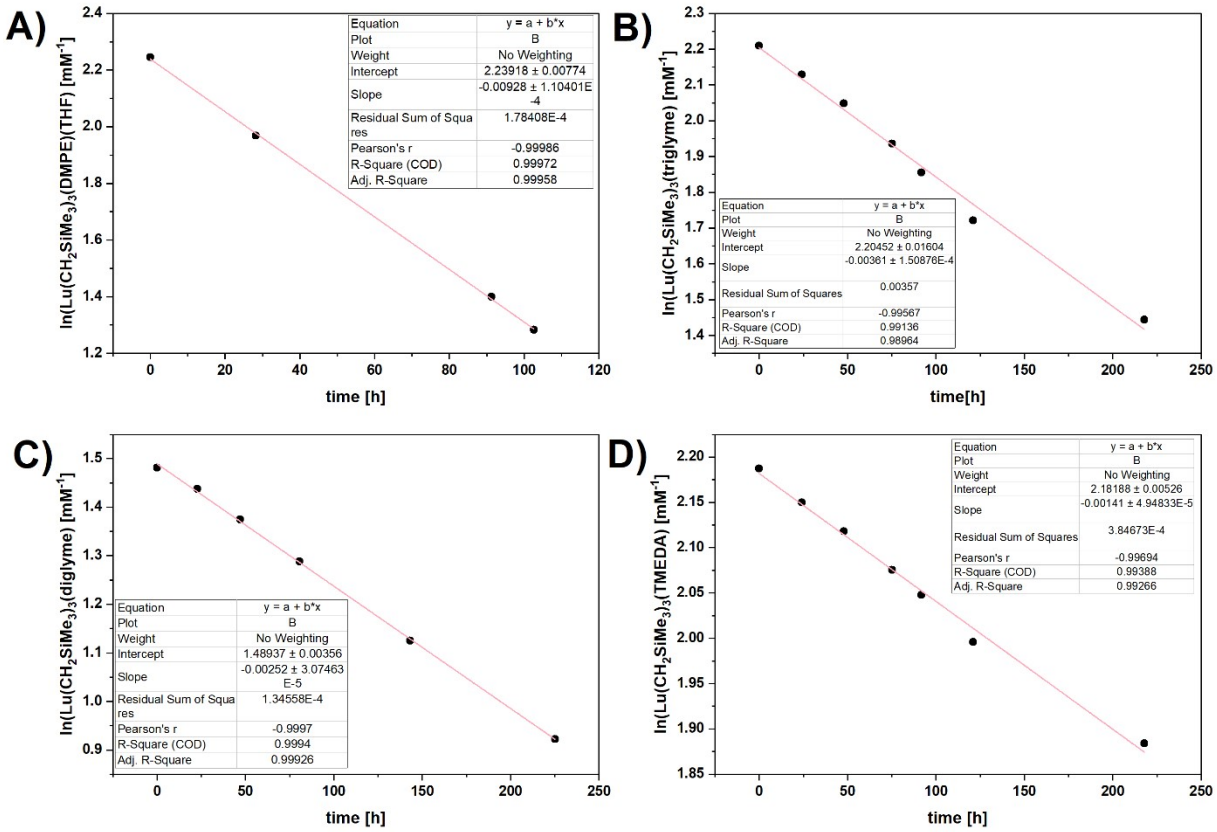

Figure S 44 Thermalstability of **A) Lu-DMPE**, **B) Lu-G_3**, **C) Lu-G_2**, and **D) Lu-TMEDA** expressed by the decrease of **Lu-donor** concentration as a function of time using the logarithmic **Lu-donor** concentration values obtained from the NMR integration values after incubation in C_6D_6, room temperature (30°C).

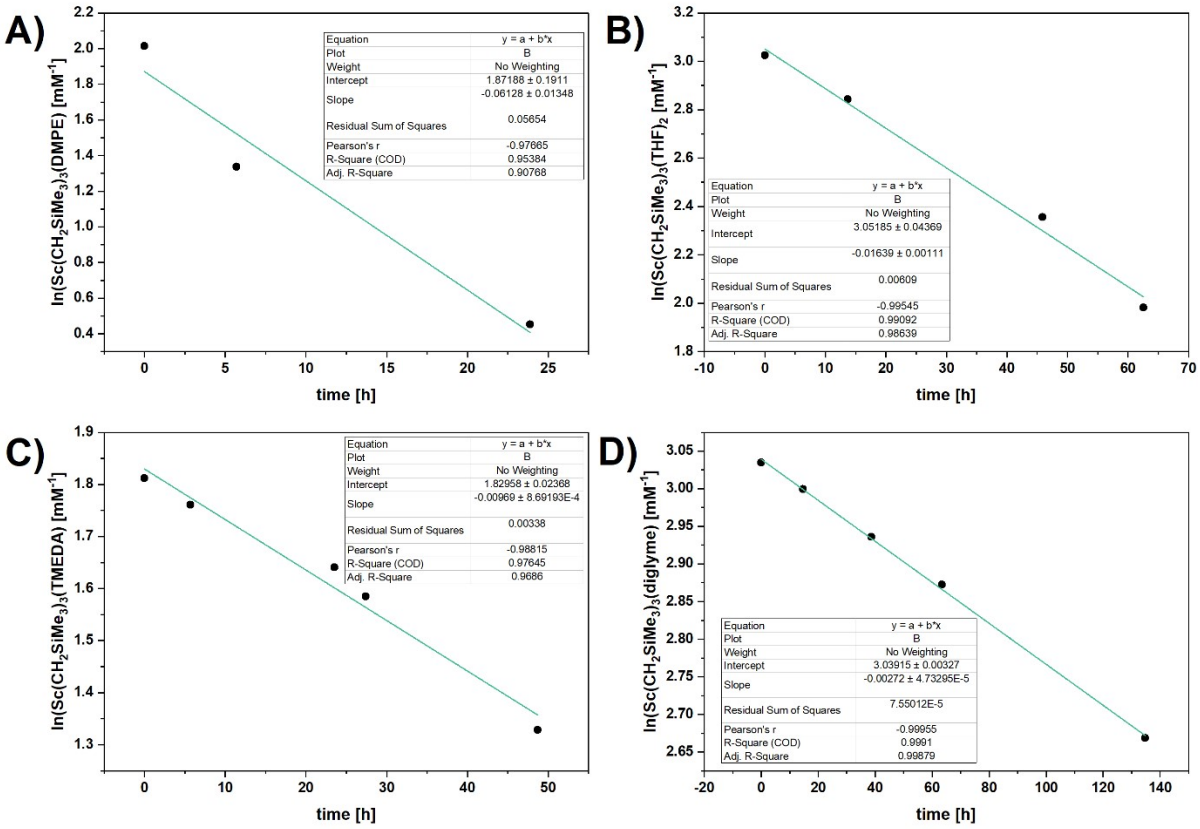

Figure S 45 Thermal stability of **A) Sc-DMPE**, **B) Sc-THF**, **C) Sc-TMEDA**, and **D) Sc-G_2** expressed by the decrease of **Sc-donor** concentration as a function of time using the logarithmic **Sc-donor** concentration values obtained from the NMR integration values after incubation in C_6D_6, room temperature (30°C).

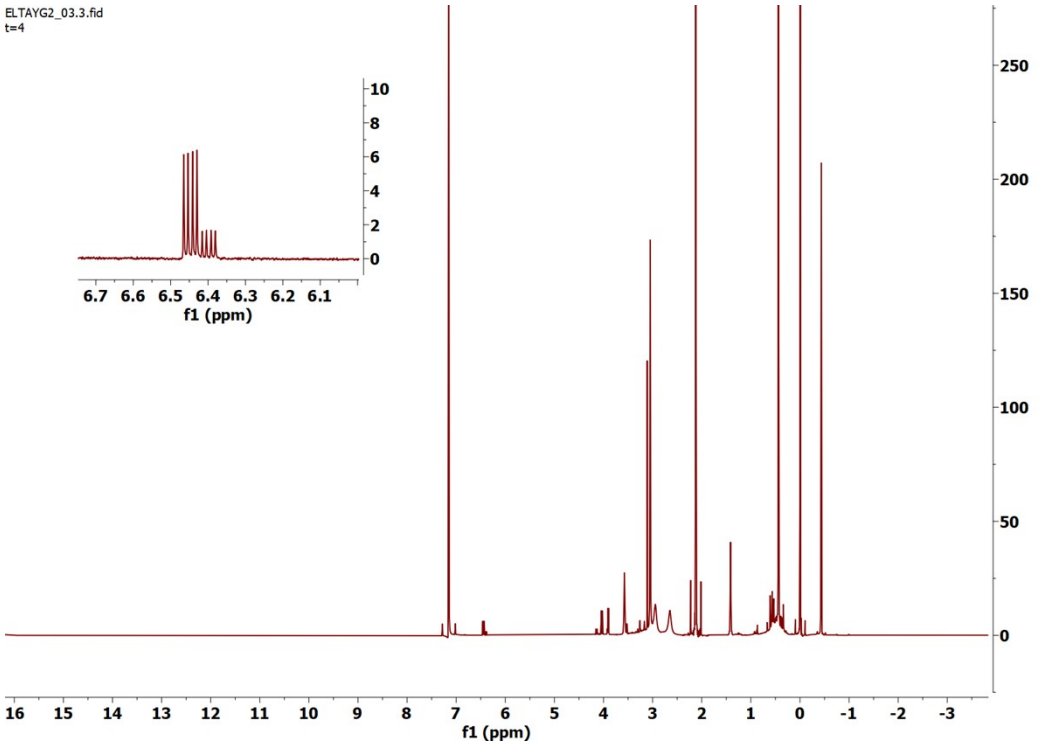

Figure S 46 ^{1}H NMR spectrum (600 MHz) of **Y-G$_2$** in d_6-benzene (t = 33 h) showing increasing resonances that can be assigned to CH_2=CHOMe vinyl methyl ether, VME (inset).

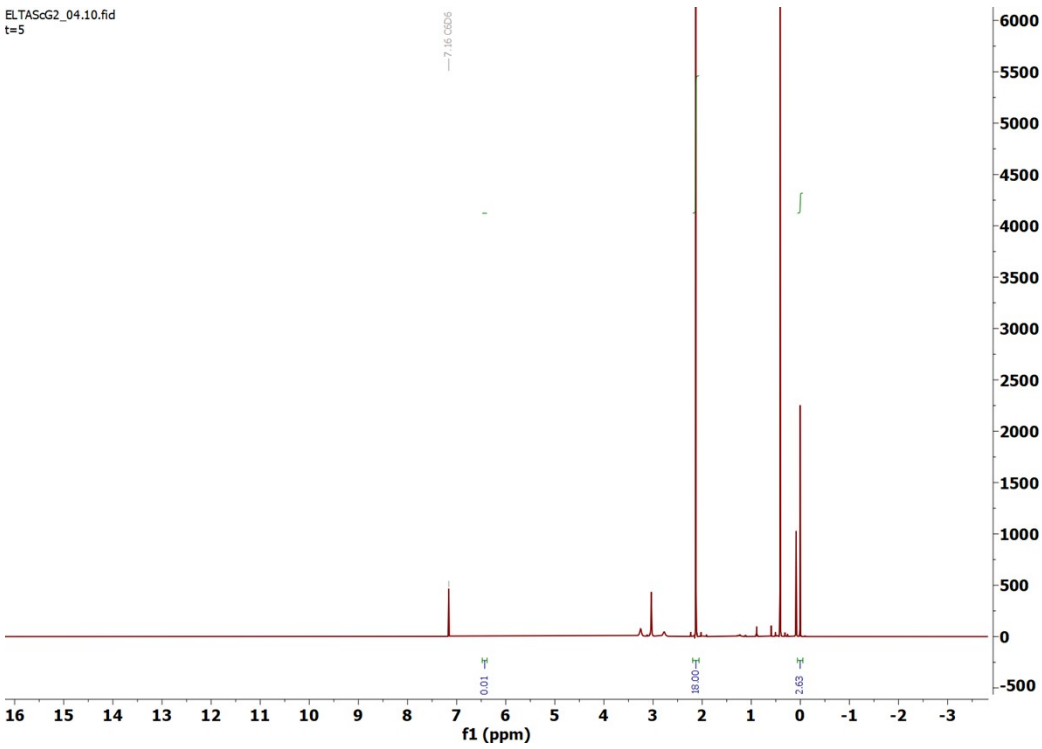

Figure S 47 ^{1}H NMR spectrum (600 MHz) of **Sc-G$_2$** in d_6-benzene (t = 134 h) showing negligible amount of vinyl methyl ether, VME.

5. Isotope labelling and speciation studies

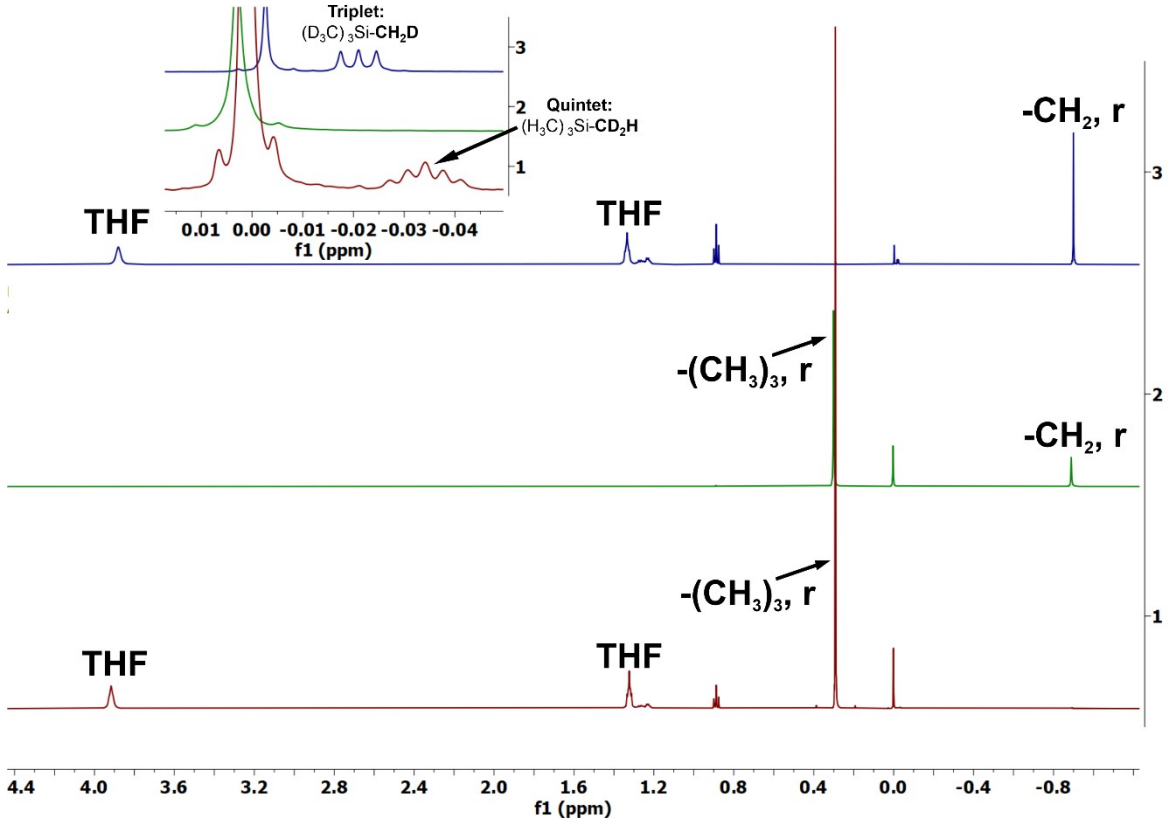

Figure S 48 Stacked ^{1}H NMR spectra (600 MHz) of Lu(d_2-r)$_3$(THF)$_2$ (red), Lu(r)$_3$(d_8-THF)$_2$ (green), and Lu(d_9-r)$_3$(THF)$_2$ (blue) in [d_6] - benzene. (9.1 mM, 30°C).

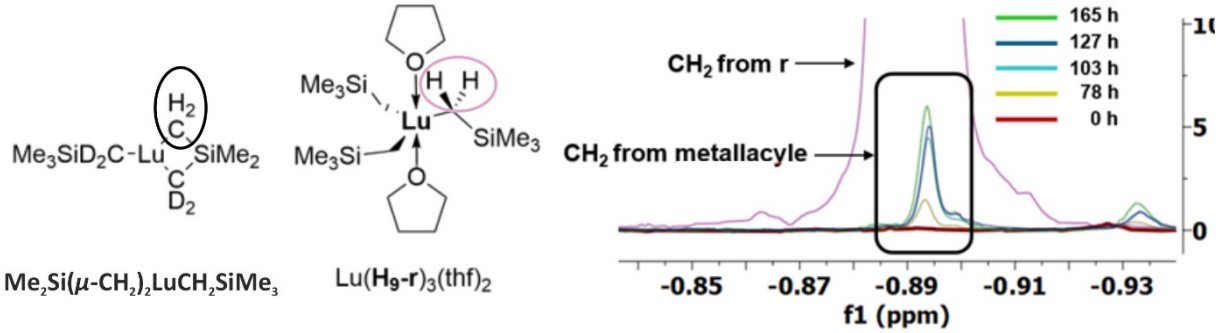

Figure S 49 ^{1}H NMR spectrum shows metalacyclic CH_2 – resonance (black box and circle) (t = 0 to 165h) growing in overlaps with -CH_2 resonance from r (lavender). 30°C in [D_6] - benzene.

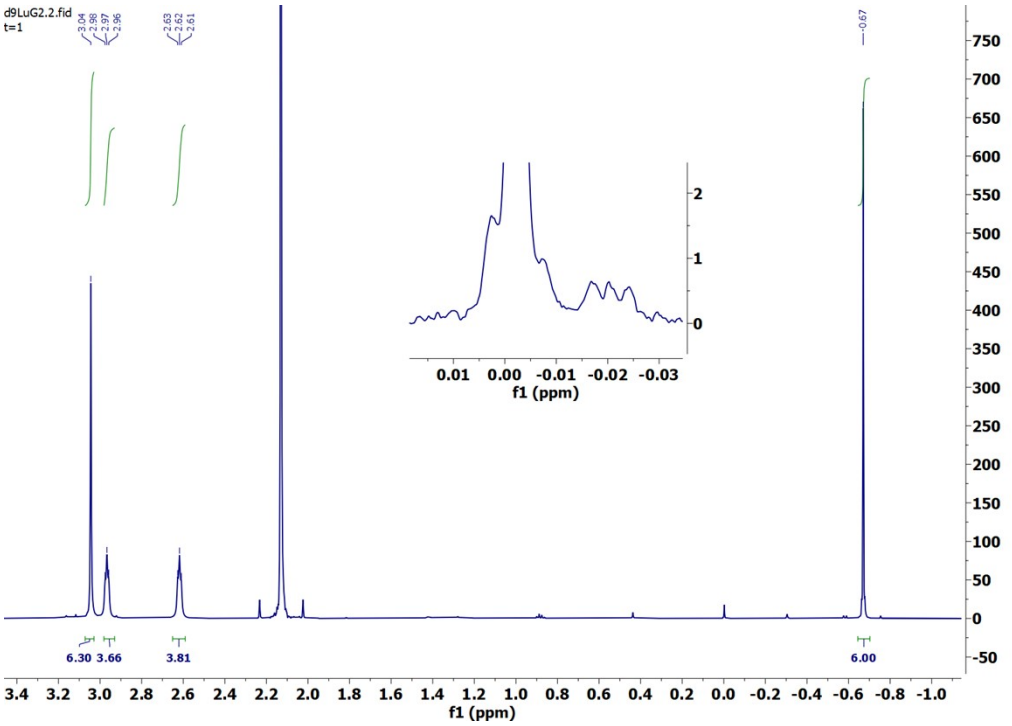

Figure S 50 ^{1}H NMR (600 MHz, C_6D_6) of $Lu(CH_2Si(CD_3)_3)_3(C_6H_{14}O_3)$ showing $CDH_2Si(CD_3)_3$ as a 1:1:1 triplet at δ 0.02. δ 3.04 (s, 6H), 2.97 (t, J = 5.4 Hz, 4H), 2.62 (t, J = 5.4 Hz, 4H), -0.67 (s, 6H).

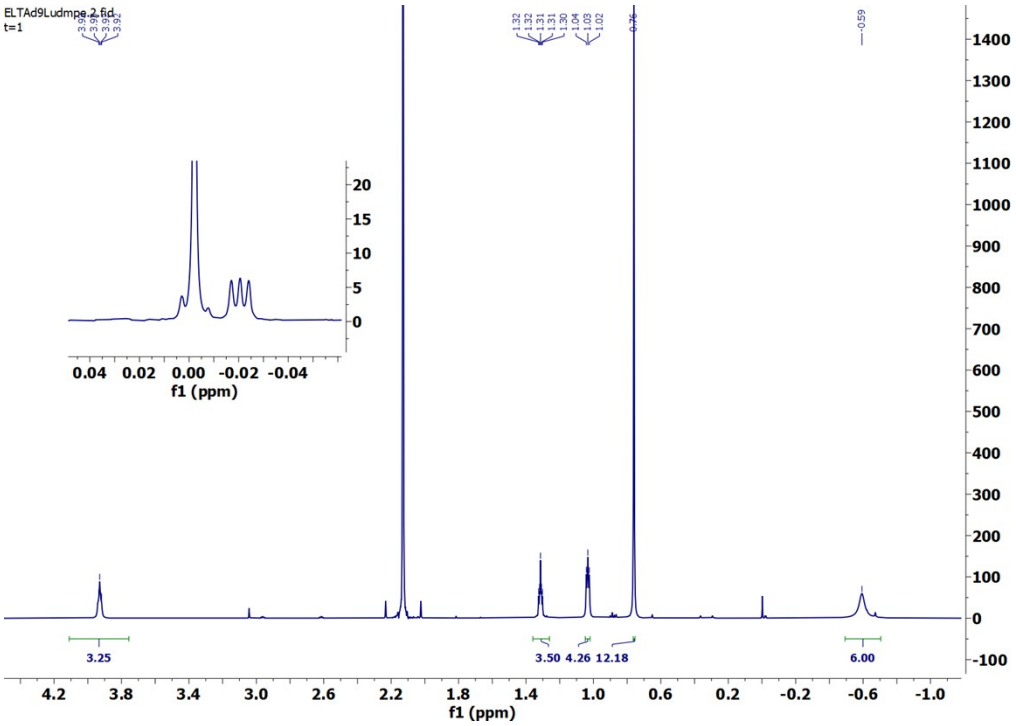

Figure S 51 ^{1}H NMR (600 MHz, C_6D_6) of $Lu(CH_2Si(CD_3)_3)_3(C_6H_{16}P_2)(C_4H_8O)$ showing $CDH_2Si(CD_3)_3$ as a 1:1:1 triplet at δ 0.02. δ 4.03 – 3.79 (m, 4H), 1.37 – 1.27 (m, 4H), 1.03 (t, *J* = 5.2 Hz, 4H), 0.76 (s, 12H), -0.59 (s, 6H).

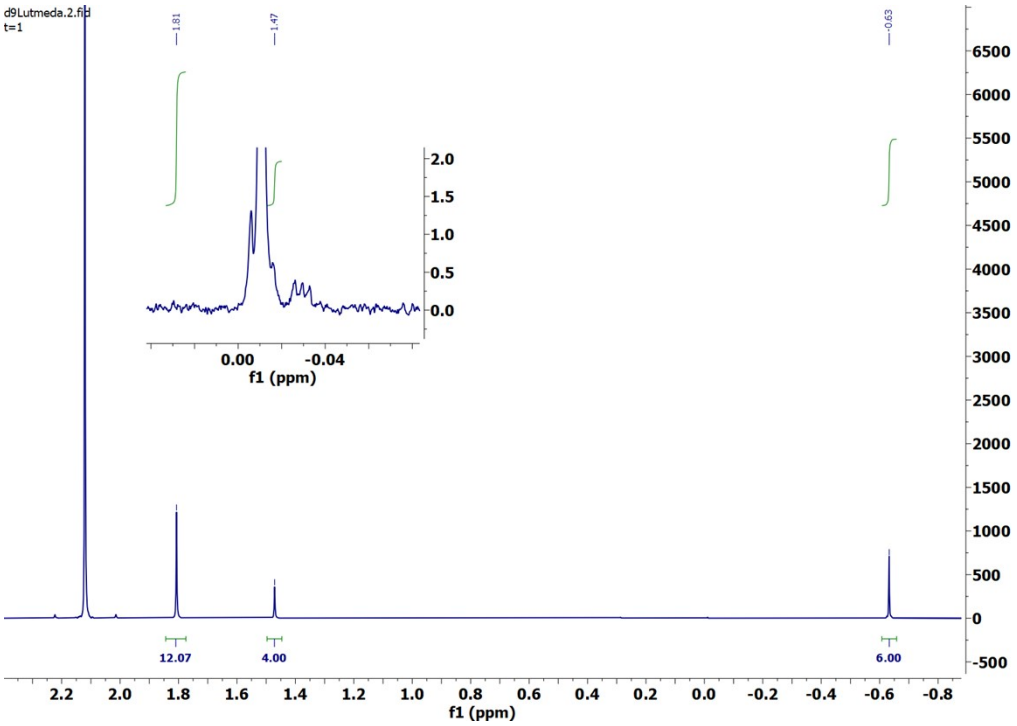

Figure S 52 ^{1}H NMR (600 MHz, C_6D_6) of $Lu(CH_2Si(CD_3)_3)_3(Me_2NCH_2CH_2NMe_2)$ showing $CDH_2Si(CD_3)_3$ as a 1:1:1 triplet at δ 0.02. δ 1.81 (s, 12H), 1.47 (s, 4H), -0.63 (s, 6H).

5.1 Synthesis of $Lu(CD_2SiMe_3)_3(C_4H_8O)_2$ (d_2-**Lu-THF**)

In an Ar-filled glovebox, anhydrous $LuCl_3$ (25 mg, 0.09 mmol) was suspended in 1.5 mL THF. To the resulting coloress solution a solution of *d_2*-((trimethylsilyl)methyl)lithium ($LiCD_2Si(CH_3)_3$) (25.7 mg, 0.27 mmol, 3 eq.) in 250 μL THF was added dropwise. The colorless reaction mixture was stirred at room temperature for 40 min. The solvent was removed under reduced pressure followed by extraction with hexane (3 × 2 mL). The filtered extracts were combined and the solvent was removed under reduced pressure yielding the title compound $Lu(CD_2SiMe_3)_3(C_4H_8O)_2$ as a white solid. Yield: 26 mg, 49% based on $LuCl_3$.

^{1}H NMR (600 MHz, C_6D_6) δ 3.97 - 3.94(s, 8H), 1.31 – 1.28 (m, 8H), 0.29 (s, 27H).). ^{2}H NMR (92 MHz, C_6D_6) δ -0.94 (s, 6H). ^{13}C NMR (151 MHz, C_6D_6) δ 71.01, 40.79, 25.06, 4.77.

5.2. Synthesis of $Lu(CH_2Si(CD_3)_3)_3(C_4H_8O)_2$ (d_9-**Lu-THF**)

In an Ar-filled glovebox, anhydrous $LuCl_3$ (25 mg, 0.09 mmol) was suspended in 1.5 mL THF. To the resulting coloress solution a solution of d_9-((trimethylsilyl)methyl)lithium ($LiCH_2Si(CD_3)_3$) synthesized according to a previously reported procedure[9] (25.7 mg, 0.27 mmol, 3 eq.) in 250 μL THF was added dropwise. The colorless reaction mixture was stirred at room temperature for 40 min. The solvent was removed under reduced pressure followed by extraction with hexane (3 × 2 mL). The filtered extracts were combined and the solvent was removed under reduced pressure yielding the title compound $Lu(CH_2Si(CD_3)_3)_3(C_4H_8O)_2$ as a white solid. Yield: 21 mg, 45% based on $LuCl_3$.

^{1}H NMR (600 MHz, C_6D_6) δ 3.98 - 3.95 (s, 8H), 1.32 – 1.29 (m, 8H), δ -0.89 (s, 6H). ^{2}H NMR (92 MHz, C_6D_6) δ 0.27 (s, 27H). ^{13}C NMR (151 MHz, C_6D_6) δ 71.01, 41.79, 25.07, 3.73.

5.3. Synthesis of $Lu(CH_2Si(CD_3)_3)_3(C_6H_{14}O_3)$ (d_9-**Lu-G_2**)

In an Ar-filled glovebox, $Lu(CH_2Si(CD_3)_3)_3(C_4H_8O)_2$ (10.05 mg, 0.017 mmol) was dissolved in 1.5 mL hexane. The colorless solution was cooled down to -78°C followed by addition of diglyme ($(CH_3OCH_2CH_2)_2O$, G_2) (9.9 mg, 0.132 mmol, 8 eq.) resulting in white precipitates which were extracted with hexane (3 x 1 mL). The combined hexanes extracts were concentrated under reduced pressure and cooled down to -40°C offering $Lu(CH_2Si(CD_3)_3)_3(C_6H_{14}O_3)$ (d_9-Lu-G_2) as a white solid. Yield: 4.2 mg, 41%, based on $Lu(CH_2Si(CD_3)_3)_3(C_4H_8O)_2$.

^{1}H NMR (600 MHz, C_6D_6) δ 3.04 (s, 6H), 2.97 (t, J = 5.4 Hz, 4H), 2.62 (t, J = 5.4 Hz, 4H), -0.67 (s, 6H).

5.4. Synthesis of $Lu(CH_2Si(CD_3)_3)_3(C_6H_{16}P_2)(C_4H_8O)$ (d_9-**Lu-DMPE**)

In an Ar-filled glovebox, $Lu(CH_2Si(CD_3)_3)_3(C_4H_8O)_2$ (20 mg, 0.033 mmol) was dissolved in 1.6 mL toluene and cooled to -40°C in the glovebox freezer. To the resulting cold clear yellow solution 1,2-Bis(dimethylphosphino)ethane ($C_6H_{16}P_2$, DMPE) (4.9 mg, 0.033 mmol, 1 eq.) in 1 mL toluene was added dropwise. The resulting clear colorless mixture was stirred for 1h at room temperature. Toluene was removed under reduced pressure at room temperature resulting in a white solid that was recrystallized from a 1:1 Et_2O/hexane mixture to yield $Lu(CH_2Si(CD_3)_3)_3(C_6H_{16}P_2)(C_4H_8O)$ as a white crystalline solid. Yield: 12.5 mg, 55% based on $Lu(CH_2SiMe_3)_3(C_4H_8O)_2$.

^{1}H NMR (600 MHz, C_6D_6) δ 4.03 – 3.79 (m, 4H), 1.37 – 1.27 (m, 4H), 1.03 (t, *J* = 5.2 Hz, 4H), 0.76 (s, 12H), -0.59 (s, 6H).

5.5. Synthesis of $Lu(CH_2Si(CD_3)_3)_3(Me_2NCH_2CH_2NMe_2)$ (d_9-**Lu-TMEDA**)

In an Ar-filled glovebox, $Lu(CH_2Si(CD_3)_3)_3(C_4H_8O)_2$ (20 mg, 0.033 mmol) were dissolved in 1.6 mL toluene and cooled to -40°C in the glovebox freezer. To the cold clear yellow solution TMEDA (3.8 mg, 0.033 mmol, 1 eq.) in 1 mL toluene was added dropwise. Toluene was removed under reduced pressure at room temperature resulting in a white solid that was recrystallized from a 1:1 Et_2O/hexane mixture to

yield $Lu(CH_2Si(CD_3)_3)_3(Me_2NCH_2CH_2NMe_2)$ as a white solid in 18% yield, 3.5 mg based on $Lu(CH_2Si(CD_3)_3)_3(C_4H_8O)_2$.

^1H NMR (600 MHz, C_6D_6) δ 1.81 (s, 12H), 1.47 (s, 4H), -0.63 (s, 6H).

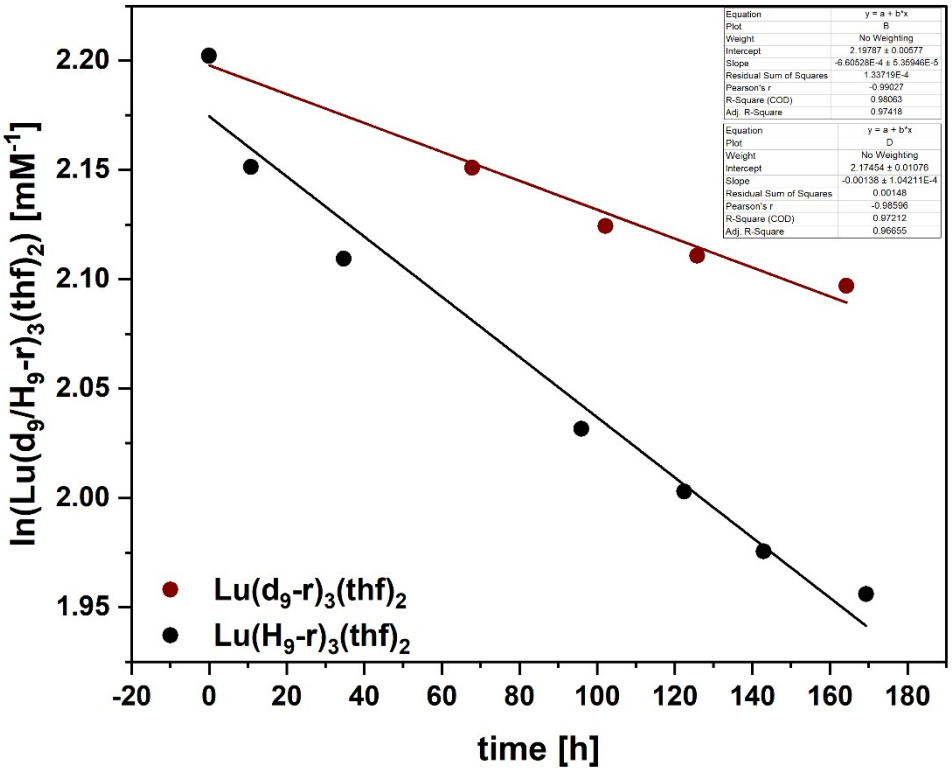

Figure S 53 Thermalstability of $Lu(CH_2Si(CD_3)_3)_3(THF)_2$ ($Lu(H_9\text{-}r)_3(THF)_2$) and $Lu(CH_2SiMe_3)_3(THF)_2$ ($Lu(H_9\text{-}r)_3(THF)_2$) expressed by the decrease of $Lu(r)_3(THF)_2$ concentration as a function of time using the logarithmic $Lu(r)_3(THF)_2$ concentration values obtained from the NMR integration values after incubation in C_6D_6, room temperature (30°C). The functions are described by the linear fits (R^2 = 0.98): ln ([$Lu(d_9\text{-}r)_3(THF)_2$]) = -6.61 (±0.5) × 10^{-4} x + 2.2 and (R^2 = 0.97): ln ([$Lu(H_9\text{-}r)_3(THF)_2$]) = -13.8 (±1.0) × 10^{-4} x + 2.17, respectively, with x being the incubation time in h. The slope of the linear fit gives the rate constants k_D = -6.61 (±0.5) × 10^{-4} h and k_H = -13.8 (±1.0) × 10^{-4} and a primary KIE k_H/k_D = 2.09.

5.6. General procedure for alkyl crossover studies

In an Ar-filled glovebox, 18.2 mM solutions of Li[YCl(CD_2SiMe_3)$_3$(THF)$_2$] and Li[YCl($CH_2Si(CD_3)_3$)$_3$(THF)$_2$] in C_6D_6 (310 μL per sample) were prepared. 300 μL per sample were combined in a YT NMR tube to yield a 600 μL solution containing 9.1 mM of equimolar Li[YCl(CD_2SiMe_3)$_3$(THF)$_2$] and Li[YCl($CH_2Si(CD_3)_3$)$_3$(THF)$_2$], respectively. The NMR sample was incubated at 30°C in an oil bath with a thermocouple. The thermolysis process was monitored by ^{1}H NMR spectroscopy.

Intermolecular:

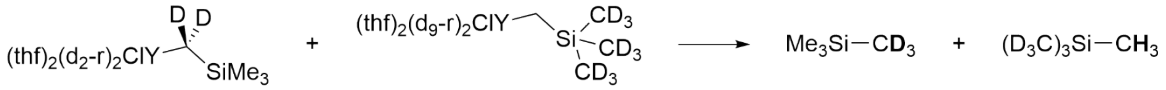

Intramolecular:

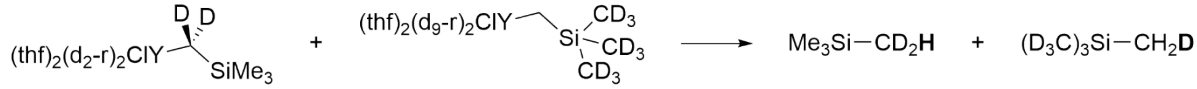

Scheme S1. Schematic representation of crossover reaction featuring of Li[YCl(d_2-r)$_3$(THF)$_2$] and Li[YCl(d_9-r)$_3$(THF)$_2$] and the corresponding crossover products according to inter- or intramolecular decomposition.

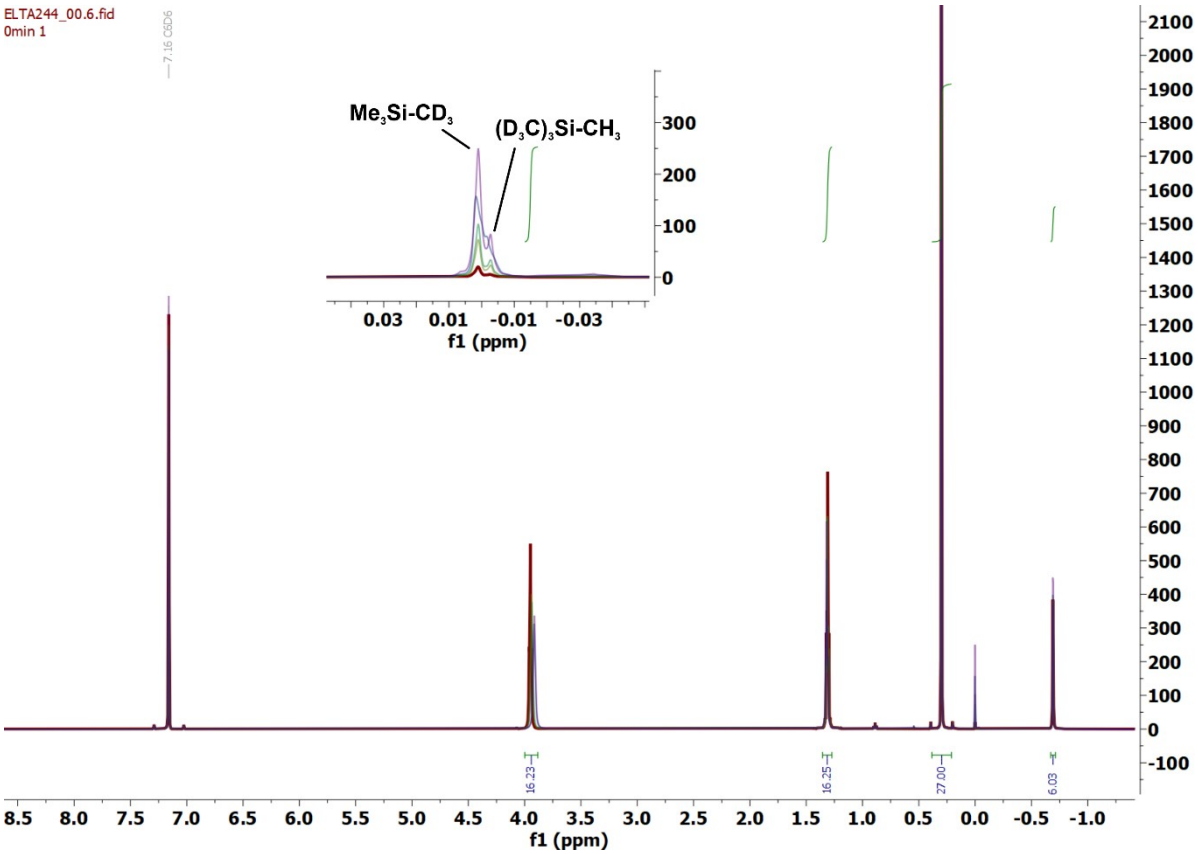

Figure S 54 Superimposed ^{1}H NMR spectra (600 MHz) of an equimolar reaction mixture containing Li[YCl(d_2-r)$_3$(THF)$_2$] and Li[YCl(d_9-r)$_3$(THF)$_2$] in C_6D_6 (30°C) recorded at t = 0 min (red), 185 min (yellow), 354 min (teal), 1425 min (lavender), 1627 min (purple). The inset shows singlet resonances at δ = 0.001 ppm and δ = -0.002 ppm, respectively, which can be assigned to the crossover products d_3-TMS and d_9-TMS of the intermolecular decomposition process. The different TMS shifts are a result of isotopic effect.[10]

6. Impact of LiCl on thermal stability of $M(r)_3(THF)_2$ M = Y, Lu

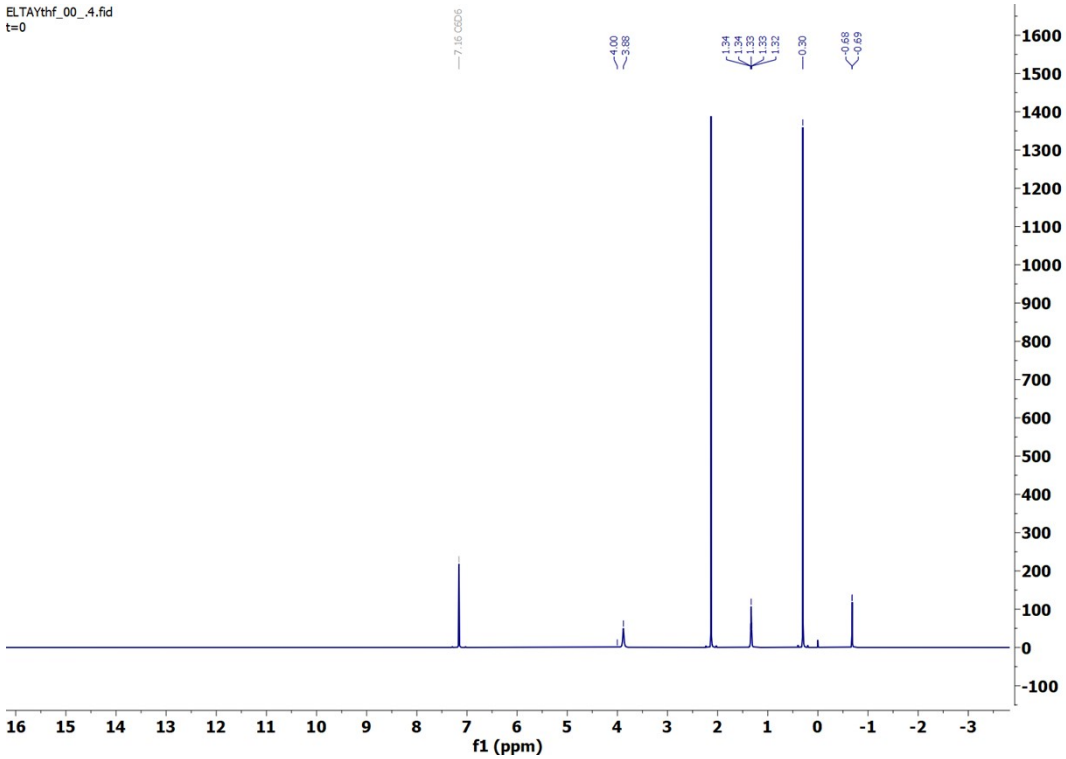

Figure S 55 ^{1}H NMR spectrum (600 MHz) of **Y-THF** prepared starting from Nar (this work) in d_6-benzene.

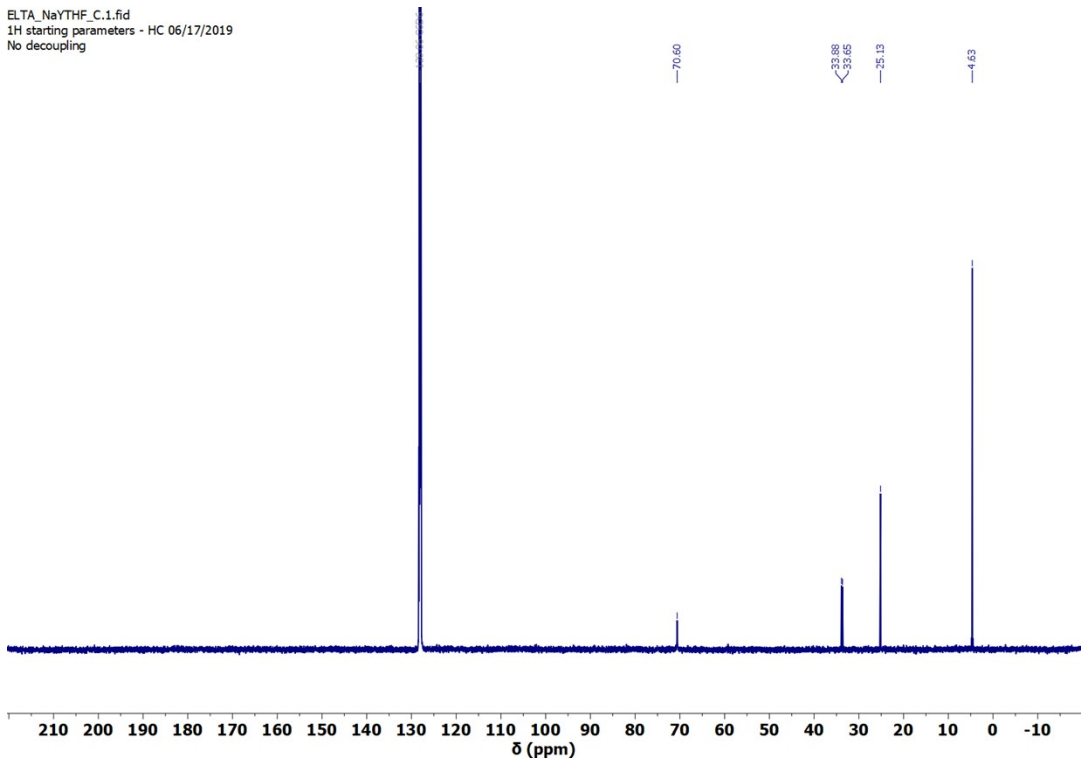

Figure S 56 ^{13}C NMR (151 MHz, C_6D_6) of **Y-THF** in d_6-benzene.

6.1 General procedure for speciation studies

In an Ar-filled glovebox, 18.2 mM stock solutions of $Lu(CH_2SiMe_3)_3(THF)_2$ or $Li[YCl(CH_2SiMe_3)_3(THF)_2]$ (synthesized according to previously published procedures[2, 11, 12]) and 12-crown-4 ether ($C_8H_{16}O_4$) were prepared in C_6D_6. 300 µL of the 12-crown-4 ether ($C_8H_{16}O_4$) stock solution were mixed with 300 µL of $Lu(CH_2SiMe_3)_3(THF)_2$ or $Li[YCl(CH_2SiMe_3)_3(THF)_2]$ in J Young teflon-valved equipped NMR tubes to yield equimolar mixtures of the corresponding complex and 12-crown-4 ether.

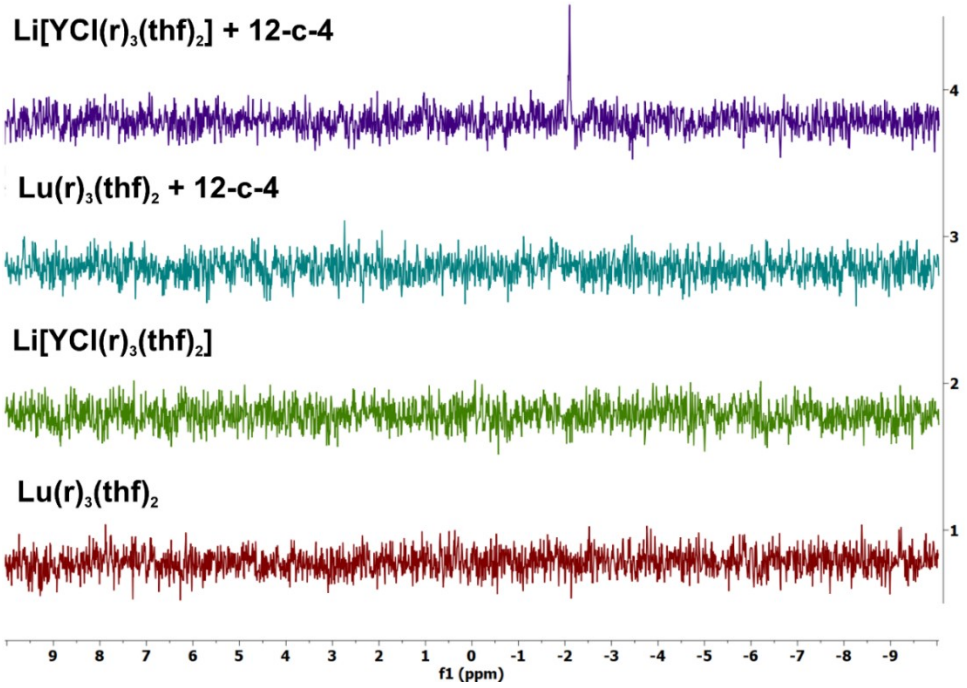

Figure S 57 Stacked ^7Li NMR spectra (156 MHz, C_6D_6) of $Lu(CH_2SiMe_3)_3(THF)_2$ and $Li[YCl(CH_2SiMe_3)_3(THF)_2]$ (prepared according to previously published procedures[2, 11, 12]) in the absence and in the presence of and equimolar amount of 12-crown-4 ether. $Li[YCl(CH_2SiMe_3)_3(THF)_2]$ does not show a visible ^7Li resonance in absence of 12-crown-4 ether which can be attributed to the quadrupolar nature of ^7Li. Addition of 12-crown-4 ether provides a symmetric coordination environment for ^7Li which can be observed as a resonance in the ^7Li NMR spectrum.

Table S11. Summary of reports on characterization of $Y(CH_2SiMe_3)_3(THF)$ synthesized from $LiCH_2SiMe_3$. (CSDS & Scifinder August, 28 2024).

entry	Citation	$^{13}C\{^1H\}$ NMR frequency and chemical shifts[a]	^1H NMR NMR frequency and chemical shifts[b]
1	*Organometallics* **2017**, *36*, 3677	cites *Catal. Sci. Technol.* **2016**, *6* (16), 6339–6353.	
2	*Inorg. Chem.* **2020**, *59*, 5835	No NMR resonances reported; reports SXRD + EA	
3	*Organometallic Chem.***2018**, *875*, 5	cites **5**	
4	*J. Am. Chem. Soc.* **2001**, *123*, 7711	cites **9** & **5**	
5	*J. Chem. Soc., Chem. Commun.* **1973**,126	N/A	2.73 (s, 2H), N/A (m, 2H), 0.30 (s, 27H), -0.65 (d, *J* = 2.5 Hz, 1H).
6	*Chem. Commun.* **2016**, *52*, 5425	N/A	(400 MHz, toluene-d_8) 4.09 (t, J = 6.4 Hz, 8H), 1.61-1.33 (m, 8H), 0.18 (s, 27H), -0.38 (s, 6H).
7	*Macromolecules* **2022**, *55*, 7488	N/A	(400 MHz) 3.95 (t, 8H), 1.31 (t, 8H), 0.29 (s, 27H), -0.69 (s, 6H).
8	*Macromolecules* **2019**, *52*, 7073	(126 MHz) 69.8, 33.8, 25.2, 4.5	(400 MHz) 4.01 - 3.87 (m, 8H), 1.36 - 1.21 (m, 8H), 0.31 (s, 27H), -0.67 (d, 6H).
9	*Organometallics* **2000**, *19*, 228	(101 MHz) 70.8, 35.7, 33.7, 25.0, 4.6	(400 MHz) 3.93 (s, 9H), 1.30 (m, 10H), 0.27 (s, 27H), -0.71 (d, *J* = 2.3 Hz, 6H).
10	Y-THF + LiCl (1 equiv.)	(151 MHz) 70.60, 33.88, 33.65, 25.13, 4.63	(600 MHz) 3.85 (s, 1H), 1.37 – 1.31 (m, 2H), 0.28 (s, 27H), -0.70 (d, *J* = 2.8 Hz, 1H).
11	this work (NaY-THF)	(151 MHz) 65.90, 33.99, 33.75, 25.15, 4.63	(600 MHz) 3.87 (s, 9H), 1.35 – 1.31 (m, 10H), 0.30 (s, 27H), -0.68 (d, *J* = 2.7 Hz, 6H).

a. all reported as δ in C_6D_6 solution. b. all reported as δ in C_6D_6 solution except as noted for entries 5 and 6. The H resonances for entry 5 have been converted from τ (tau) (in the original report) to δ by subtraction from 10; the THF resonances were not reported.

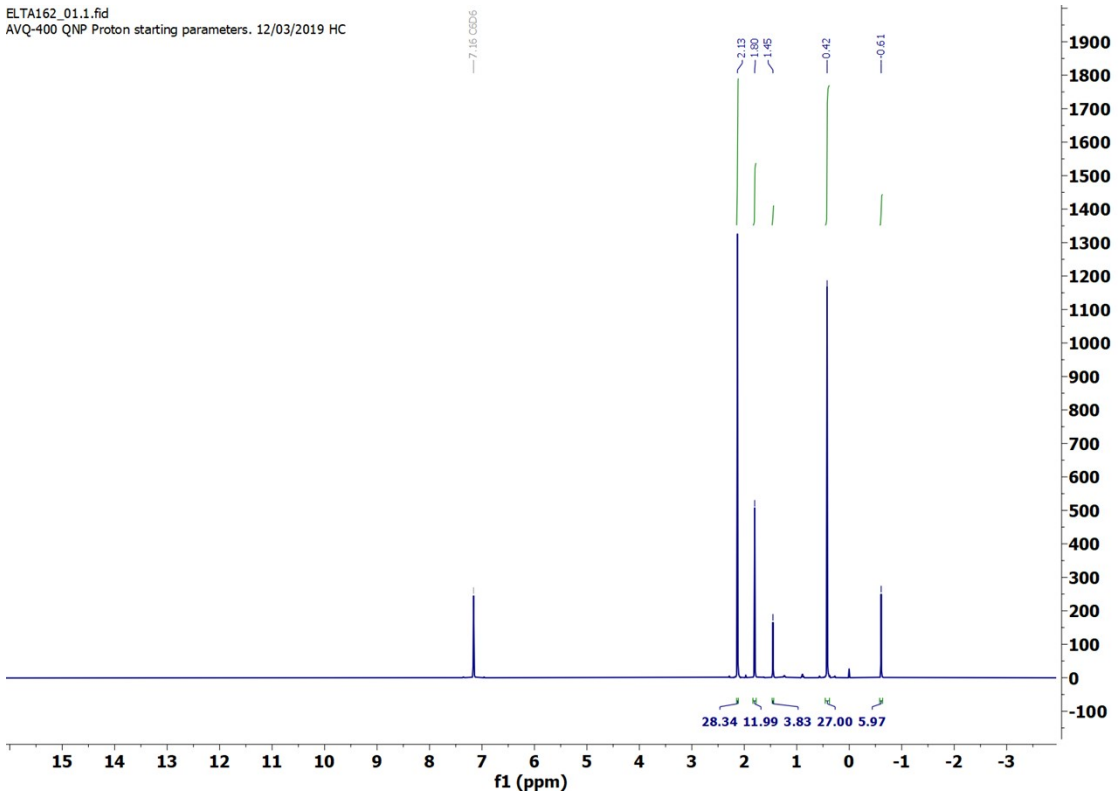

Figure S 58 Li[YCl(r)$_3$(THF)$_2$] in C_6D_6 after addition of an equimolar amount of 12-crown-4 ether. ^{1}H NMR (400 MHz, C_6D_6) of δ 2.13 (s, 28H), 1.80 (s, 12H), 1.45 (s, 4H), 0.42 (s, 27H), -0.61 (s, 6H).

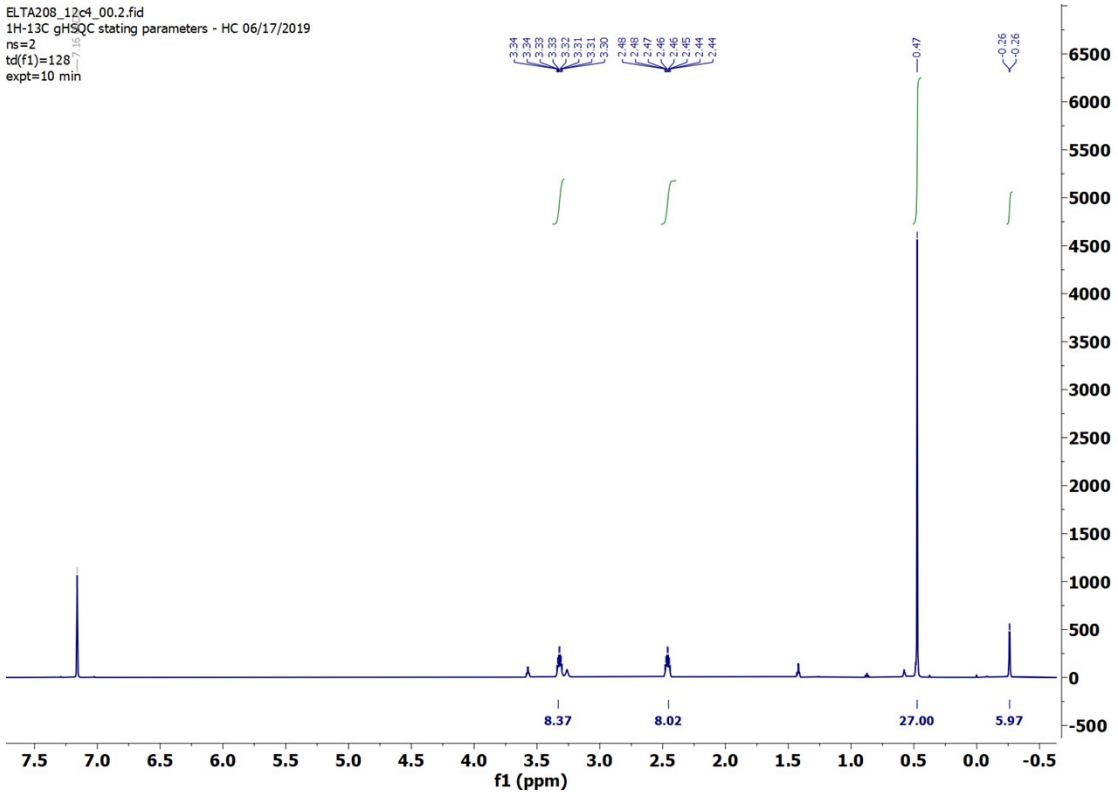

Figure S 59 Y(r)$_3$(12-crown-4) synthesized according to the literature (Okuda *et al.*)[13] ^{1}H NMR (600 MHz, C_6D_6) δ 3.32 (tt, J = 7.1, 3.7 Hz, 8H), 2.46 (tt, J = 6.8, 3.7 Hz, 8H), 0.47 (s, 27H), -0.26 (d, J = 3.2 Hz, 6H).

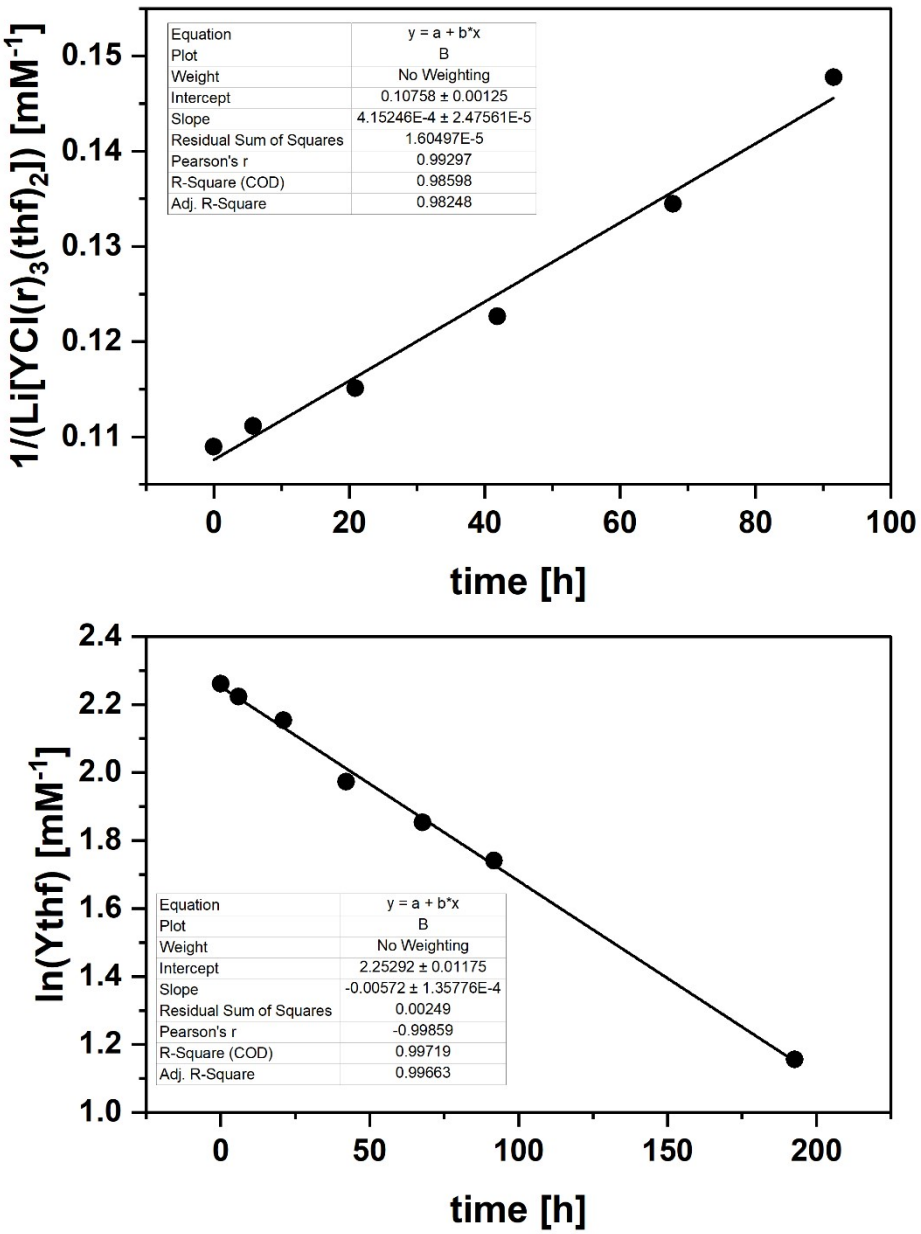

Figure S 60 Thermalstability of $Li[YCl(r)_3(THF)_2]$ (prepared according to previously published procedures[2], upper figure) and $Y(r)_3(THF)_2$ prepared from Nar (this work, bottom figure) expressed by the decrease of **Y-donor** concentration as a function of time using the logarithmic **Y-donor** concentration values obtained from the NMR integration values after incubation in C_6D_6, room temperature (30°C).

6.2. General procedure for LiCl spiking experiments

In an Ar-filled glovebox, five 4 mL vials were charged with $Lu(CH_2SiMe_3)_3(THF)_2$ (3.2 mg, 0.006 mmol) and dissolved in varying amounts of THF (833.3 µL to 1 mL). To each stirred THF solution, varying amounts (0 µL to 166.7 µL) of a 33.3 mM LiCl solution in THF were added to yield 1 mL solutions of $Lu(CH_2SiMe_3)_3(THF)_2$ with LiCl concentrations ranging from 0% to 100% (0 to 1 equivalent). After stirring the solutions for five minutes at room temperature, the volatiles were removed under reduced pressure, and the residues were redissolved in C_6D_6.

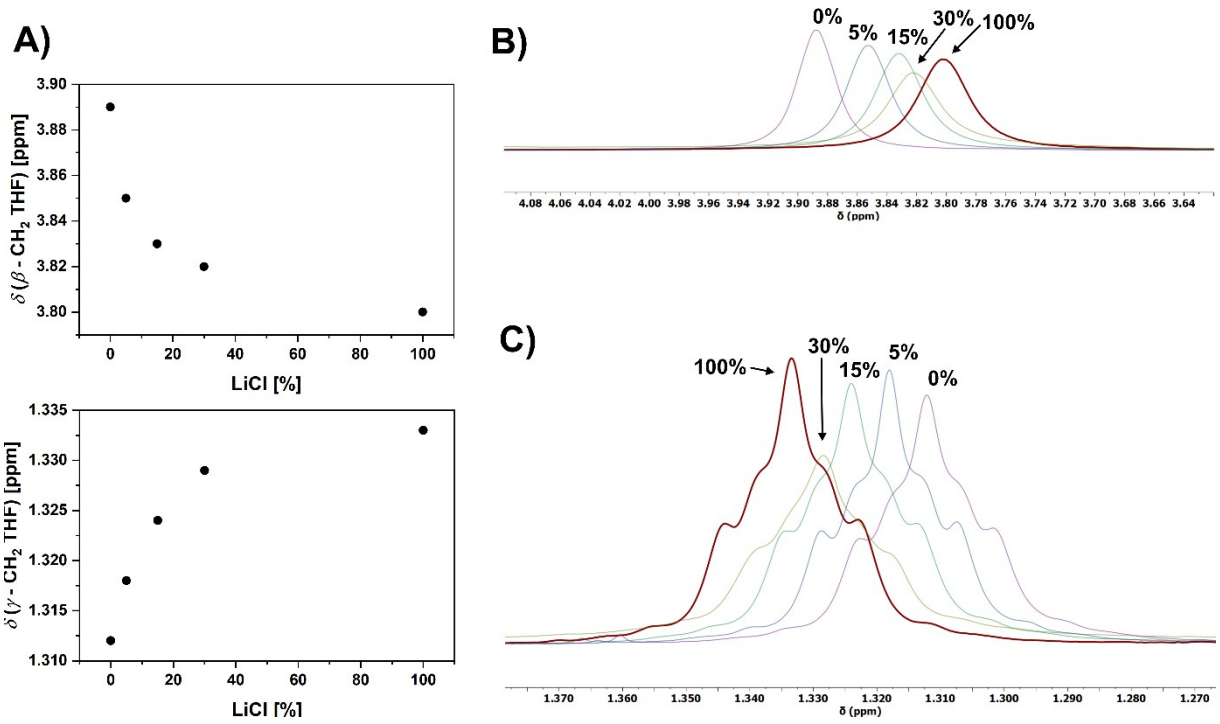

Figure S 61 Impact of LiCl concentration on the ^{1}H NMR shifts of the β- & γ-CH_2 resonances in THF.

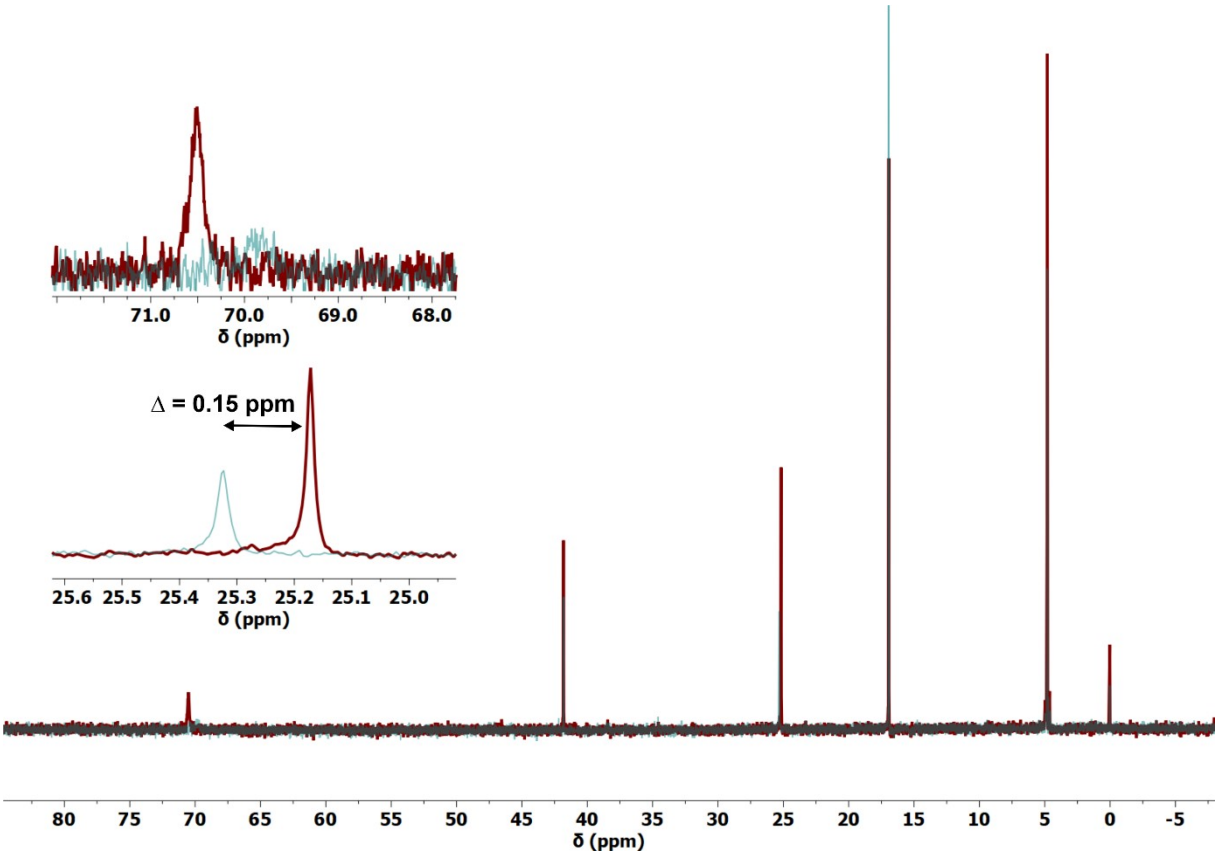

Figure S 62 Superimposed ^{13}C NMR spectra of $Lu(CH_2Si(CH_3)_3)_3(THF)_2$ in the absence (red) and presence of 1eq. LiCl (cyan) showing impact of LiCl concentration on the ^{13}C NMR shifts of the β- & γ-CH_2 resonances in THF.

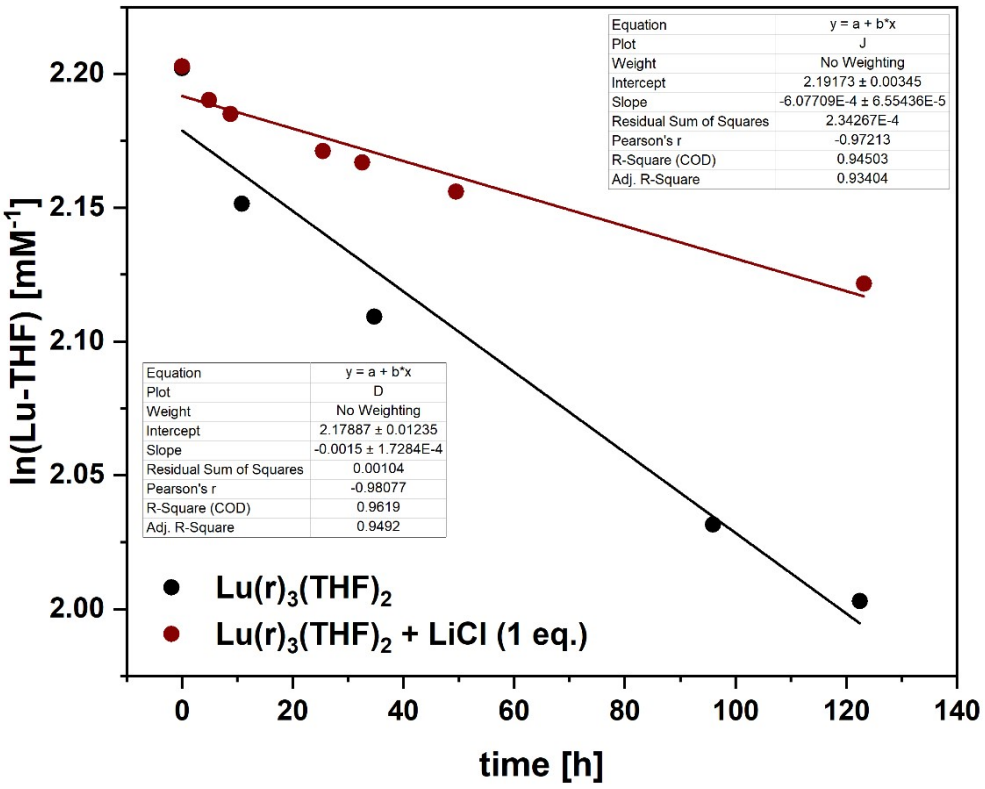

Figure S 63 Thermal stability of $Lu(CH_2Si(CH_3)_3)_3(THF)_2$ (**Lu-THF**) in the absence (black) and in the presence of 1 equivalent LiCl (red) expressed by the decrease of $Lu(r)_3(THF)_2$ concentration as a function of time using the logarithmic $Lu(r)_3(THF)_2$ concentration values obtained from the NMR integration values after incubation in C_6D_6, room temperature (30°C). The functions are described by the linear fits ($R^2 = 0.96$): ln ([$Lu(r)_3(THF)_2$]) = -1.5 (±0.2) × 10^{-3} x + 2.18 and ($R^2 = 0.95$): ln ([$Lu(r)_3(THF)_2$] + 1 eq. LiCl) = -6.1 (±0.7) × 10^{-4} x + 2.19, respectively, with x being the incubation time in h. The slope of the linear fit gives the rate constants k_1 = -1.5 (±0.2) × 10^{-3} and k_2 = -6.1 (±0.7) × 10^{-4}.

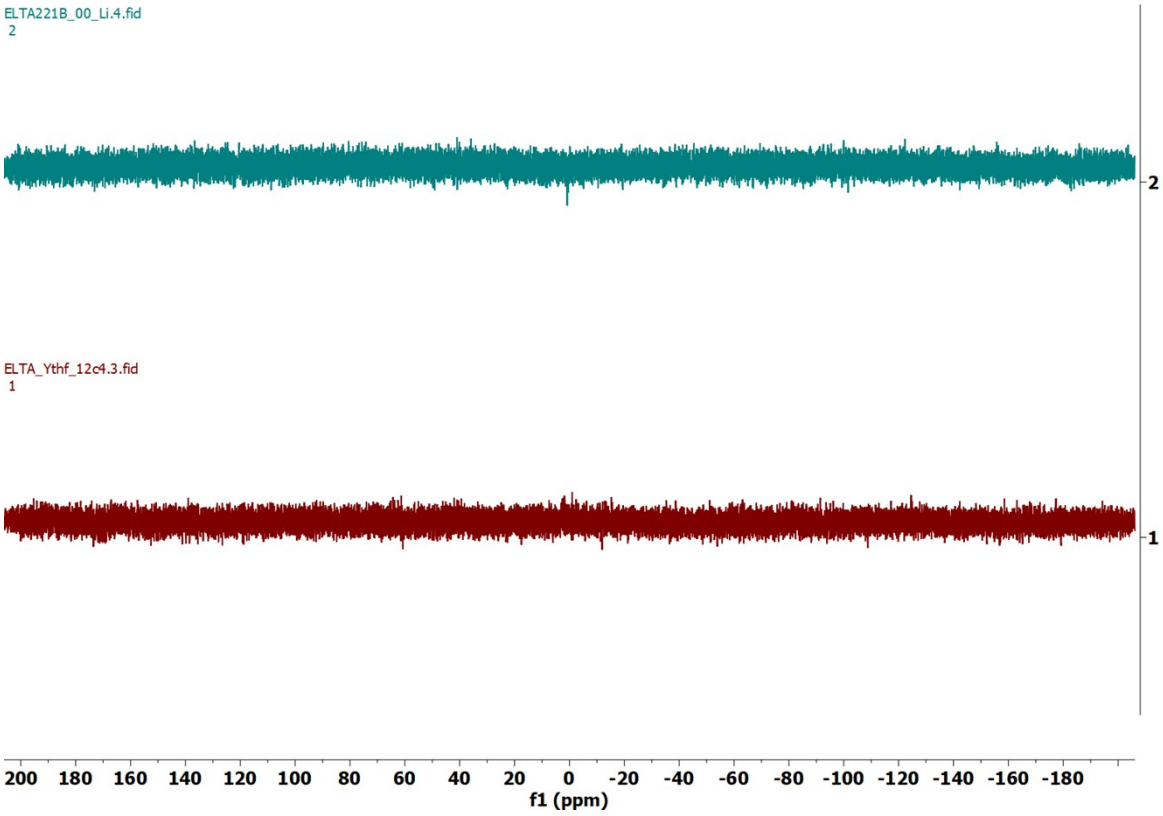

Figure S 64 Stacked ^{7}Li NMR spectra (156 MHz, C_6D_6) of $Y(r)_3(THF)_2$ prepared from Nar (this work) in the absence (red) and in the presence (cyan) of an equimolar amount of 12-crown-4 ether demonstrating the complex bulk is lithium free.

Figure S 65 Qualitative Cl^- test showing no AgCl formation in the case of H_2O (**1**, as a blank acidified with conc. HNO_3), $Y(r)_3(THF)_2$ (**2**, prepared starting from Nar after digestion with H_2O acidified with conc. HNO_3), and AgCl precipitates for $Li[YCl(r)_3(THF)_2]$ (**3**, after digestion with H_2O acidified with conc. HNO_3).

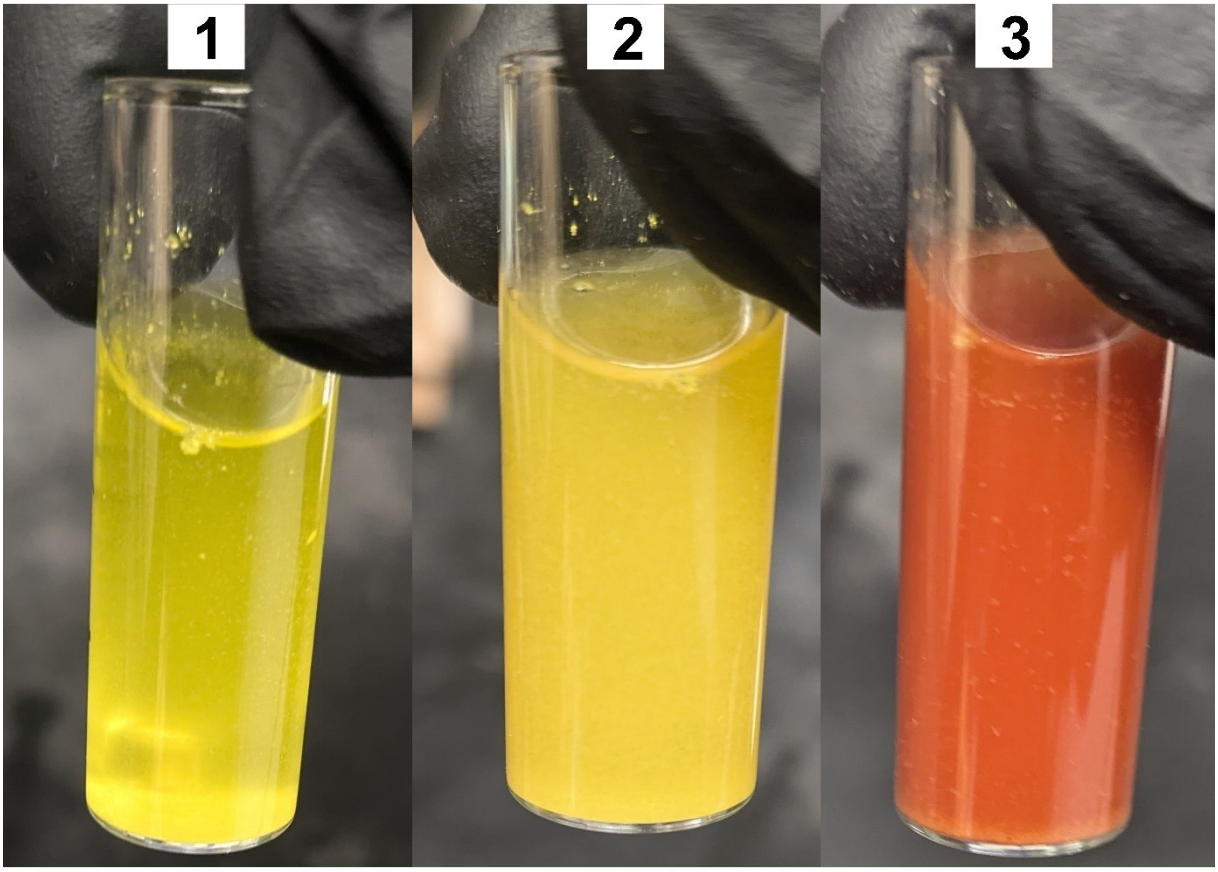

Figure S 66 Quantitative Cl^- test using Mohr's method showing an aqueous solution of **Y-THF** prepared from Li(r) (**Li[YCl(r)$_3$(THF)$_2$]**) in the presence of K_2CrO_4 (**1**). Dropwise addition of an aqueous $AgNO_3$ solution results in gradual AgCl precipitation (**2**) followed by formation of red Ag_2CrO_4 at the endpoint of the titration (**3**).

7. References

1. H. Schumann, D. M. Freckmann and S. Dechert, *Zeitschrift für anorganische und allgemeine Chemie*, 2002, **628**, 2422-2426.
2. S.-M. Chen, Y.-Q. Zhang, J. Xiong, B.-W. Wang and S. Gao, *Inorganic Chemistry*, 2020, **59**, 5835-5844.
3. K. A. Rufanov, D. M. M. Freckmann, H.-J. Kroth, S. Schutte and H. Schumann, *Zeitschrift für Naturforschung B*, 2005, **60**, 533-537.
4. A. G. B. Getsoian, B. Hu, J. T. Miller and A. S. Hock, *Organometallics*, 2017, **36**, 3677-3685.
5. A. Mortis, C. Maichle-Mössmer and R. Anwander, *Dalton Transactions*, 2022, **51**, 1070-1085.
6. O. V. Dolomanov, L. J. Bourhis, R. J. Gildea, J. A. Howard and H. Puschmann, *Journal of applied crystallography*, 2009, **42**, 339-341.
7. G. M. Sheldrick, *Acta Crystallographica Section A: Foundations and Advances*, 2015, **71**, 3-8.
8. R. Clark and J. Reid, *Acta Crystallographica Section A: Foundations of Crystallography*, 1995, **51**, 887-897.
9. J. W. Bruno, G. M. Smith, T. J. Marks, C. K. Fair, A. J. Schultz and J. M. Williams, *Journal Of The American Chemical Society*, 1986, **108**, 40-56.
10. P. E. Hansen, *Progress in Nuclear Magnetic Resonance Spectroscopy*, 1988, **20**, 207-255.
11. S. C. Kosloski-Oh, K. D. Knight and M. E. Fieser, *Inorganic Chemistry*, 2023, DOI: 10.1021/acs.inorgchem.3c03161.
12. G. Cai, Y. Huang, T. Du, S. Zhang, B. Yao and X. Li, *Chemical Communications*, 2016, **52**, 5425-5427.
13. S. Arndt, P. M. Zeimentz, T. P. Spaniol, J. Okuda, M. Honda and K. Tatsumi, *Dalton Transactions*, 2003, 3622-3627.